SEMI-AUTOMATED RECONSTRUCTION OF VASCULAR NETWORKS IN KNIFE-EDGE SCANNING MICROSCOPE MOUSE BRAIN DATA

A Thesis

by

ANANTH DILEEPKUMAR

Submitted to the Office of Graduate and Professional Studies of
Texas A&M University
in partial fulfillment of the requirements for the degree of

MASTER OF SCIENCE

Chair of Committee,	Yoonsuck Choe
Committee Members,	James Caverlee
	Jim Xiuquan Ji
Head of Department,	Nancy M. Amato

August 2014

Major Subject: Computer Science

ABSTRACT

The Knife-Edge Scanning Microscope (KESM) enables imaging of an entire mouse brain at sub-micrometer resolution. The data from KESM can be used in the reconstruction of neuronal and vascular structures in the mouse brain. Tracing the vascular network of the brain and reconstructing the topology allows us to map the circulatory pathways inside the brain. Studying these cerebro-vascular networks is important to understand and measure the consumption and access to energy, oxygen and nutrients by different regions of the brain. Presently, there are both manual and automated methods to trace the vascular network from images of the brain. The manual methods are limited by the time consuming nature of the process and the extensive manual labor required. Today, vascular reconstruction techniques focus either on tracing vessels at the macro-level in a whole brain or tracing micro vessels in a small section of the brain. In this thesis, I attempt to develop a new, more targeted approach to semi-automatically trace a single blood vessel and its associated network of branches.

In my approach, the user provides the algorithm with a single seed point of a vessel to start exploration and can guide the system towards specific sub-branches or sub-networks to explore. This new approach is expected to help quickly trace the vascular network of the brain as well as reduce the manual effort involved and save computing power by limiting the scope of the reconstruction to a smaller sub-network of blood vessels.

DEDICATION

to my family

ACKNOWLEDGEMENTS

I would like to thank my advisor, Dr. Yoonsuck Choe for his earnest support and guidance throughout my research work. Without his advice and encouragement, this research would not have been possible. I would also like to thank my committee members, Dr. James Caverlee and Dr. Jim Xiuquan Ji for their valuable comments and advice. I'm also grateful to my friends, colleagues and the department faculty and staff for all the rich memories and for making my time at Texas A&M University such a great experience.

I would like to express my gratitude to my family, especially my Mom and Dad for all the love and support.

Part of this research was funded by the National Science Foundation through the Collaborative Research in Computational Neuroscience program (NSF #1208174, NSF #0905041).

TABLE OF CONTENTS

Page

LIST OF FIGURES

LIST OF TABLES

CHAPTER I

INTRODUCTION

1.1 Motivation

Understanding the cerebrovascular architecture of the brain is crucial to study various processes in the brain as well as diseases afflicting it. Since the cerebrovascular network is the circulatory system of the brain, it is important to understand the consumption and access to nutrients, oxygen, and energy by different regions of the brain. There is also a need to study the location of blood vessels in relation to other anatomical structures of the brain. In addition to providing insights into the energy and nutrient requirements of the brain, a clear understanding of the structural abnormalities of the vascular network can help diagnose neurological disorders. For instance, there is evidence that Alzheimer's disease has a neurovascular cause [1][5]. It is also possible to construct a statistical model of regions of the brain from vascular reconstructions of several brain specimens. Such a statistical model can provide topological features that are common in vascular networks of most brains. This can help us understand the trajectory, origin and destinations of major blood vessels, identify regions where there are crucial branches in the network, etc. It is therefore essential that we have the tools to map the topology of the vascular networks of the brain in detail.

High resolution images of the brain are required to reconstruct the vascular networks of the brain. Today, sophisticated imaging techniques are available which can

provide huge volumes of high resolution images of the brain which let researchers study and trace the vascular networks.

The researchers at the Brain Network Laboratory (BNL) at Texas A&M University developed the Knife-Edge Scanning Microscope (KESM) to scan images of mammalian brains at sub-micrometer resolutions [2]. These data sets can be used to trace the vascular network of the brain in great detail [3].

The techniques that are used today to reconstruct vascular structures of the brain are limited to either the reconstruction of macroscopic vessels of the whole brain, which do not yield significant insight into how the vessels are interconnected through finer capillaries at the microscopic scale, or the reconstruction of microscopic vessels of a small region of the brain, which do not yield information about their origins or ultimate destinations.

1.2 Goal of Research

The goal of this research is to develop a novel method to perform targeted semi-automated traces of vascular networks originating at a chosen cross sectional point of a particular blood vessel. The reconstruction of the vascular network would be targeted toward the exploration of only those subnetworks constituted by the branches of the specific blood vessel, referred to as the seed vessel.

1.3. Approach and Methods

Exploration of the neurovascular network originating at a particular vessel is performed through a series of steps outlined in this section. This is primarily an image processing problem and I used several image processing techniques to process the image sets, extract features from them as well as to trace the vascular networks through the cross sectional slices. First, the images were preprocessed to remove noise using simple noise reduction and smoothing algorithms. Next, regions of interest in the images were identified and the boundaries of cross sections of blood vessels were detected. Following this step, blood vessels of interest were identified and adjoining blood vessels were also tracked to identify potential merges or splits in the network of vessels. Next, branching of the blood vessels were identified using a combination of heuristics and image processing algorithms. Finally, on a global level, each new branch point was collected, analysed and the new vessels which spring from these branches were recursively explored using a breadth-first approach. The network exploration can either be automated or semi-automated with the user directing the reconstruction.

1.3.1 Preprocessing

The first stage of the process to trace vessels from the images of the mouse brain is to determine an Area of Interest (AoI), which is a cropped portion of about 120 × 100 pixels from the original image which completely contains the initial seed cross section of the vessel as well as regions surrounding it. This reduces the computing costs as subsequent image processing algorithms are applied only to a restricted area of the

original image. Next, the image is inverted so that the vessel cross sections are highlighted. The next step is to clean up the image using noise reduction algorithms and filters. Gaussian filters were used to accomplish this. They simultaneously smooth the image and reduce noise. The AoI can be shifted as the exploration of the vessel progresses to regions where the vessel moves to.

1.3.2 Edge and Region Detection

The next step is to identify the boundaries (in image processing terminology, this process is called edge detection. Henceforth, the boundaries shall be referred to simply as 'edges') of the cross section of the vessel in each successive slice. The convex polygon bounded by these edges would henceforth be referred to as 'regions'. These regions are the cross sections of blood vessels. Detecting edges helps determine the shape of the cross section. Edges can help identify several useful properties of the regions and by extension those of the blood vessel being traced. The Canny edge detection algorithm is used to identify edges in a particular AoI [4].

Once edges have been identified, several properties of the cross section, such as the centroid and the area of the cross section can be identified. The centroid can be used for tracing the vessel. The cross sectional area can be used to approximate the width and size of the vessel. The cross sectional area also helps determine whether the vessel is about to split or merge with another vessel. The algorithm does not store information about the shapes of the vessel cross section. The information about the cross sectional area is stored for each cross section however.

1.3.3 Trace Extension

The blood vessel can be traced through progressive slices and can be split into sub-branches based on the characteristics of its cross sectional region in each slice. From each cross section, various information about the vessel can be collected, such as the slice number, the coordinates of the centroid of the vessel (which is used to trace the vessel), cross-sectional area, etc. The exploration can progress in the direction of extension of the blood vessel. This means that the exploration can proceed in either direction of the z-axis for a given vessel. The reconstruction algorithms can handle most orientations of the vessel except where it is nearly perpendicular to the z-axis. Here the cross sections of the vessel or segments of the vessel would lie in within a few parallel planes perpendicular to the z-axis.

1.3.4 Branching

Determining instances where each vessel branches or merges with other vessels is essential to map out the vascular network branching out from the given seed vessel. A combination of heuristics and image processing algorithms are used to predict and validate branching events. Watershed algorithm is a classic image processing algorithm that can be used to identify distinct but adjacent regions [13]. This helps determine instances where a vessel is on the cusp of a split or has just merged with another vessel.

1.3.5 Vascular Network Exploration

Each vessel can be tracked between points of branching. The points of branching can be identified as nodes of a graph and the vessel themselves as the edges. This abstraction can be useful in applying graph theoretic algorithms to explore the vascular network efficiently. The network is explored either automatically using a breadth-first exploration strategy or semi-automatically by requiring the user to direct the reconstruction as it progresses.

1.4 Significance

This thesis extends the manual methods for neuro-vascular network reconstruction [17]. It also creates a new tool for performing targeted exploration of vascular networks in the brain. The tool created as part of this thesis is semi-automated with limited need for human intervention and assistance. This novel method can trace the entire vascular sub-network rooted at a particular blood vessel or it can explore the sub-network as an interactive process with the user guiding the exploration at each branch of the network. This thesis is expected to contribute to the ongoing research into the structure and architecture of vascular networks of the brain in a significant way.

1.5 Outline

This thesis is organized in the following manner. In the subsequent chapter, background of the present cerebrovascular reconstruction strategies will be briefly summarised. In Chapter III, the entire strategy for the semi-automated vascular network

reconstruction is expounded upon. In Chapter IV, the experimental results of the reconstruction performed on KESM data as well as validation using synthetic data is presented. Finally, in Chapter V, the results are discussed, possible future work in this process is explored, and open issues and conclusions are presented.

CHAPTER II

BACKGROUND AND PRIOR WORK

2.1 Background

Over the past few years, researchers have produced several techniques, processes and instruments to image, reconstruct and analyse the neuro-vascular network. The Knife-Edge Scanning Microscope is one of such instruments, envisioned and invented at Texas A&M University's Brain Networks Laboratory (BNL), which can image whole mouse brains at sub-micrometer resolution [2]. The instrument can digitize an entire mouse brain specimen embedded in a plastic block at 180MB/s. An entire mouse brain, which typically occupies a volume of ~1cm^3, can be digitized in less than 100hrs. The instrument line samples the tissue at 300 nm sampling resolution at its maximum capability.

2.1.1 Knife-Edge Scanning Microscope

The Knife-Edge Scanning Microscope was designed to image cross sections of whole mouse brains at sub-micrometer resolution. The KESM thus straddles the technology space between imaging techniques which produce ultra-high resolution images of a small volume of brain tissue and techniques which produce low-resolution images of whole brains. The KESM instrument serves the dual purpose of a microtome and a microscope. It can cut slices as thin as 0.5μm from tissue specimens embedded in

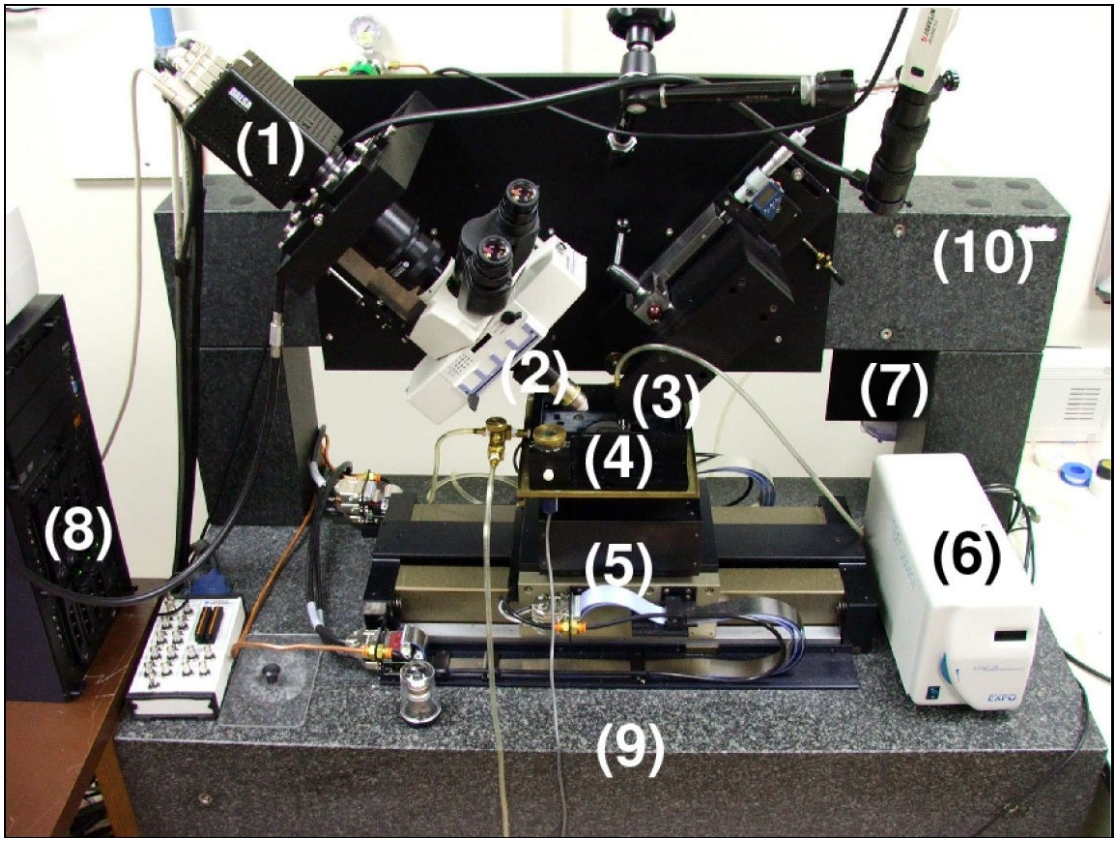

Figure 1. The knife-edge scanning microscope. This figure shows the major components of the KESM instrument: (1) The high-speed line-scan camera, (2) The microscope objective, (3) the diamond knife and light collimator, (4) The specimen tank, (5) The specimen stage with 3 degrees freedom of movement, (6) white-light microscope illuminator, (7) water pump (in the back) for the removal of sectioned tissue, (8) PC server for stage control and image acquisition, (9) granite base, and (10) granite bridge. Adapted from [2], [12]

plastic [2]. The instrument consists of a specimen stage, an illuminator, a diamond knife (the microtome), a microscope, and high-sensitivity line-scan camera (Figure 1) [2][12].

The specimen can be perfused with varying stains and depending on the type of stain used, KESM can image different types of microstructures of the brain tissue: the Golgi stain for neuronal structure, the India ink stain for vasculature, the Nissl stain for

soma. The stained specimen is mounted on a three axis specimen stage and is moved across the diamond knife. The instrument is illustrated in Figure 1 and Figure 2.

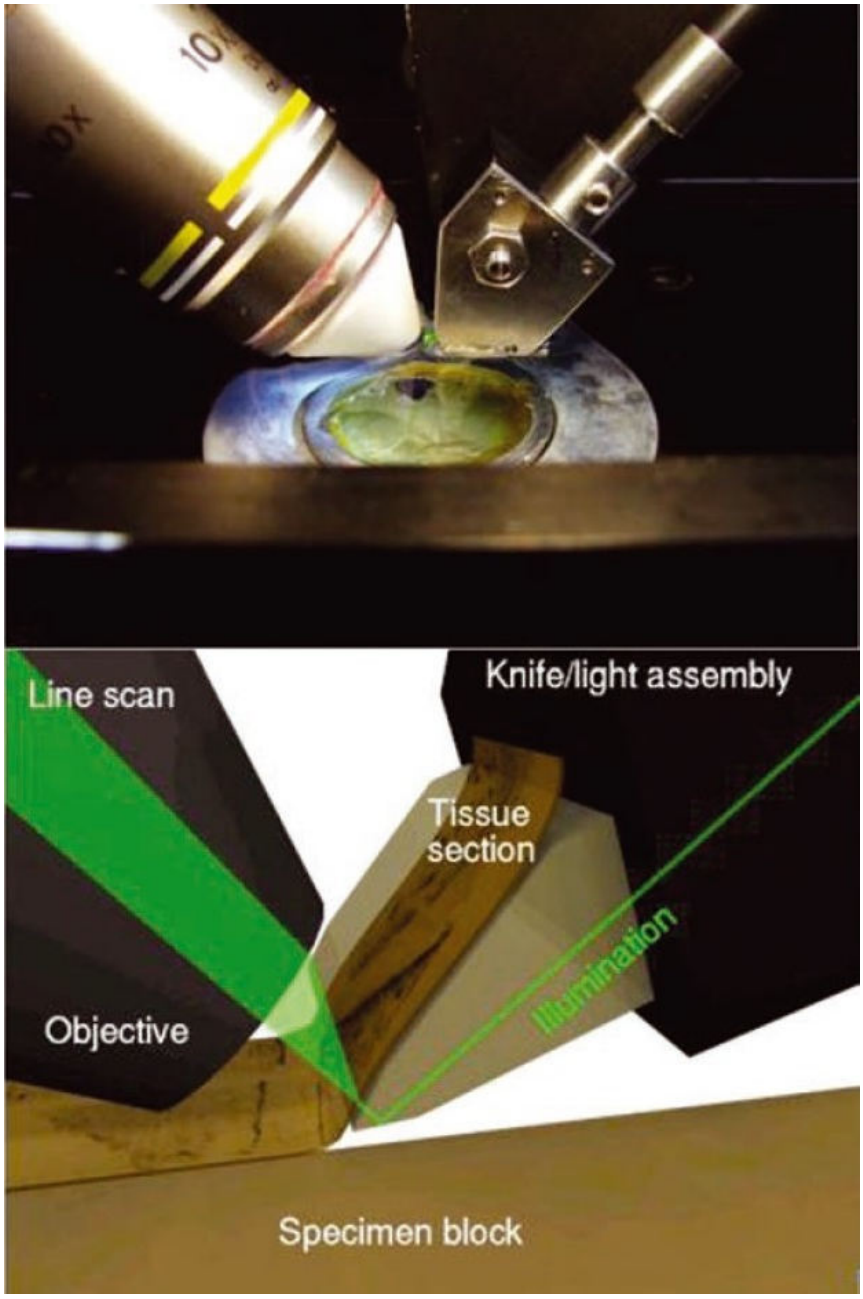

Figure 2. Illustration of tissue sectioning and imaging in KESM. A photograph of the objective, knife and specimen (top), and a cartoon of the light transport through the diamond knife and through the objective for imaging (bottom). Adapted from [2].

This process sections the specimen and the slice slides up the diamond knife which also illuminates the tissue from the rear. The high-sensitivity line scan camera images the tissue as it slides across the tip of the knife. The line scan camera sends the data to two frame-grabber boards. One sweep across the knife results in an image of size 80MB approx.Two frame grabber boards send the data collected to a buffer stored in a computer server [2].

2.1.2 Imaging Vascular Network Using KESM

The KESM instrument can be used to image neurovascular structures by perfusing the brain specimen with India-ink stain. KESM produces high-contrast images at a resolution of 0.6μm × 0.7μm × 1.0μm [7]. Since the images produced are high contrast, they can be easily segmented using thresholds to build a high resolution model [7][15]. A $1cm^3$ specimen requires ≈ 100hrs to image. Figure 3 shows visualization of the vascular networks in the KESM India ink data.

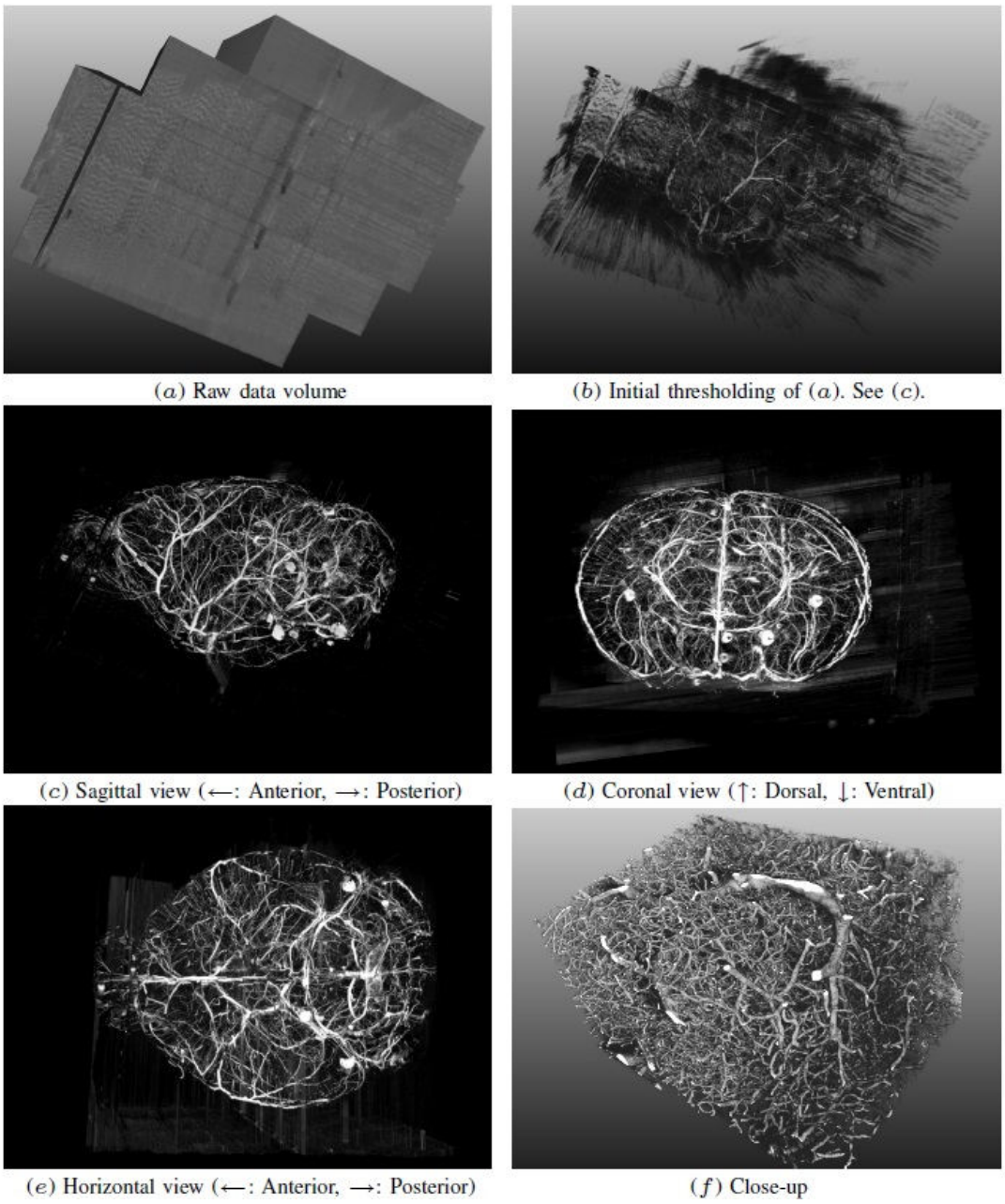

Figure 3. Visualization of the vascular networks in the KESM India ink data. (a) 3D view of raw data in the sagittal plane. (b) A lightly thresholded version of (a). (c)−(e) Fully thresholded versions of (a) but in a different view (∼ 5mm). (f) Close-up of the intricate details (∼ 1.5mm). Adapted from [7], [15]

2.2 Prior Work

2.2.1 Vascular Reconstruction in Mouse Brain Using KESM Data

There has been prior work done to develop techniques to reconstruct the vascular network of mouse brains from images collected by the KESM instrument. Most notably, local maximum intensity projection (MIP) approach to trace the 3-dimensional vascular network from KESM image sets was developed by Han et al. [3, 6]. In this technique, first seed points are selected manually by the user to initiate the tracing. Some of these seed points might not be centered in the vessel. This is corrected geometrically by centering the seed point along both a horizontal and a vertical line segment which touch the edges of the blood vessel [6]. This is illustrated in Figure 4.

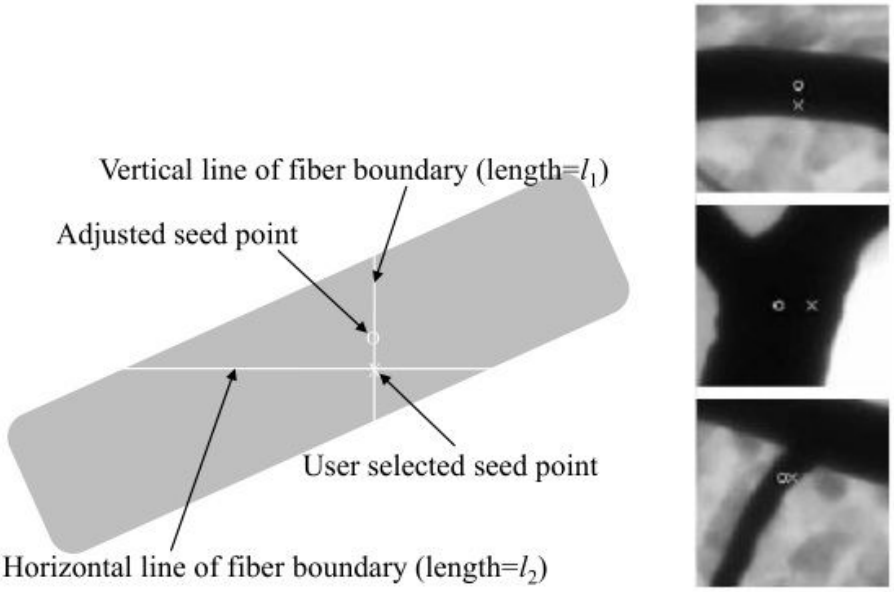

(a) (b)

Figure 4. Centering seed points provided by the user. (a) Centering of selected seed points. (b) Seed point selected in the real image (marked with an 'x') data and the centered seed point (marked with an 'o'). Adapted from [6].

Next, a local volume size centered at the seed point is determined using boundary detection. This is followed with local volume evaluation and local MIP processing. Next the direction of the blood vessel is determined using 2D tracing methods. This allows the 3D vessel direction to be predicted. The vessel direction is then adjusted using a momentum operator.

2.2.2 Vascular Reconstruction in Mouse Brains

In recent years, there has been an increase in research into new imaging as well as reconstruction techniques to study the vascular networks of the mouse brain. In this section I review the current techniques which are used to reconstruct neurovascular networks of the whole mouse brain.

In [16], Xue. et al. describes a methodology to reconstruct the neurovascular network of the whole mouse brain using Maximum Intensity Projection (MIP). The India-ink perfused mouse brain was imaged using a Micro-CT as well as the MOST system. For imaging the brain at high resolution using the MOST system, the brain has to be dehydrated. This shrinks the blood vessels. The MOST images are used in the reconstruction and the reconstructed model is compared with the Micro-CT images (which images the brain in it's normal size and shape) to determine shrinkage. This shrinkage is measured using the affine registration in Amira software. This shrinkage factors are used to recover the diameter of blood vessels from the MOST dataset [16]. The blood vessels in the thalamus were studied using this technique.

2.2.3 Manual Methods

The present manual methods for tracing vascular networks from KESM data involve iterating manually through the image slices and recording the approximate medial points of the cross section of each vessel. This involves a considerable manual labor and is time consuming. Cassot et al. developed algorithms adapted to very large data sets to automatically extract and analyze center lines together with diameters of thousands of brain microvessels from thick sections of india ink-injected human brain, using confocal laser microscopy [17].

CHAPTER III

APPROACH AND METHODS

This chapter elaborates on the methods and processes of my approach. The process involves mainly five steps: image preprocessing, edge detection, region identification, trace extension, branching, and network exploration. These steps are discussed in detail in the following sections.

3.1 Data Acquisition

The KESM instrument has been used to collect different types of whole mouse brain image data depending on the type of stains used. The KESM can scan slices of brain tissue stained with Golgi, India-ink and Nissl stains. India-ink staining technique was used to image the vascular networks of the whole mouse brain for the first time using KESM in 2008 [14].

The full scan of a India-ink-stained mouse brain at a sub-micrometer resolution (0.6 um × 0.7 um × 1.0 um voxel size) is used to trace the cerebro-vascular network of the mouse brain [7] [14]. This data was available from the Brain Networks Laboratory and is being used in this thesis. Figure 5 shows the typical images of vascular structures collected through the KESM instrument.

The vasculature of the whole mouse brain specimen was stained using India Ink perfusion. The specimen is submerged in water to improve the resolution. The specimen was sectioned using the diamond knife and simultaneously imaged by KESM.

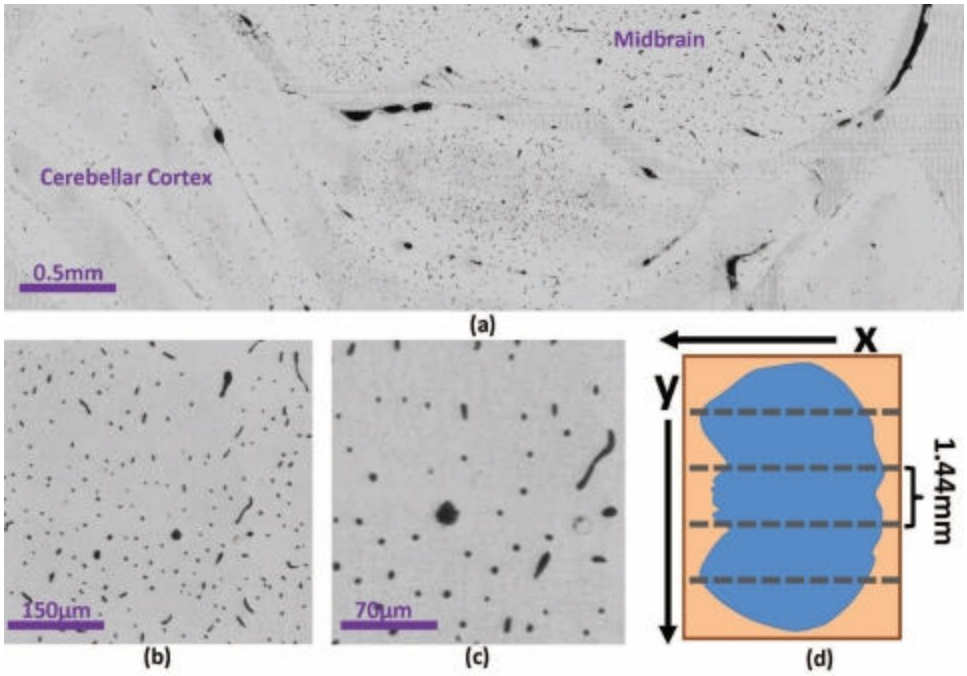

Figure 5. India-ink stained vascular structures imaged using KESM. (a) Single coronal KESM section of the mouse cerebellum and midbrain. (b) 500μm zoomed in view of (a). (c) 200μm view of the same section. (d) A single tissue cross-section at any depth z is composed of several adjacent sections with a width that falls within the objective Field Of View (FOV). Adapted from [7]

3.2 Scikit-image Image Processing Suite

Scikit-image is a suite of image processing algorithms available for the Python programming language. The software tool was written in Python and uses algorithms from the Scikit-image toolkit. It is available free of charge and without restrictions [8].

3.3 Matplotlib

Matplotlib is a python plotting tool which is used in this thesis to present the outputs of the reconstruction as a series of 3-dimensional plots of the traces [20]. The library is written in Python.

3.4 Preprocessing

The first stage of the process to trace vessels from the india-ink stained slices of the mouse brain is to preprocess the data to apply the image processing algorithms like Canny's edge detection algorithms or the watershed algorithms for segmentation. This involves both converting the image to a manageable size and inverting the image. The images were cropped down to 120x100 pixel to enable quick processing. This does not remove any useful information since the algorithm makes sure the cropped image always contains the vessel/vessels that are being traced. Images with irregularities such as long streaks or smears which obfuscate large portions of the image are manually identified and discarded from the KESM data set before the tracing commences.

3.4.1 Identifying Area of Interest

The first step in the preprocessing is to determine an area of interest (AoI), which is a cropped portion of the original image of about 120 pixels × 100 pixels size which completely contains the initial cross section of the vessel as well as regions surrounding it. This reduces the computing costs as subsequent image processing algorithms are applied only to a smaller area of the original image. Henceforth, the AoI of the original KESM image would simply be referred to as the 'image' for convenience.

3.4.2 Image Inversion

The image is then converted to grayscale and then inverted to the negative. Figure 6 shows an original India-Ink stained tissue image obtained by KESM and the

final grayscale, inverted image. It shows a zoomed in original KESM image next to its inverted counterpart. Further algorithms are performed on this resulting inverted image. The grayscale image is an 8-bit per pixel intensity image. The luminous intensity at each pixel is recorded as an 8 bit value.

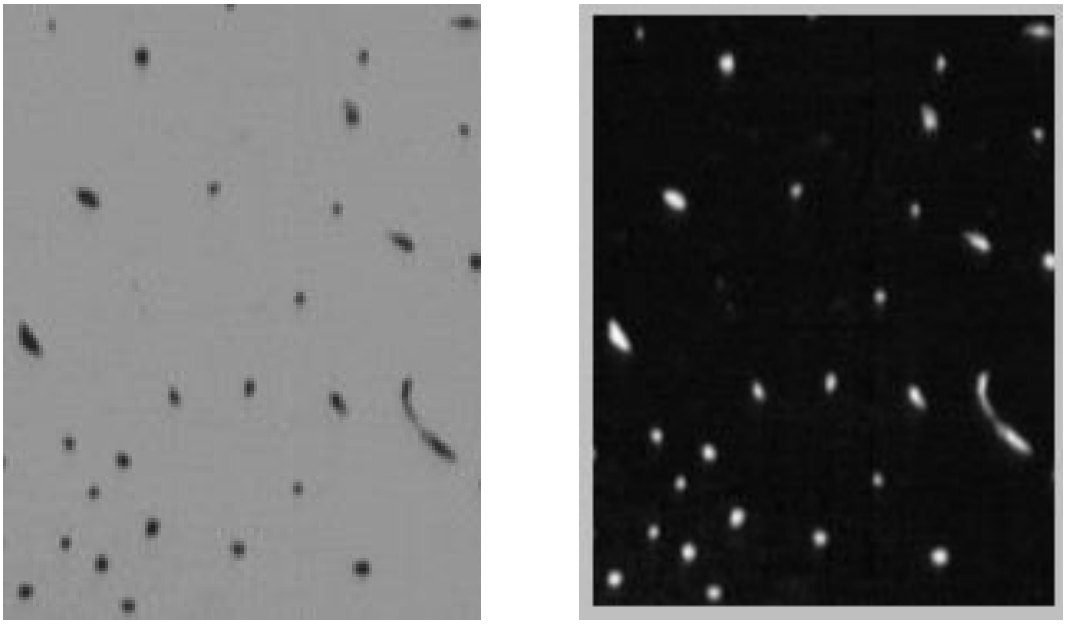

(a) (b)

Figure 6. Inverting image. (a) The original image zoomed in to the AoI, (b) The inverted grayscale image of (a).

3.4.3 Noise Reduction

The next step is to clean up the image using noise reduction algorithms and filters. Several image filtering algorithms and packages are available for this pre-processing step. The Gaussian filter provided by scikit-image is used to blur the image. The 2-dimensional Gaussian filter was used with the standard deviation, $\sigma = 2.0$

for mild smoothing. This smoothed image was then filtered using intensity thresholding filter to further highlight the vessel cross sections in the image. Figure 7 shows the result of noise reduction algorithms on the image. The Gaussian filter was applied as an intermediary step of the Canny edge detection algorithm implemented in the scikit-image suite, which will be described in the next section. In certain cases, a contrast enhancement filter might be necessary for the images. Contrast enhancement brings the features of each image into sharper focus.

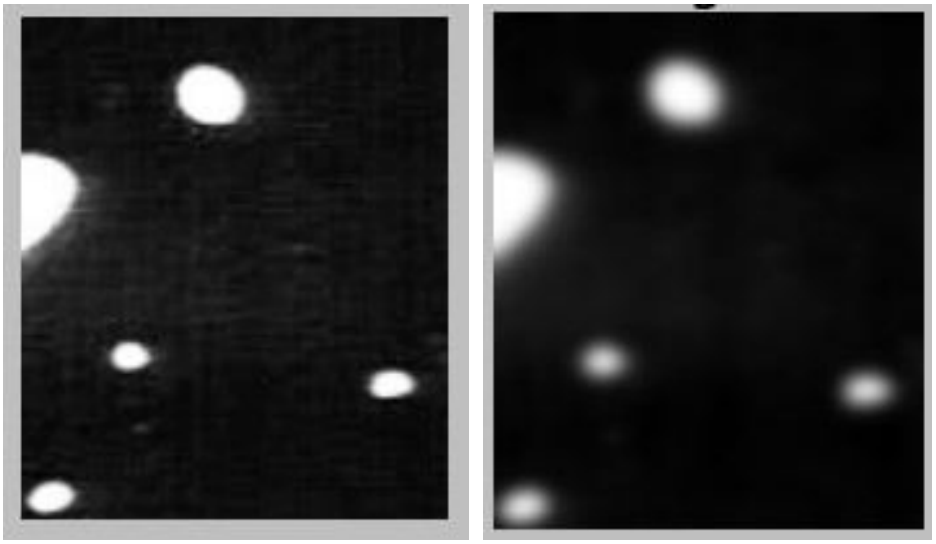

(a) (b)

Figure 7. Gaussian filter. (a) Image after inversion, (b) Image after applying Gaussian filter with $\sigma = 2.0$. The gaussian filter produces a noticeable blurring effect as can be observed from the figure.

3.5 Edge Detection

Once the preprocessing steps are complete, we can apply subsequent algorithms to the cleaned up images. The next step in the tracing was to identify the edges of the

cross section of the vessel in each successive slice. Edges can help identify several useful properties of the image. Edge detection helps identify distinct regions of the image such as the cross sections of individual vessels. It can also help recognize vessels that are about to merge to subsequent slices. Detecting edges helps determine the shape of the cross section, as well as determine if the region is closed or not.

3.5.1 Canny Edge Detection

The edges of the vessels were detected using the Canny edge detection algorithm [4]. The Canny edge detection algorithm implemented in scikit-image suite comes with a built in Gaussian filter. A standard deviation value of $\sigma = 2.0$ for the Gaussian filter gives smoother edges after processing by the Canny algorithm.

These are the steps of the Canny edge detection algorithm:

- Reduce noise in the image using the Gaussian filter.
- Next, the intensity of the edges are determined by computing the gradient at each pixel using Sobel operators. These operators performs 2-dimensional gradient measurement on the image. The Sobel operator uses a pair of 3×3 convolution masks to calculate the gradient along each coordinate axis (see Figure 8). The edge strength at each pixel is approximated by the formula:

$$|G| = |G_x| + |G_y|$$

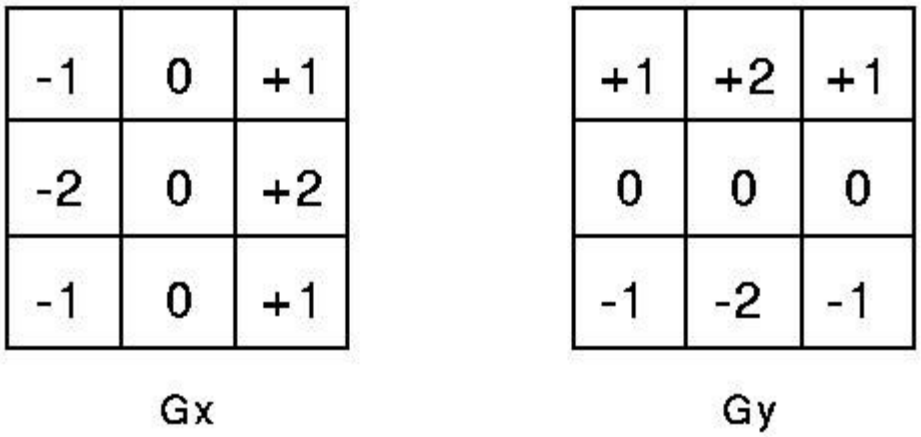

Figure 8. Convolution masks to calculate the gradient along each coordinate axis.

- Next, the edge direction is calculated from G_y & G_x.

$$\theta = \tan^{-1}(|G_y| / |G_x|)$$

Since a pixel has only 8 neighbours, the direction has to be discretized into 4: The horizontal, the vertical, the diagonal and the antidiagonal.

- Once the edge directions are known, thinning of the edges (also called, non-maximum suppression) is done. This traces the edges along the edge direction and suppresses pixels that are not edges.
- Finally perform hysteresis thresholding to eliminate streaks. Hysteresis thresholding further reduces the gradient array. It uses two thresholds, T1 and T2 with T1 < T2. If the magnitude of the pixel is below T1, it is set to zero (a non-edge pixel). If the magnitude is above T2, The gradient array is now further reduced by hysteresis. Hysteresis is used to track along the remaining pixels that have not been suppressed. Hysteresis uses two thresholds and if the magnitude is below the first threshold, it is set to zero (made a non edge). If the magnitude is

above T2, it set to 255 (‘True’ value, or an edge pixel). If the magnitude is between the two thresholds, the pixel is set to zero unless there is a path from this pixel to 8-connected to another pixel with gradient above T2 the high threshold, in which case, it is set to 255 (an edge pixel).

Figure 9 shows the results of the canny edge detection algorithm on a preprocessed image.

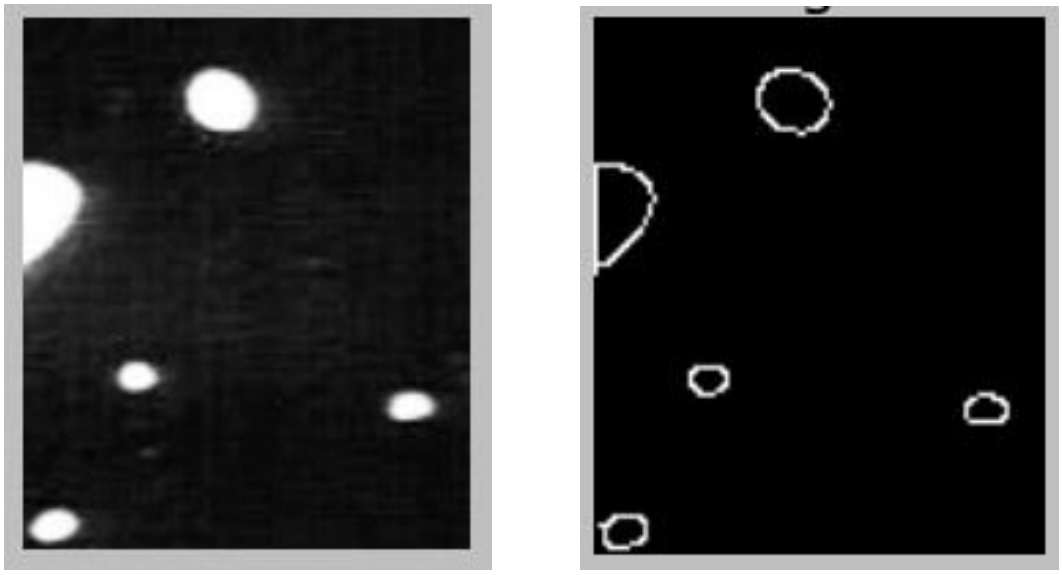

(a) (b)

Figure 9. Edge detection using Canny edge detection algorithm. (a) Original image after inversion, (b) Image after smoothing and noise reduction using Gaussian filter and application of Canny edge detection algorithm.

3.6 Region Detection

The next step is identifying regions corresponding to the cross section of blood vessels in the images. For the purposes of this thesis, a 'region' is defined as the cross section of vascular structures highlighted after the preprocessing and edge detection algorithms are applied. Figure 10 shows 5 regions in the image. Regions are identified using the package skimage.measure.regionprops of the scikit-image suite [9] [10] [11]. The package identifies regions in the image and computes several properties of each region, such as its centroid and area. The centroid will be used in the subsequent steps to trace the vessel. The cross sectional area can be used to approximate the diameter of the vessel. The package also extracts other information about the cross sectional region like the rectangular bounding box which exactly bounds the identified region. The shape of the region also helps determine whether the vessel is about to split or merge with a neighbouring region.

Figure 10. Regions in an image. This figure shows an image with 5 regions. Regions which touch the image boundary are also considered as valid regions.

3.7 Trace Extension

Once regions are identified in a particular slice, the next step is to extrapolate the vessel being traced in previous slices to the current slice. The algorithm can be configured to either ignore or accept regions that touch the image boundary. There is a tradeoff between comprehensive exploration and accuracy in detecting branch events when using this configuration. If the algorithm is configured to ignore regions that touch the image boundary, it would make more accurate branch event detection but would compromise on the exploration of the complete network. If on the other hand, the algorithm is configured to accept regions which touch the image boundary, it would explore the network more comprehensively, but this could lead to less accurate branch event detection. This is because, the algorithm takes into account the area of the region when predicting branch events as discussed in section 3.8.

At any step of the extension, let's assume the previous slice was S^n, and that the current slice being examined is S^{n+1}. Now the trace extension involves matching the region corresponding to the cross section of the vessel in the previous slice, say R^n_i, to a region R^{n+1}_j in the current slice. The centroid of the region R^n_i, say C^n_i, is used as an estimate of the new centroid of the region R^{n+1}_j in the current slice.

Thus C^n_i is an estimate for the actual centroid C^{n+1}_j. We can now compute the actual centroid C^{n+1}_j by determining the region which is closest to the coordinate C^n_i in the image plane of the slice S^{n+1}.

Let $P = (x_0, y_0)$ be a point or pixel coordinate in the image. Then the distance between the region R and the point P is defined as :

distance(R, P) = min sqrt($(x_i - x_0)^2 + (y_i - y_0)^2$) $\quad \forall (x_i, y_i) \in R$

Then, region R_k is defined to be the region closest to the point P in an image if

k = argmin distance(R_k, P)

This identifies a unique region R^{n+1}_j in the current slice S^{n+1} as the next cross section of the vessel in the series of cross sections that make up the vessel. This process is repeated until the vessel terminates or splits or is merged with another vessel.

At the same time this process of extension progresses, the algorithm also keeps track of other regions in the same slice to estimate the trajectories of the vessels and predict any impending splits or merges. In order to track all the regions, information about the regions in the previous slice is also stored and processed to recognize patterns.

Let there be g regions in the slice S^n and h regions in the subsequent slice S^{n+1}. A proximity matrix keeps track of the proximity of each of the g regions in S^n to the h regions in S^{n+1}.

	R^{n+1}_1	R^{n+1}_2	...	R^{n+1}_h
R^n_1	distance(R^n_1, R^{n+1}_1)	distance(R^n_1, R^{n+1}_2)	...	distance(R^n_1, R^{n+1}_h)
...	...	...	...	...
R^n_g	distance(R^n_g, R^{n+1}_1)	distance(R^n_g, R^{n+1}_1)	...	distance(R^n_g, R^{n+1}_h)

Table 1. Table illustrating the proximity matrix.

The proximity matrix is used to match each of the regions in the previous slice S^n to regions in the current slice S^{n+1}. A region R^n_i is matched to a region R^{n+1}_j if and only if

- R^{n+1}_j is the region in the slice S^{n+1} closest to R^n_i.
- R^n_i is the region in the slice S^n closest to R^{n+1}_j.

Note that R^{n+1}_j and R^n_i lie in different slices, hence to determine distances, the regions are reduced to their centroids and the distances are computed between these two points in the 2-dimensional coordinate space. This is a restrictive criteria to match regions in one image to the regions in the subsequent image. Hence it rules out erroneous matches. In certain cases, this would obviously result in either of two scenarios:

1. A few of the regions from S^n not being matched to any region in S^{n+1}. This would imply one of the following events:
    a. The vessel has terminated at a vessel tip.
    b. The vessel has moved out of the field of the image.
    c. The vessel has merged with another vessel and the new combined vessel has a cross section in S^{n+1}.
2. The converse, where a few of the regions from S^{n+1} not being matched to any region in S^n. This would imply one of the following events:
    a. These unmatched region correspond to a new vessel taking shape (This particular region was the cross section of the tip of a new vessel).
    b. A new vessel has entered from outside the image boundary.
    c. A vessel from the previous slice has split into two vessels. S^n has the region corresponding to the original parent vessel while S^{n+1} has the

regions corresponding to the child vessels which sprouted from the parent vessel.

The vessel can be thus be extended through the series of slices and can be split into sub-branches based on the characteristics of its cross sectional region in each slice. The exploration can progress in the direction of extension of the trace. This means that the exploration can proceed in either direction of the z-axis for a given vessel, assuming the s axis lies perpendicular to each slice.

3.8 Branching

One of the crucial steps in the reconstruction is identifying branching events in the vascular network. As noted in the previous section, one way this can be accomplished is by tracking all the regions from slice to slice. Another is using heuristics about region features to detect branching events. This section discusses different types of branching including i) Vessel bifurcation, ii) Vessel fusion iii) Oblique fusion of multiple vessels. This section also describes how each type of branching event is detected and then validated.

3.8.1 Vessel Bifurcation

Splitting of vessels is usually one of the branching events which is easier to determine. Figure 11 below shows the sequence of slices which illustrates how a vessel splits into two.

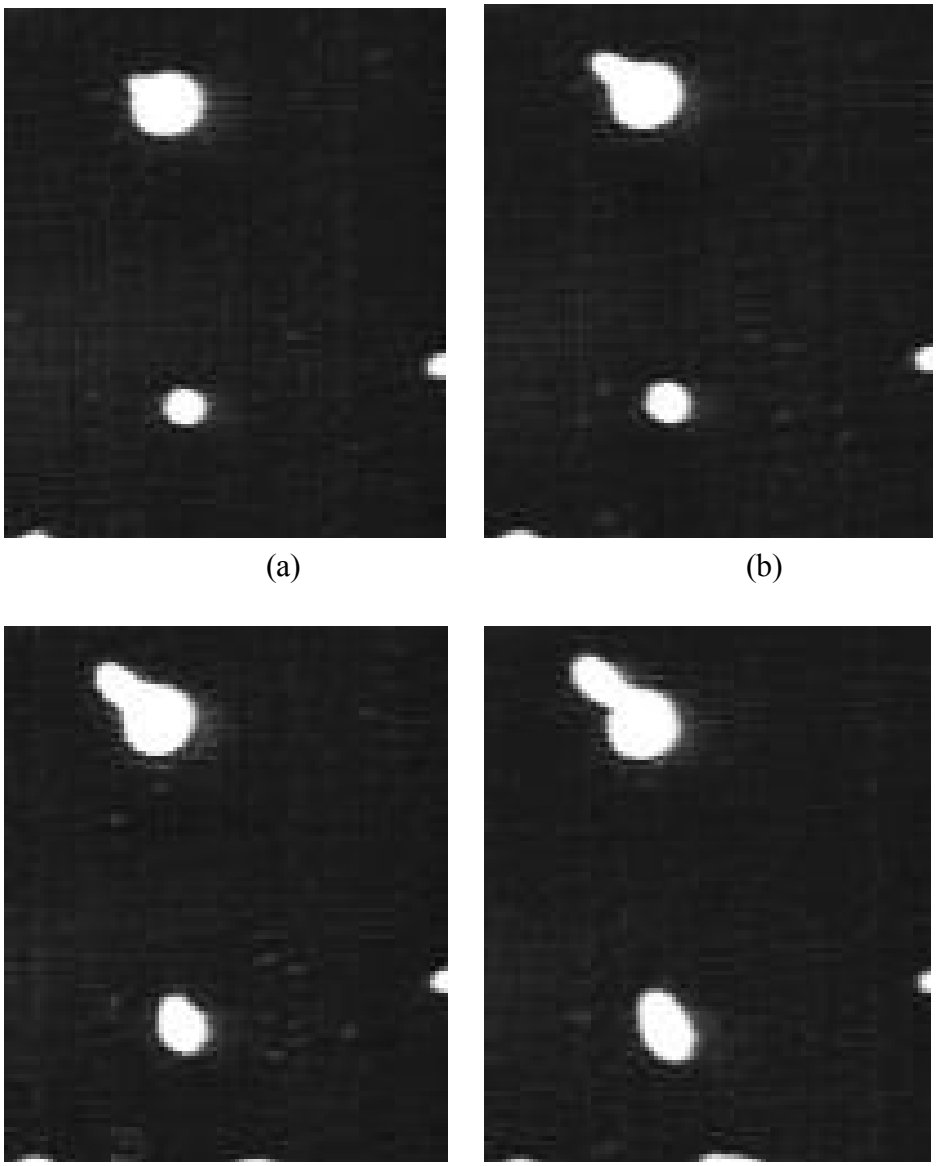

(a) (b)

(c) (d)

Figure 11. Vessel bifurcation. In the series of images (a-f) above, the vessel, whose cross section is visible at the top of each image, splits into two over the course of 6 images.

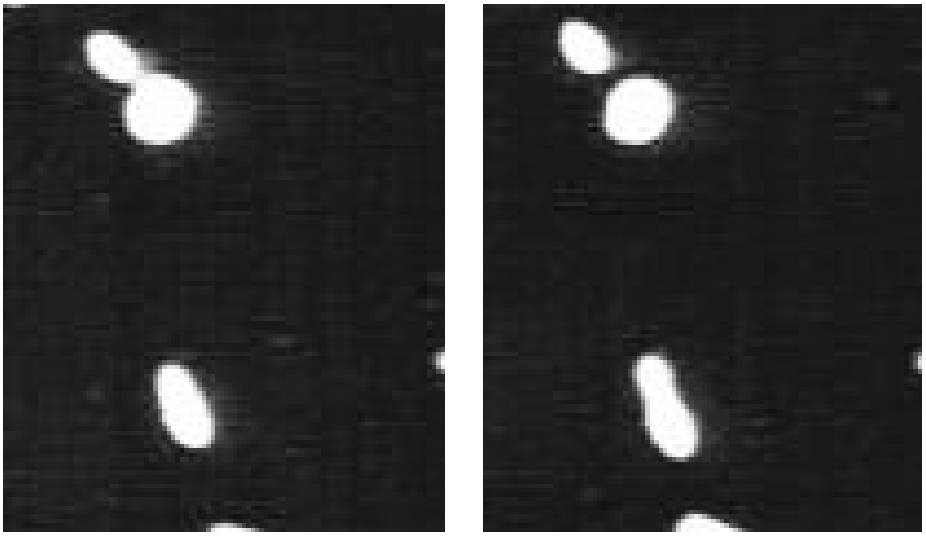

(e) (f)

Figure 11 Continued.

As is clear from Figure 11 (e) & (f), the vessel has split into two. The region from the first slice has split into two in the second slice. In the Figure 12 below, it is clear how the centroids of the regions move as the corresponding vessels split into two.

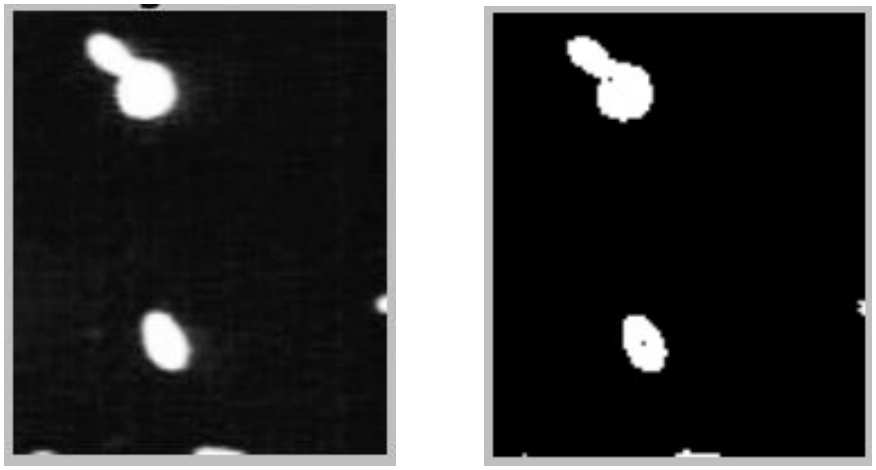

(a) (b)

Figure 12. Vessel bifurcation showing the movement of centroids. (a), (c), (e) are the original images which show the gradual split in the blood vessel. (b), (d), (f) show the filtered images with the centroid of each region marked with a black pixel.

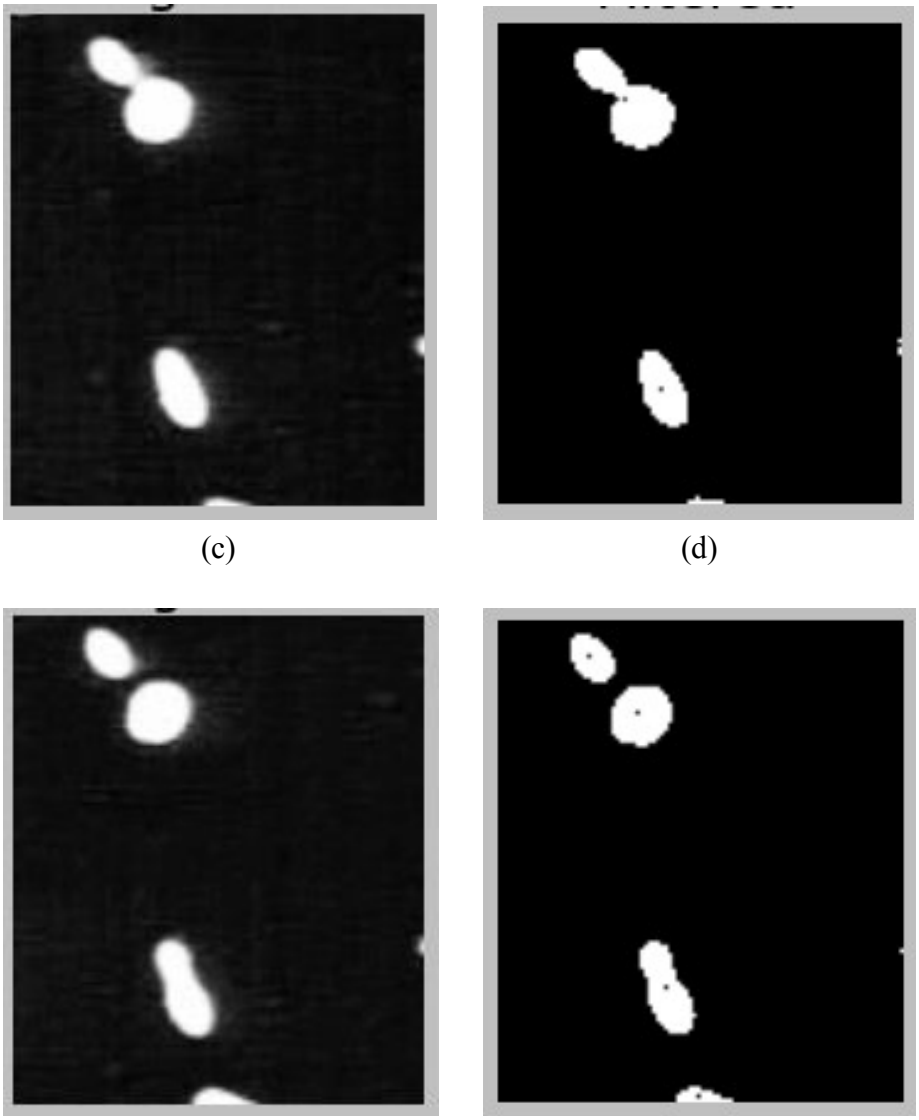

(c) (d)

(e) (f)

Figure 12 Continued.

The first step in recording the bifurcation is to detect that the vessel has split. This is done using a combination of heuristics and image segmentation using the watershed algorithm.

3.8.1.1 Heuristics for Vessel Bifurcation

To recognize that the vessel has split, we can use knowledge of the average cross sectional area of the vessel before the split. Since we already keep track of the area of the cross section of the vessel in each slice, we can compute the average area of cross section of the vessel as reconstruction of the vessel progresses. However, since the vessel can arbitrarily expand or constrict along its length, and also increases in cross sectional area immediately before the split, it is appropriate to weight the cross sections that are recent and discount the areas that are not so recent. Hence, I keep a running weighted average of the cross sectional areas. I use a weight of 0.1 to compute the average.

Let A^n_i be the area of the region R^n_i for a the vessel being traced. Let n = 0 for the first cross sectional region of the vessel. Then the recursive equation for the running weighted average is given by:

$$\overline{area}_0 = A^0_i$$

$$\overline{area}_n = (A^n_i + 0.1 \times \overline{area}_{n-1} \times n)/(n+1)$$

At each slice we compute $\overline{area}_n$, and compare it with $\overline{area}_{n-1}$.

$$\Delta\overline{area} = (\overline{area}_n - \overline{area}_{n-1})/\overline{area}_{n-1}$$

As a vessel is about to split, the cross section of the vessel would gradually increase in area and finally when the vessel splits, the area of the cross section of the vessel would decrease dramatically. This feature of the series if used as a heuristic to predict when a vessel is likely to have split. If $\Delta\overline{area} <= -\text{threshold}_{detection}$, the vessel is

predicted to have split. The threshold value $threshold_{detection}$ is configurable by the user. An appropriate value for the threshold which was used in experiments was 0.30. $threshold_{detection}$ should be a positive value and henve -$threshold_{detection}$would be a negative value since the cross sectional area of the vessel decreases slightly when the vessel splits. The smaller the value of this threshold, the more liberal the prediction of branches which would mean higher the misprediction rate and more costly computations for the watershed algorithm outlined in the next sub-section. The higher the value, the more conservative the predictions, and higher is the rate of non-detection of branch events. The threshold proportion of 0.30 is the average proportion of change in area when a region splits into two for the sample dataset that was used. This is a conservative estimate of how much area a region would lose after splitting. Next, this prediction needs to be corroborated. Once a bifurcation is predicted, the next step is to validate the prediction. I use the watershed algorithm to validate the prediction.

3.8.1.2 Watershed Algorithm

The watershed algorithm is used to segment images and separate overlapping features in an image [13]. I use the watershed algorithm to confirm the prediction from the previous step. The watershed algorithm can be applied to the last slice where the

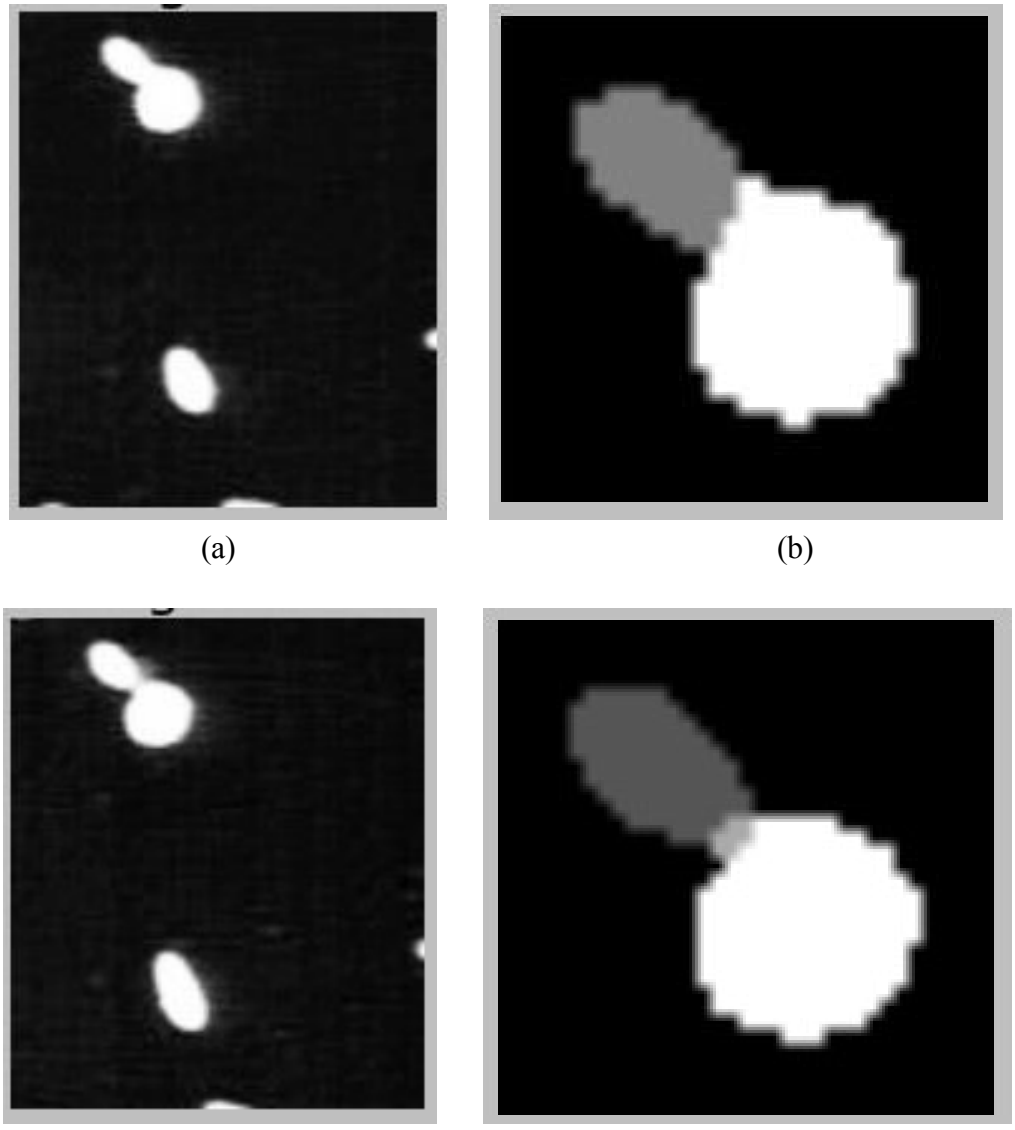

(a) (b)

(c) (d)

Figure 13. Application of watershed algorithm. (a-b) Slice S^n showing a vessel in the cusp of bifurcation/splitting. (c-d) Slice S^{n+1} showing the vessel immediately after bifurcation. (a) Original image of slice S^n, (b) image after the application of the watershed algorithm to (a) on the region being traced. It clearly shows two distinct sub-regions within the region which indicates a vessel about to be split. (c) Original image of slice S^{n+1}, (d) image after the application of the watershed algorithm to (c) on the region being traced.

vessel was confirmed to be still whole. Hence the watershed algorithm is applied to the region R^n_i in the slice S^n. This produces distinct watershed segmentations that indicates the presence of two sub-regions in the image. Figure 13 illustrates this.

Using the watershed algorithm to analyse the region R^n_i corresponding to the cross section of the vessel immediately before the split, it becomes clear there are two sub-regions within it. Centroids for these sub-regions can be computed and used to trace the child vessel in the next slice. The watershed algorithm is also used to validate the prediction of a split by the weighted average area method outlined in section 3.8.1.1. If the algorithm reveals two overlapping sub-regions in the region R^n_i, then the prediction by weighted average area method is validated.

If the watershed algorithm confirms the prediction of the branch event, the next step is to determine the correct two regions R^{n+1}_j and R^{n+1}_k which are the first cross sectional regions of the two child vessels.

3.8.1.3 Region Proximity Method

One method to correctly identify the two new regions (which are the result of the split of the region from the previous slice) out of the many regions in the current slice is using the proximity matrix. At the event of the branching, say between slice S^n and S^{n+1}, the region R^n_i of S^n splits into regions R^{n+1}_j & R^{n+1}_k in S^{n+1}. The region R^n_i would be matched to one of the regions R^{n+1}_j or R^{n+1}_k using the proximity matrix. Let us assume that region is R^{n+1}_j. Now to positively identify R^{n+1}_k as the new region, I analyse all the regions in S^{n+1} and order them in the non-increasing order of distance of their centroids

from the centroid of R^n_i. Here again, the user can configure the algorithm's behavior. The user can specify a distance threshold $threshold_{search}$. Only regions whose distances from the centroid of R^n_i is at most $threshold_{search}$ is evaluated as candidate regions. Among this ordered list, the region closest to the centroid of R^n_i is set as R^{n+1}_j, and the following regions in the list are evaluated using the Area Validation criterion outlined in the next section. The first region to meet this criterion is set as R^{n+1}_k.

3.8.1.4 Area Validation

For each set of regions being evaluated in the previous section Area Validation is run to test whether the two regions could be the cross sections of the succeeding child vessels. The area validation criterion is expressed below:

$$|A^n_i - A^{n+1}_j - A^{n+1}_k| / A^n_i <= threshold_{validation}$$

The proportional difference in areas of the three regions should be less than $threshold_{validation}$, which is again set by the user. The first pair of regions R^{n+1}_j and R^{n+1}_k which meet this criterion is set as the first cross sectional regions of the two child vessels.

3.8.2 Vessel Fusion

Merging vessels involve the same process as a split, except in the reverse direction, hence merging of vessels is handled by the exact same procedures as for splitting vessels. Since the algorithm is direction-agnostic, with respect to the series of slices, it can trace a vessel in either direction along the z-axis. The procedure to detect the merging of two vessels is similar to the procedure to detect a split in a single vessel.

If a region R^n_i from slice S^n cannot be matched to any region in S^{n+1}, then it indicates a potential merging of adjacent vessels. This prediction is confirmed by using the watershed algorithm, and the new vessel cross sections are correctly identified using the proximity matrix method described in the previous section. Suppose the vessel being traced has a region R^n_i in slice S^n and another vessel has region R^n_j in the same slice. Let these vessels merge into the region R^{n+1}_k in slice S^{n+1}. R^{n+1}_k is identified readily using the proximity matrix method, and we already know the region R^n_i. Hence the only variable to be identified is the region R^n_j. The changes in the various steps described for Vessel Bifurcation is outlined below:

3.8.2.1 Heuristics for Vessel Fusion

The heuristic for vessel fusion is exactly the same as for vessel bifurcation except that the proportional change in cross sectional area would be positive since there is an increase in the cross sectional area when a vessel merges with another. Hence,

$\Delta\overline{area} <= + \text{threshold}_{\text{detection}}$

is the condition being evaluated. The same threshold ($\text{threshold}_{\text{detection}}$) which was used for vessel bifurcation is used here for symmetry.

3.8.2.2 Watershed Algorithm

As in the case of vessel bifurcation, the watershed algorithm is used to confirm the prediction from the heuristic condition. The watershed algorithm is applied to the

region R^{n+1}_k to segment it. If the output reveals two distinct segments, then the prediction from the heuristic is confirmed.

3.8.2.3 Region Proximity Method

The algorithm has to correctly identify the region R^n_j from amongst the regions in slice S^n. This is again similar to the method outlined for vessel bifurcation. The regions in S^n are ordered in order of non-decreasing distance to the centroid of the region R^n_i. Each region is then evaluated using the Area Validation criterion.

3.8.2.4 Area Validation

The area validation criterion for vessel fusion is similar to the criterion used for vessel bifurcation.

$|A^{n+1}_k - A^n_i - A^n_j| / (A^n_i + A^n_j) <= \text{threshold}_{\text{validation}}$

The proportional difference in areas of the three regions should be less than $\text{threshold}_{\text{validation}}$, which is the same parameter used in vessel bifurcation. The first pair of regions R^n_i and R^n_j which meet this criterion is are set as the last cross sectional regions of the two merging vessels.

3.8.3 Oblique Merge

The oblique merge event occurs in the image sequence when the vessel being tracked does a double turn along the z-axis within the span of a handful of images, typically 4-6 images. In this branching event a region bifurcates into two new regions in

a given slice and in the subsequent slice, one of these new regions fuses with another region. This is best illustrated through an example. Figure 14 illustrates the changes that the regions involved undergo during the course of an oblique merge.

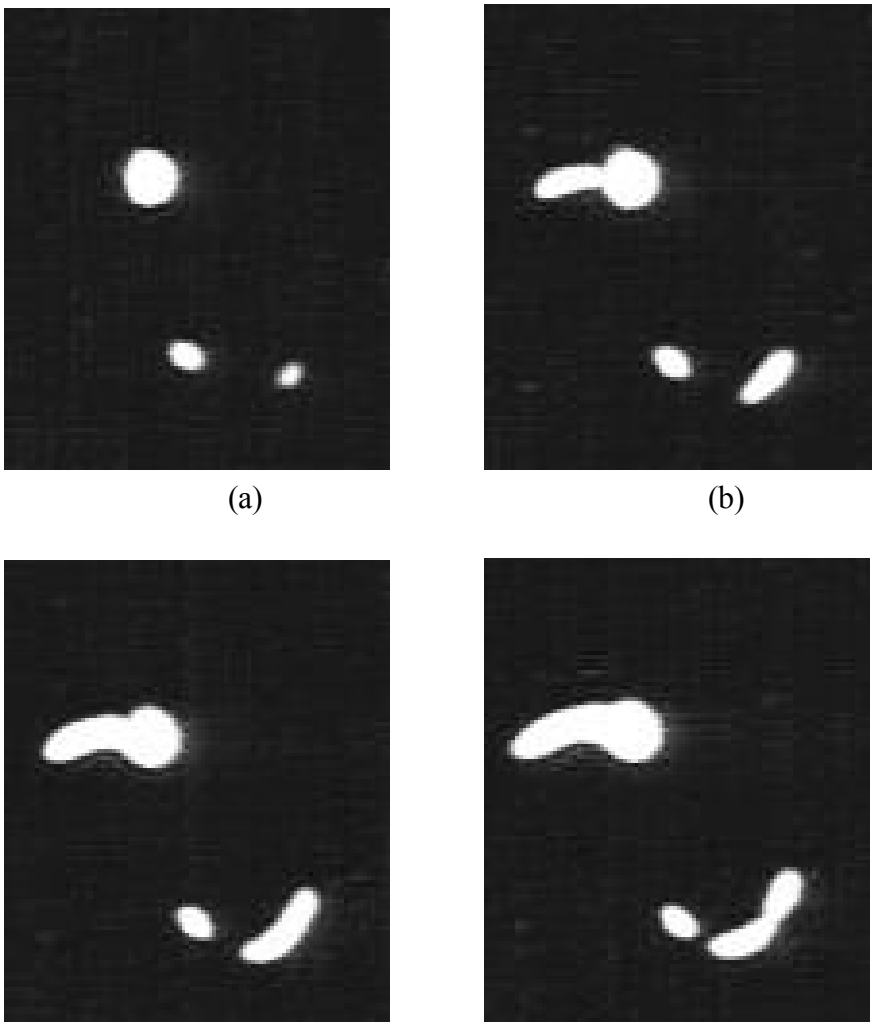

(a) (b)

(c) (d)

Figure 14. Images showing the oblique merge. (a) through (i) illustrate how the oblique merge of vessels happens. The vessels being tracked is the group of vessels in the lower right quadrant of the images. The critical events occur in (d) & (e) where a portion of the region on the right splits off in (d) and merges with the region on the left in (e).

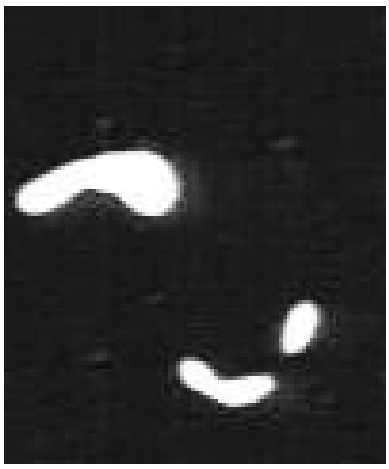

(e)

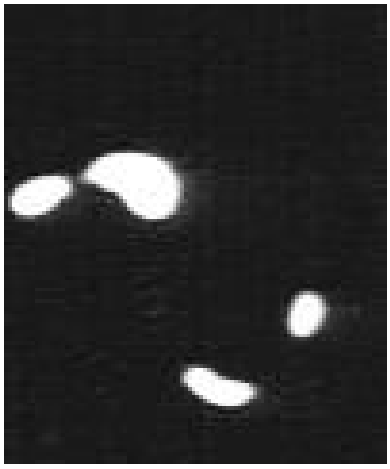

(f)

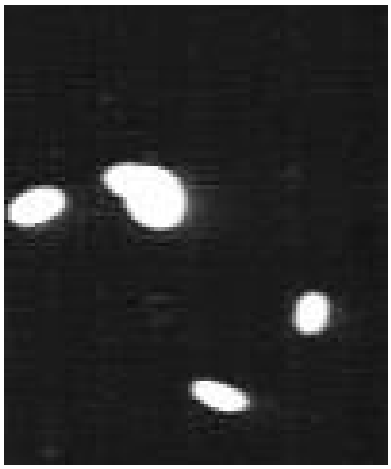

(g)

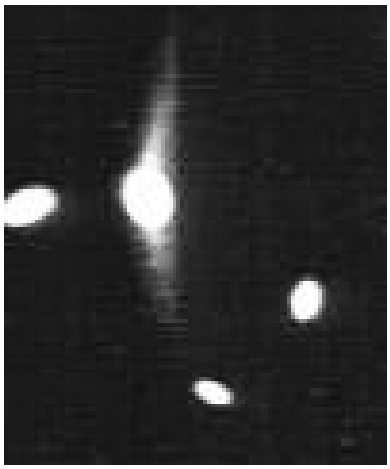

(h)

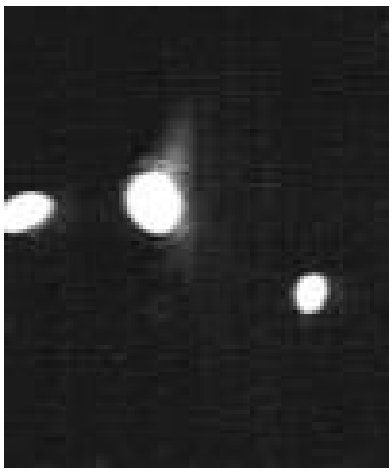

(i)

Figure 14 Continued.

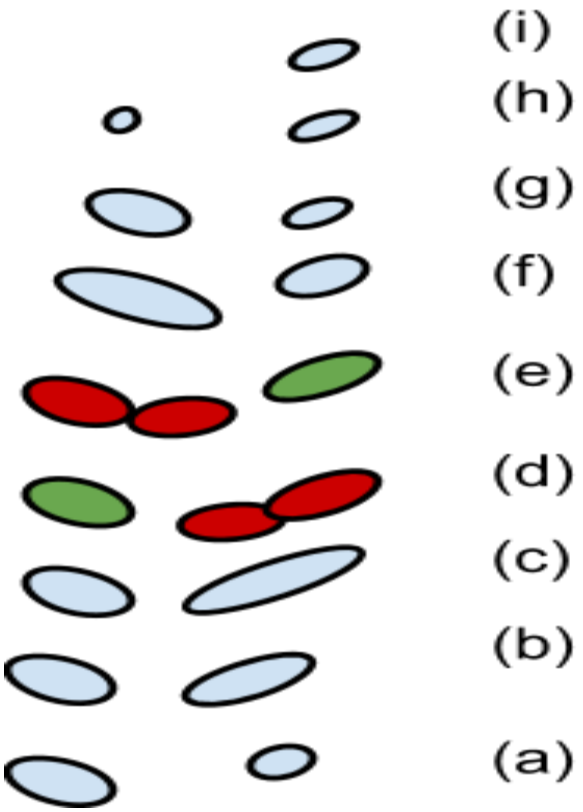

Figure 15. Illustration of the oblique merge. In the image above, only the cross sectional regions of interest from Figure 14. are shown.

As is clear from the Figure 15. above, this is nothing more than the vessel doing a double U-turn along the z-axis. It can be identified by isolating the regions indicated in red in the figure. Here a vessel that appears to split into two has one of its child regions merged into another region in the subsequent slice. This type of vessel movement would actually result in the algorithm splitting the vessel into two parts: The first segment ends in the first reversal, the second segment begins at the second reversal. Here we need to track only the local changes in the region structure. We do not need to have a global contextual knowledge of the vessel movement.

3.9 Vascular Network Exploration

The vascular network exploration step builds on top of trace exploration described in previous sections. As vessel exploration progresses and branching is documented, the alternative vessel routes are added to a priority queue data structure of vessels to be explored. This subsequent exploration is performed in multiple ways:

- A breadth first exploration of the vascular network using a queue data structure.
- A depth first exploration of the network using a stack data structure.
- User-guided exploration, where the user is presented with choices of vessels to explore.

Each vessel can be tracked between points of branching. The points of branching are identified as nodes of a graph and the vessel themselves as the edges. This mapping of the vascular network to a graph is a useful abstraction which renders the network suitable to the application of graph theoretic algorithms by subsequent processing tools.

CHAPTER IV

RESULTS AND ANALYSIS

In the first part of this chapter, I present the results of the reconstruction performed on the India-ink datasets from the KESM instrument. In the second part of this chapter, I compare the accuracy and efficiency of the results of the methodology outlined in this thesis with the results of reconstruction performed manually and from synthetic data.

Reconstruction was performed using the algorithm on a subset of images from the data set, comprising of a collection of 273 grayscale images of size 120 × 100 pixels. This section also measures the accuracy of branches detected.

4.1 Results

The reconstruction methodology presented in chapter 3 was tested on a sample data set of 273 grayscale images numbered from 03941_0_74_62.jpg.gif through 04215_0_74_62.jpg.gif. Images in this collection were already inverted to their negatives. The KESM instrument cannot reimage a section to rectify errors or irregularities. Hence, as mentioned in the section on preprocessing, images with extensive irregularities like long, obscuring streaks were manually identified and removed from the collection before preprocessing of images began. Four adjacent images images were removed from the original collection of 273 images. Hence about

1.46% of the original images had to be discarded. The removed images are shown in Figure 16 below.

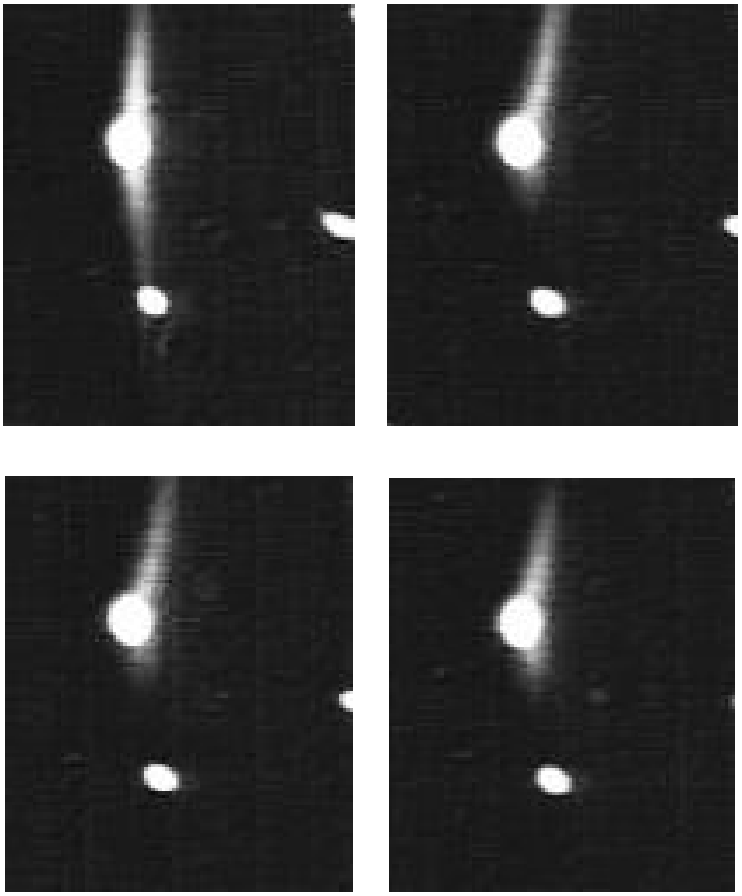

Figure 16. Images removed from data set. Examples of images that were manually identified and removed due to the presence of abnormalities in the image. These images exhibit unusual streaks which render them unusable.

Several different test cases were used to evaluate the reconstruction. The results of these exploration is presented below. The reconstruction was performed using breadth first exploration. Vessels were explored in both directions along the z-axis. The reconstructed vessel coordinates were superimposed on image overlays of the KESM

data using the software Paraview [18]. These series of image overlays are also presented in this section. The image stack used by Paraview was generated from the KESM image sequence using another software called ImageJ [19].

4.1.1 Experiment 1

The seed point (22.0, 45.0) was selected from Slice No: 1 of the data set. The vascular network associated with this seed point was explored in full. The topology of the vascular network which was reconstructed is described in Figure 17 below. There were four recorded vessel bifurcations and five instances where the vessel being explored went out of the scope of the image boundary. The reconstruction shows that the vessels that were fully explored (from beginning to end, without the vessel going out of scope of the image) spanned on average 23 slices.

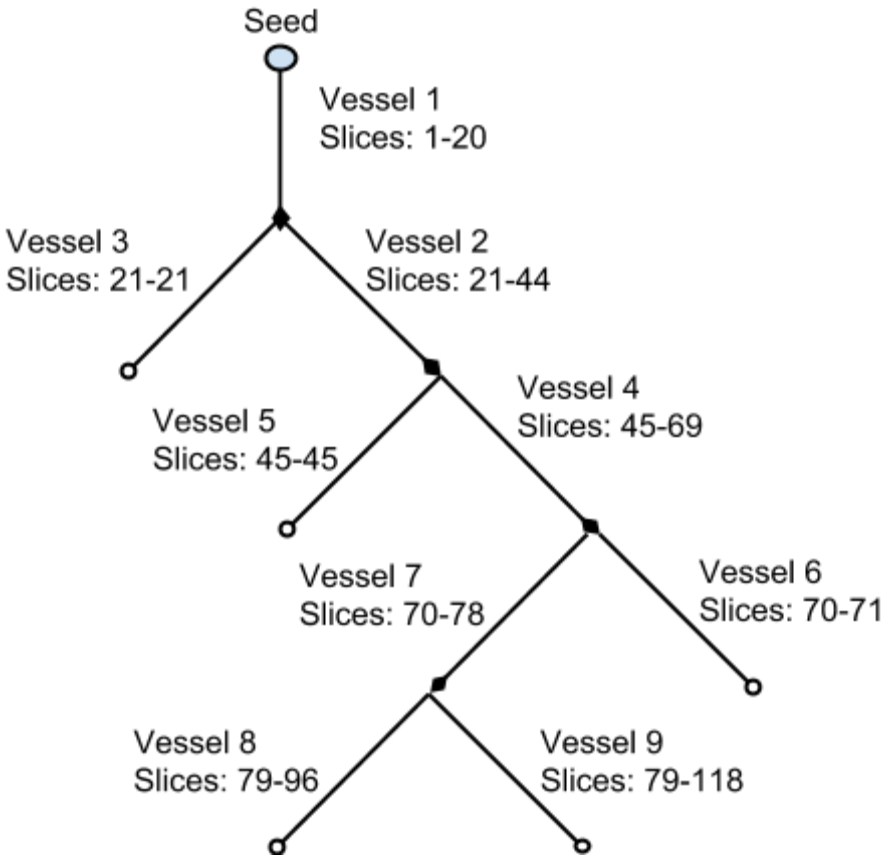

Figure 17. Topology of the vascular network for experiment 1.

The reconstruction of this network in Figure 18. shows the various branches of the network plotted in 3-dimensional space. There are multiple splits along the length of the main branch. This was a simple case since there are only branch bifurcation events in this network. In the following cases, the algorithm is used to reconstruct more complex networks.

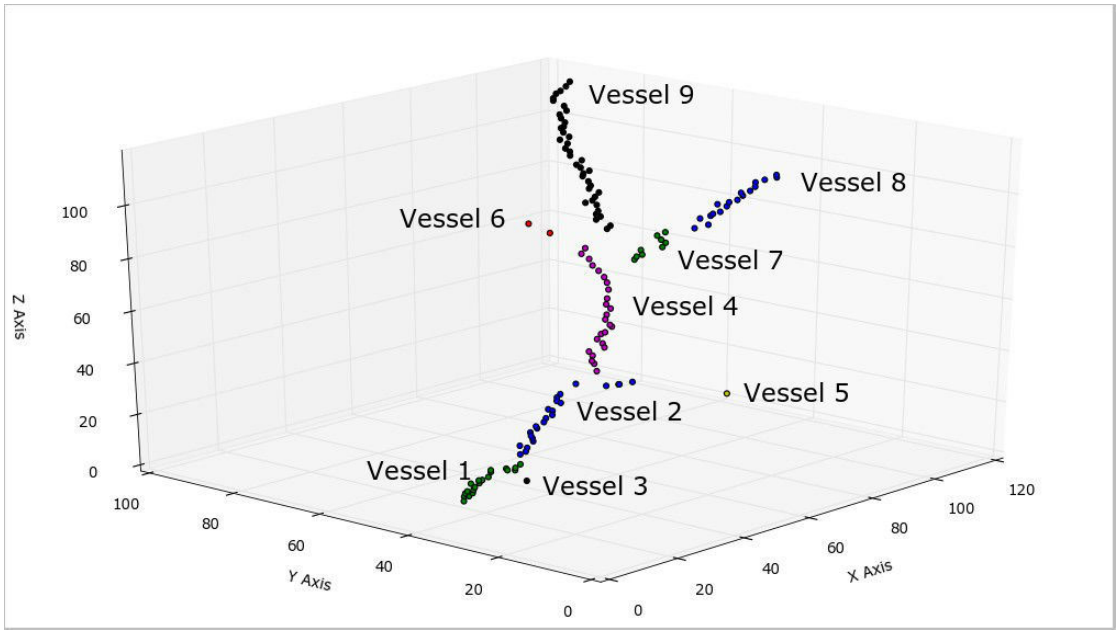

Figure 18. Trace of vascular network for experiment 1, plotted in 3-dimensional space. Each segment of a vessel between distinct branching points is colored in a different color.

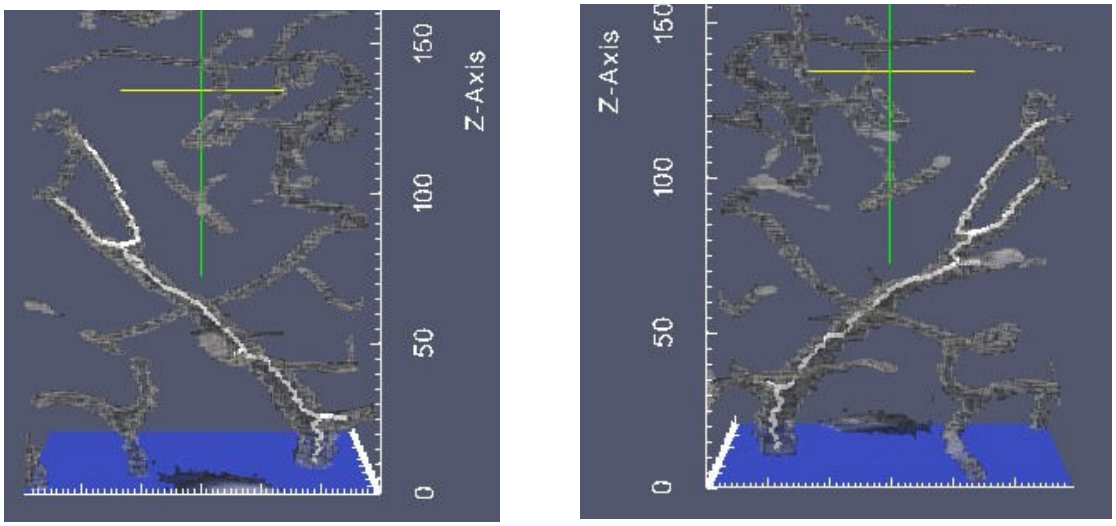

(a) (b)

Figure 19. Image overlays for experiment 1. Viewed along (a) the positive X-axis, (b) the negative X-axis, (c) the positive Y-axis, (d) the negative Y-axis.

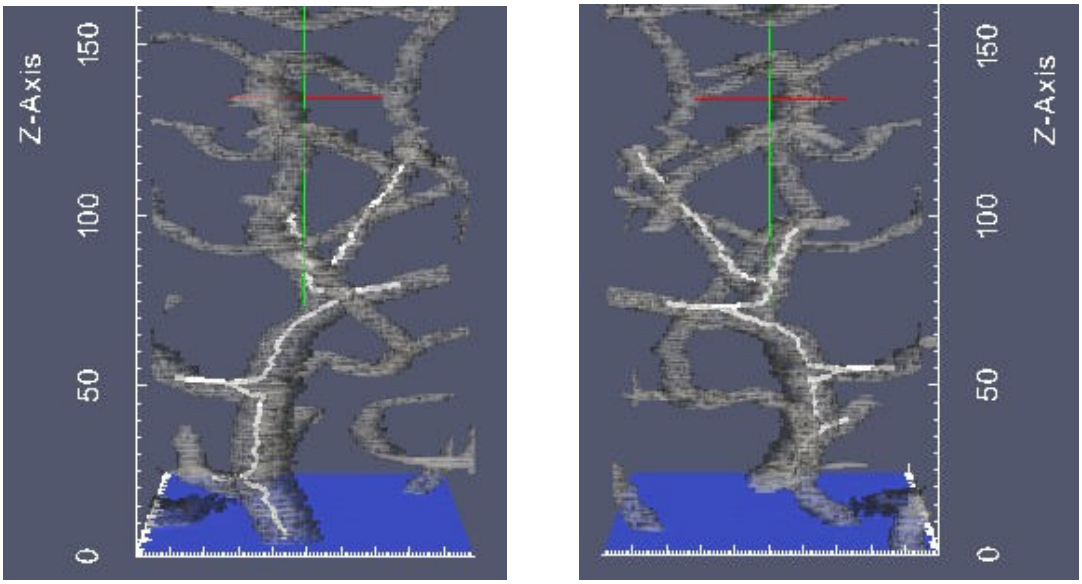

(c) (d)

Figure 19 Continued.

Figure 19 shows the image overlay (obtained through Paraview [18]) of the raw data and volume on the reconstruction. The image overlays show that, since the algorithm was configured to ignore regions that touch the image boundary, the tips of the vessels 3, 5, 6, 8 and 9 could not be explored completely. The reconstruction report is available in the Appendix.

4.1.2 Experiment 2

The seed point (81.0, 25.0) was selected from Slice No: 1 of the data set. This vascular network comprised of fewer vessels than the previous test case. The network associated with this seed point was also explored in full. The network topology is illustrated in the Figure 20. There was a single vessel bifurcation, a single recorded oblique merge, a single merge, one instance where the vessel being explored went out of

the boundary of the image, and two instances where the vessel being explored terminated normally at a vessel tip.

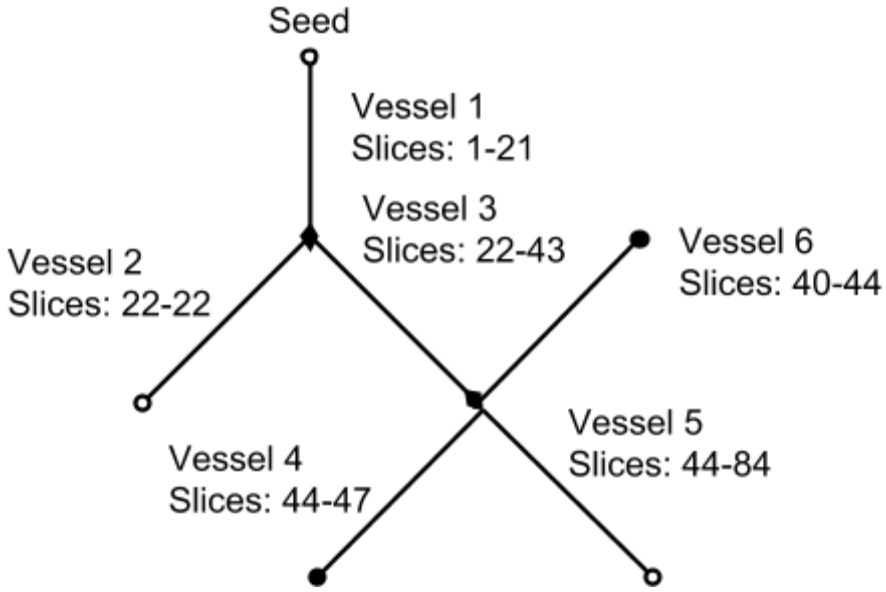

Figure 20. Topology of the vascular network for experiment 2.

The reconstruction report is available in the Appendix. The reconstruction of this network in Figure 21 shows the various branches of the network plotted in 3-dimensional space. One interesting feature of this exploration was the unusual termination of Vessel 6. The software marks the vessel as having terminated by merging with another vessel. This can be verified to be indeed the case. However, the resulting child vessel as well as the second parent vessel is not explored by the algorithm. This is a consequence of the special nature of these two vessels. Both of the unexplored vessels happen to touch the edge of the image boundary which are ignored by the algorithm.

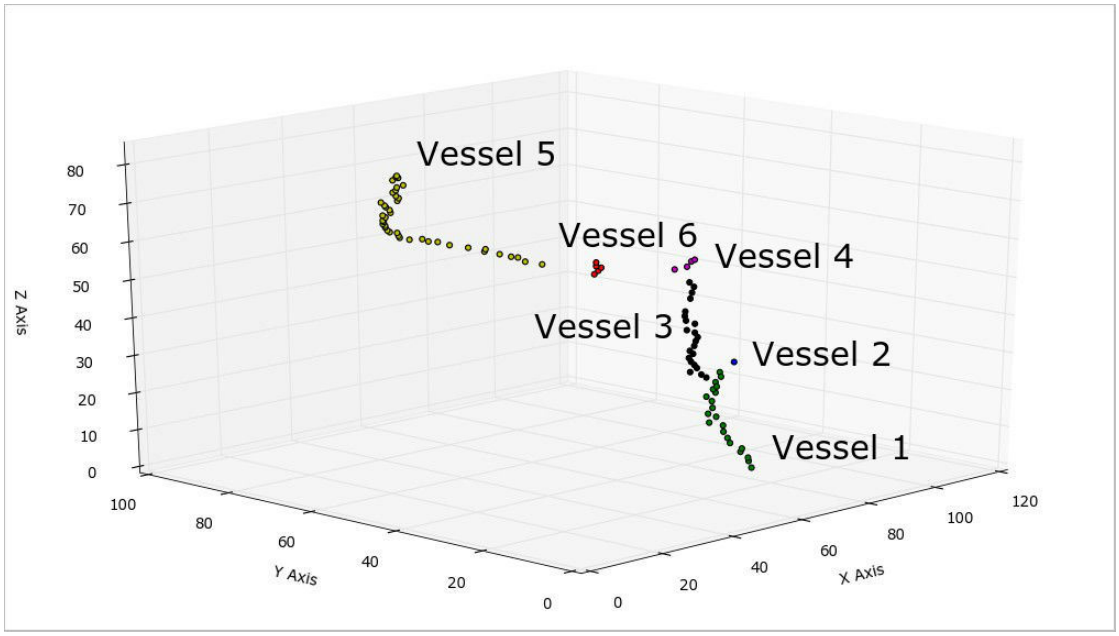

Figure 21. Trace of vascular network for experiment 2, plotted in 3-dimensional space. Each segment of a vessel between distinct branching points is colored in a different color.

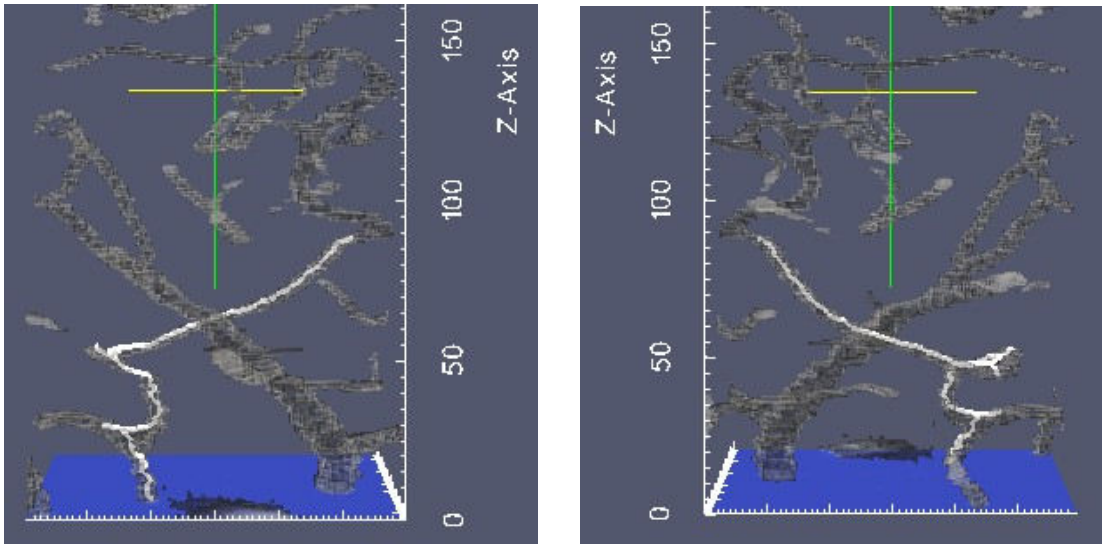

(a) (b)

Figure 22. Image overlays for experiment 2 (Variant 1). Viewed along (a) the positive X-axis, (b) the negative X-axis, (c) the positive Y-axis, (d) the negative Y-axis. The algorithm was configured to ignore regions that graze the image boundaries.

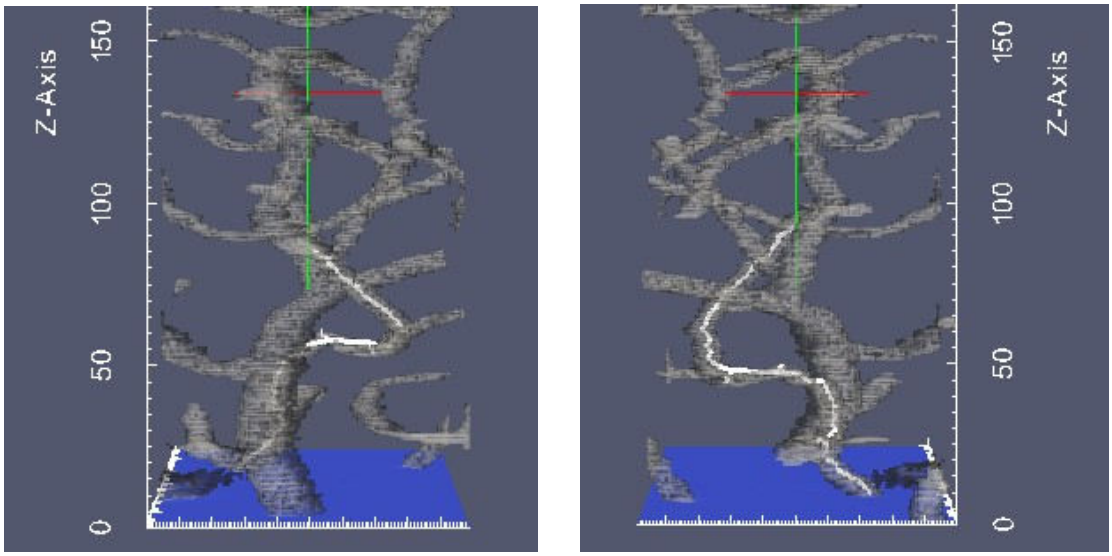

(c) (d)

Figure 22 Continued.

From the image overlays in Figure 22, it can be seen that the network was not completely explored since the algorithm ignored regions that grazed the image boundary.

In order to contrast the behaviour of the algorithm, another variant of the experiment was performed with the algorithm configured to explore every region, including those that touch the image boundary. In Figure 23, the image overlays contrasts the previous run in Figure 22 with a second run where the algorithm did not ignore regions which grazed the image boundaries. However, in this second run, the accuracy of branch event detection is compromised as two branches are not detected. The reconstruction reports for both variants of the experiment is presented in the Appendix.

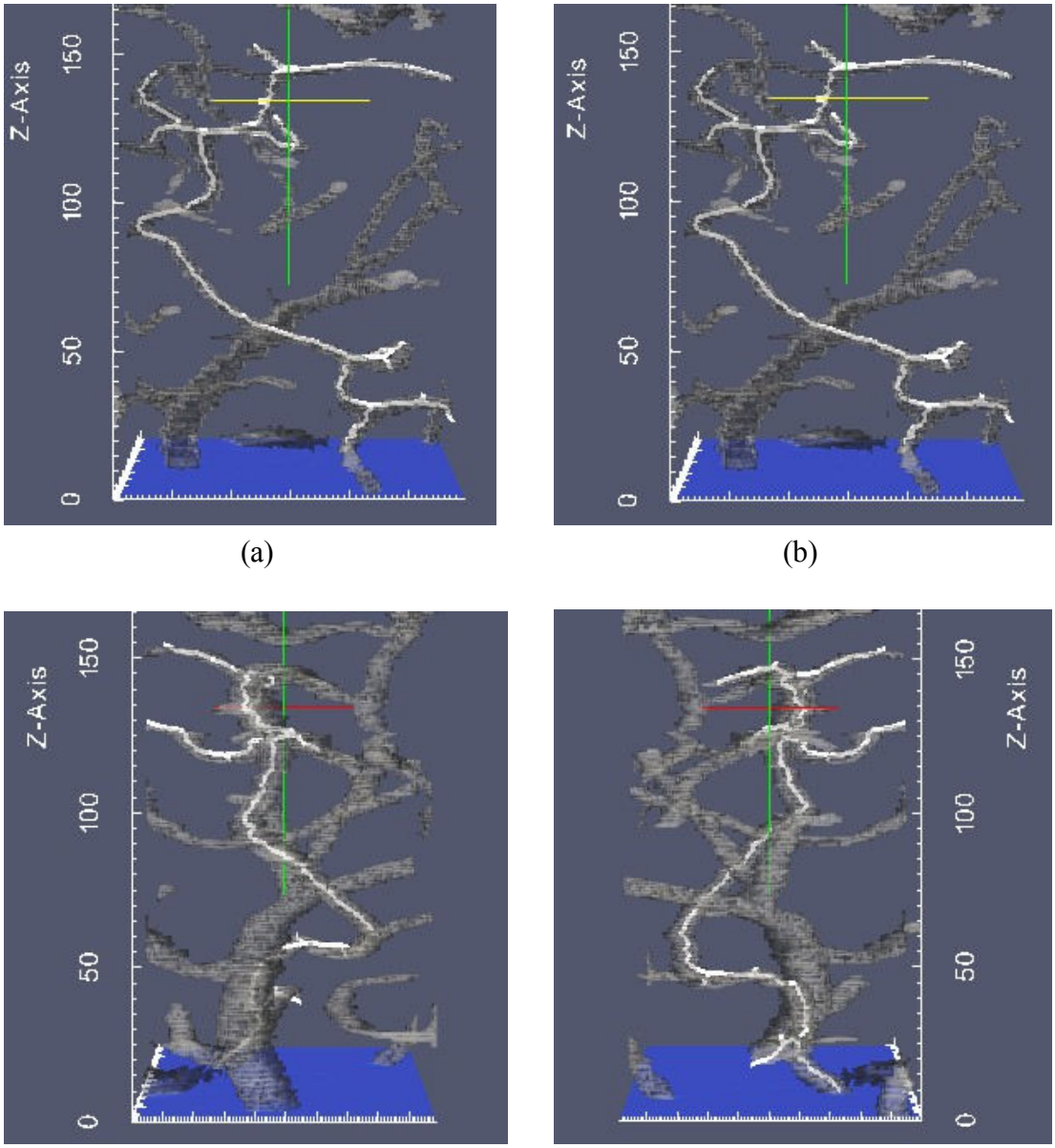

Figure 23. Image overlays for experiment 2 (Variant 2). Viewed along (a) the positive X-axis, (b) the negative X-axis, (c) the positive Y-axis, (d) the negative Y-axis. The algorithm was configured to accept regions that graze the image boundaries.

4.1.3 Experiment 3

The seed point (74.0, 53.0) was selected from Slice No: 63 of the data set. This vascular network is the same network explored in Experiment 1. The difference is that the seed point is now from the Vessel 5 illustrated in Figure 20. This experiment was run to demonstrate the versatility of the algorithm. It can explore the complete vascular network from a seed point selected from any vessel in that particular data volume. This versatility is a direct result of the localized processing of the image data by the algorithm while ignoring the global context of the blood vessels. Here again, the vascular network associated with this seed point was explored in full. The network topology is illustrated in the Figure 24 below. The reconstruction was successful and reproduced the same network from Experiment 1. This experiment shows that the algorithm is direction agnostic, that reconstruction can proceed in either direction of the z-axis.

The reconstruction report is available in the Appendix.There were four recorded vessel bifurcations and five instances where the vessel being explored went out of the image boundary. The only difference in the topology, from Experiment 1, is that a few of the branching events that were recorded as vessel bifurcations in Experiment 1, have now been recorded as a vessel coalescence in Experiment 3 depending on the order in which the images were processed.

Exploration of Vessel 5 proceeds first from Slice 63 towards Slice 69 (see z-axis label in Figure 26), and recognizes the split in the vessel at Slice 70. Next the exploration restarts again from Slice 64, towards Slice 45 with the aim of locating the origin of the vessel. Once the exploration reaches the origin of the vessel, approaching

from Slice 45 to Slice 44, the appearance is that of a vessel fusion in contrast to the vessel bifurcation recognized by the software in Experiment 1 when it approached Slice 45 from Slice 44. This also establishes the relationships between the vessels accurately.

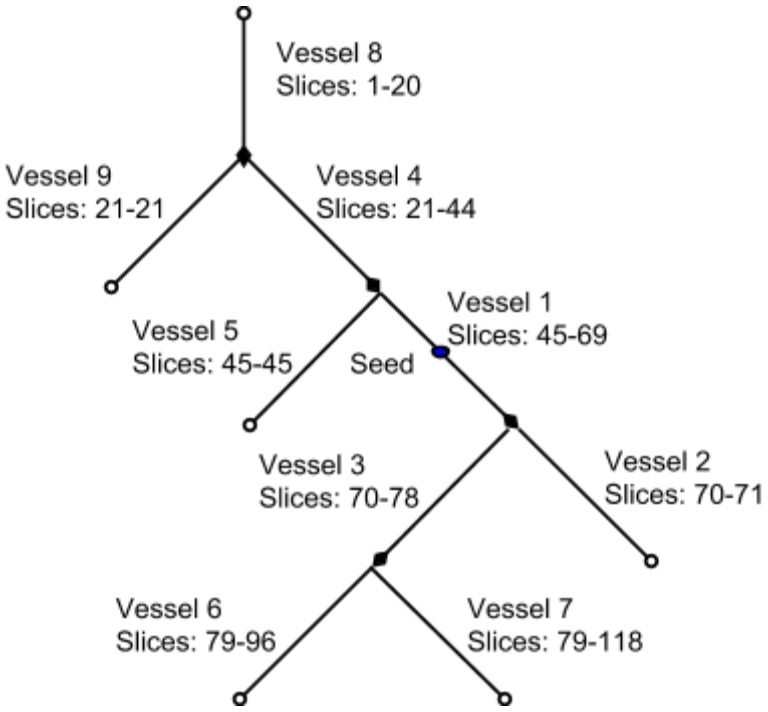

Figure 24. Topology of the vascular network for experiment 3. Note that this network is the same as the network shown in Figure 17. The difference is the seed point as well as the labelling of vessel segments by the algorithm.

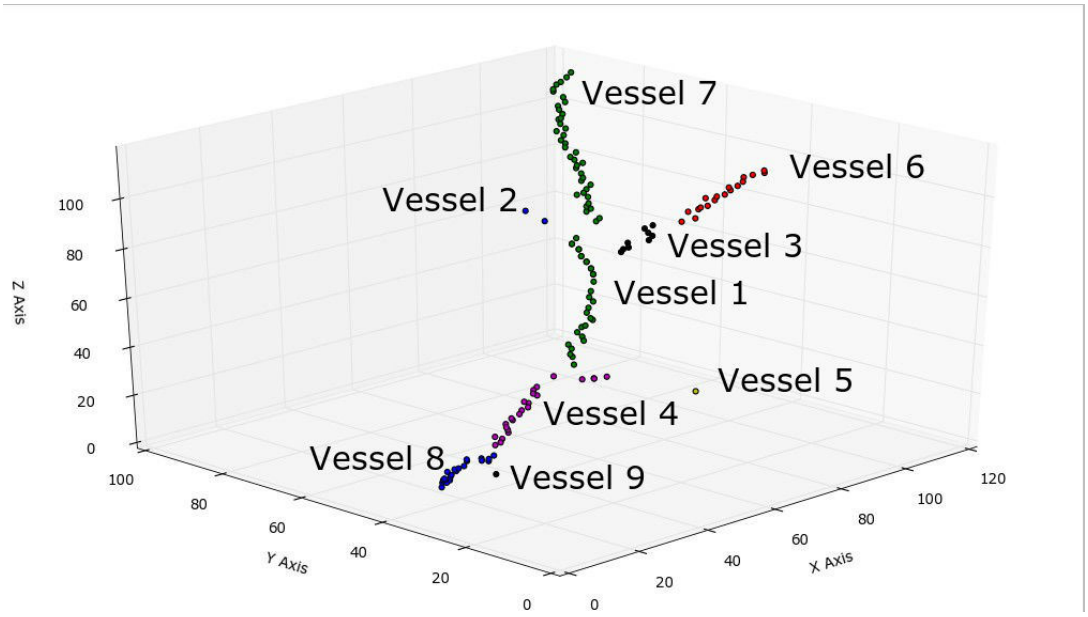

Figure 25. Trace of vascular network for experiment 3, plotted in 3-dimensional space. Note that this network is the same as the network shown in Figure 18. The difference is the seed point as well as the labelling of vessel segments by the algorithm.

The reconstruction of this network in Figure 25. shows the various branches of the network plotted in 3-dimensional space. Figure 26 shows the image overlays .

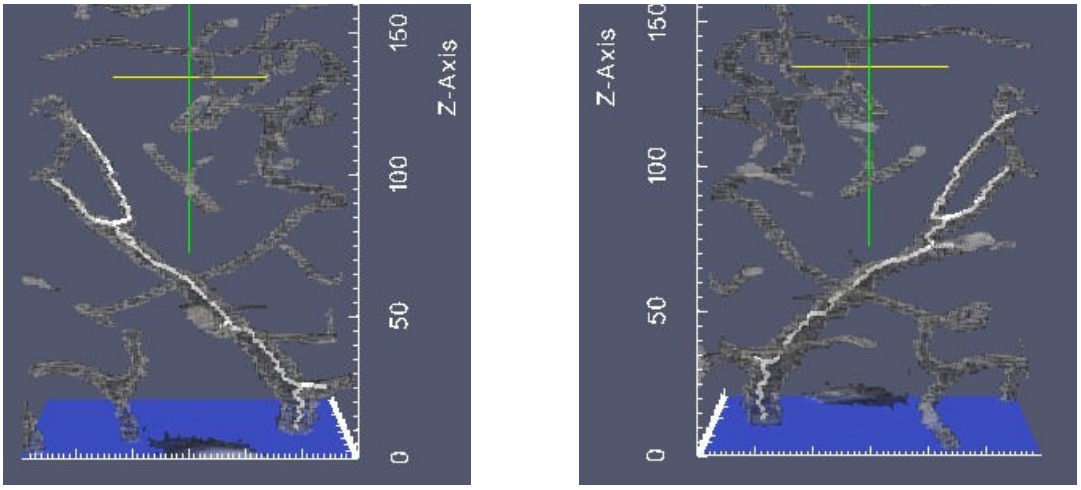

(a) (b)

Figure 26. Image overlays for experiment 3. Viewed along (a) the positive X-axis, (b) the negative X-axis, (c) the positive Y-axis, (d) the negative Y-axis. Note that this network is the same as the network shown in Figure 19.

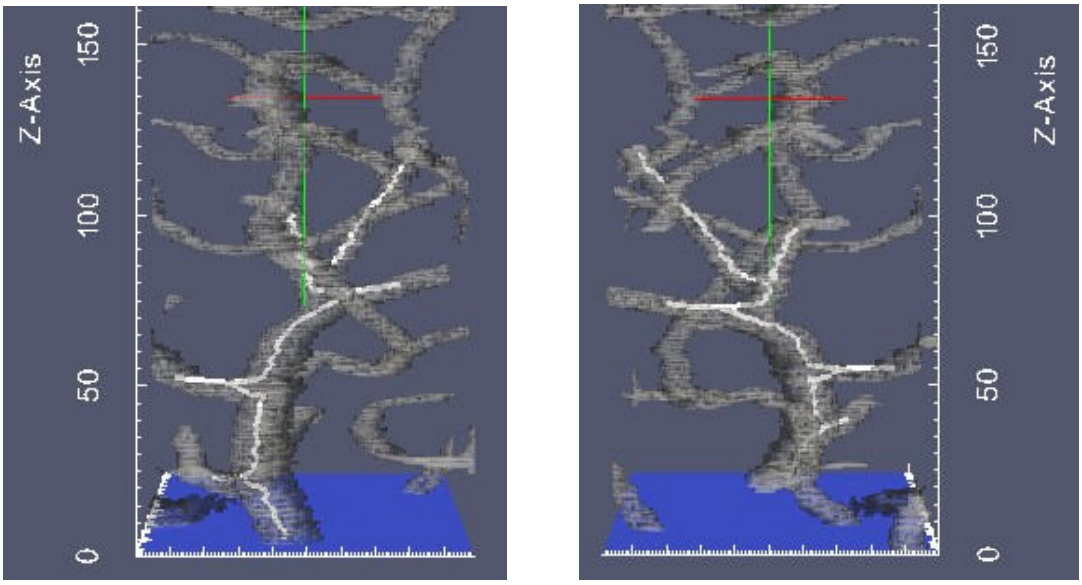

(c) (d)

Figure 26 Continued.

4.1.4 Experiment 4

The seed point (28.0, 68.0) was selected from Slice No: 210 of the data set. This vascular network is much more complex than the previous networks. It has 17 distinct blood vessels. The network is visualized in Figure 28 and the topology is illustrated in Figure 27. The reconstruction report is available in the Appendix. This network comprises 17 vessels and 8 branch points. There are 6 vessel bifurcations and 2 vessel fusions. The entire network spans over 67 slices (Slice 158 - Slice 224). Of the 17 vessels which are part of the network, 7 blood vessels could not be explored completely as they moved out of the image boundary.

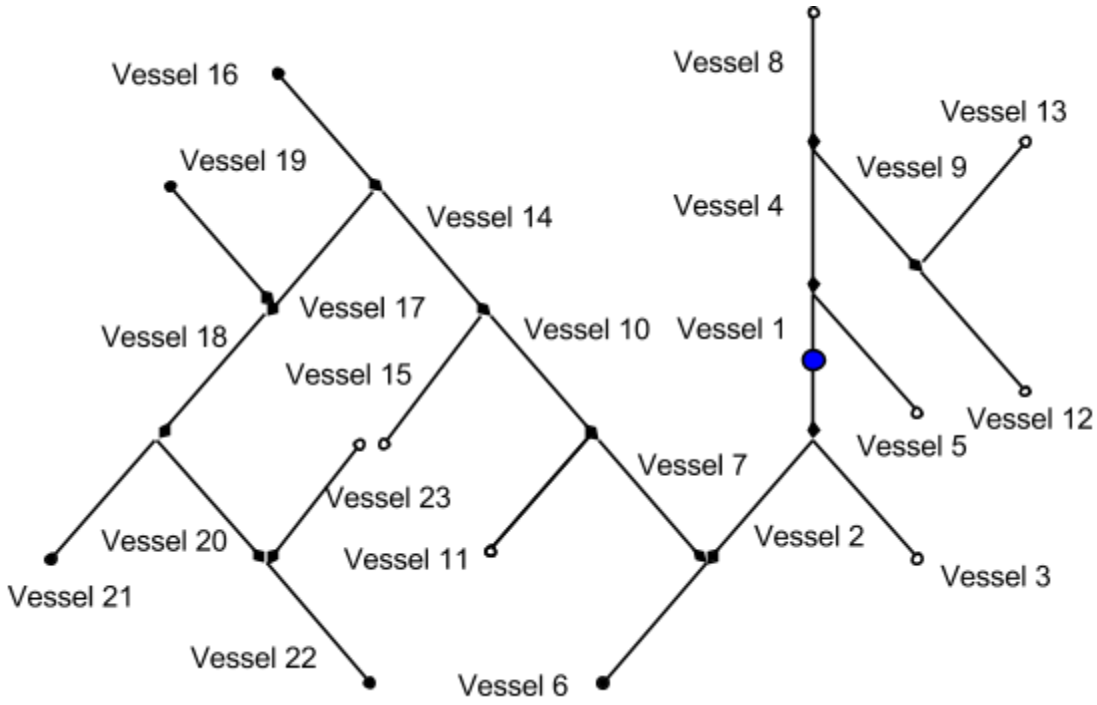

Figure 27. Topology of the vascular network for experiment 4. The seed point is marked in blue.

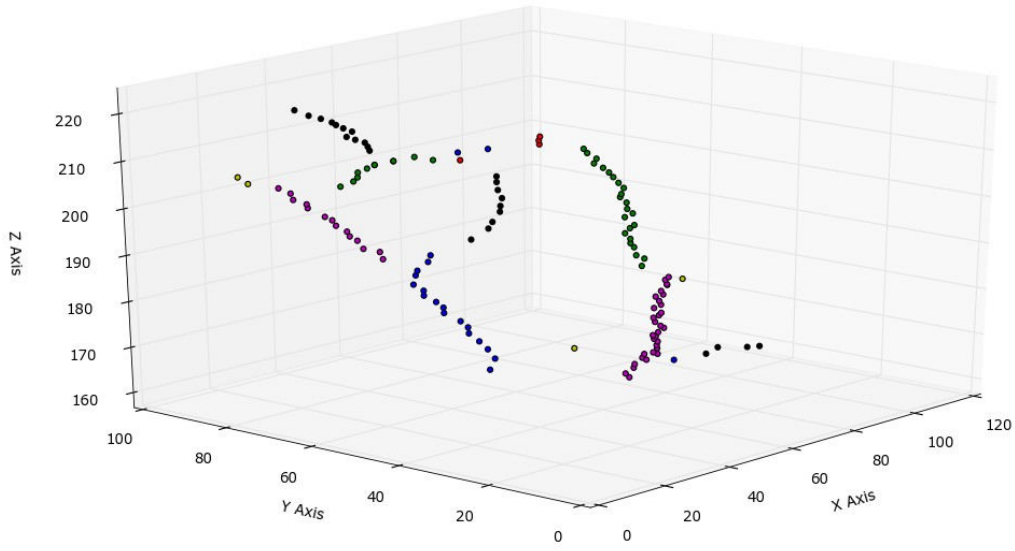

Figure 28. Trace of vascular network for experiment 4, plotted in 3-dimensional space. Each segment of a vessel between distinct branching points is colored in a different color.

Figure 29 shows the image overlays for the vascular network explored in experiment 4.

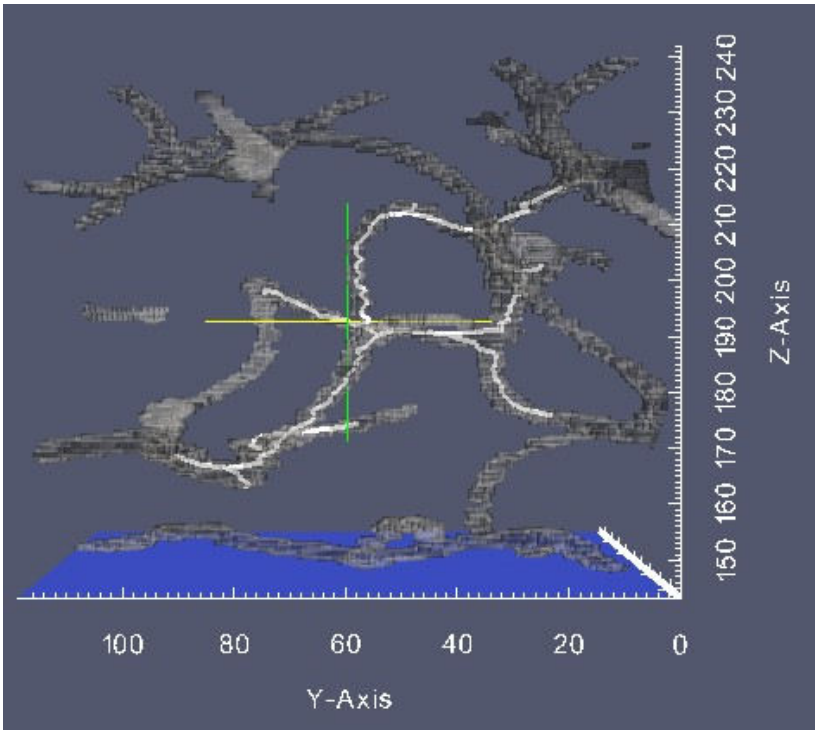

(a)

Figure 29. Image overlays for experiment 4. Viewed along (a) the positive X-axis, (b) the negative X-axis, (c) the positive Y-axis, (d) the negative Y-axis.

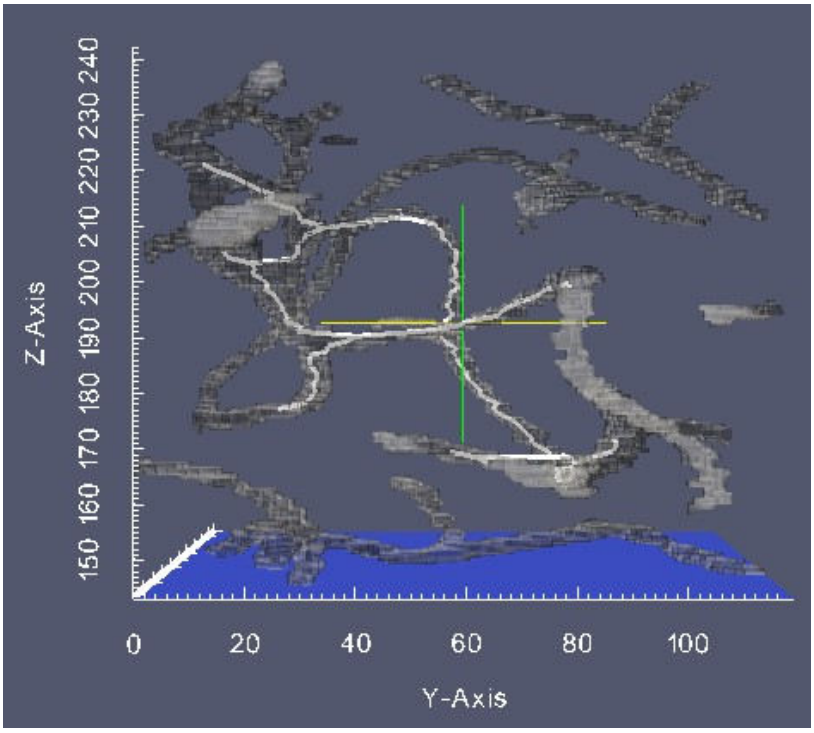

(b)

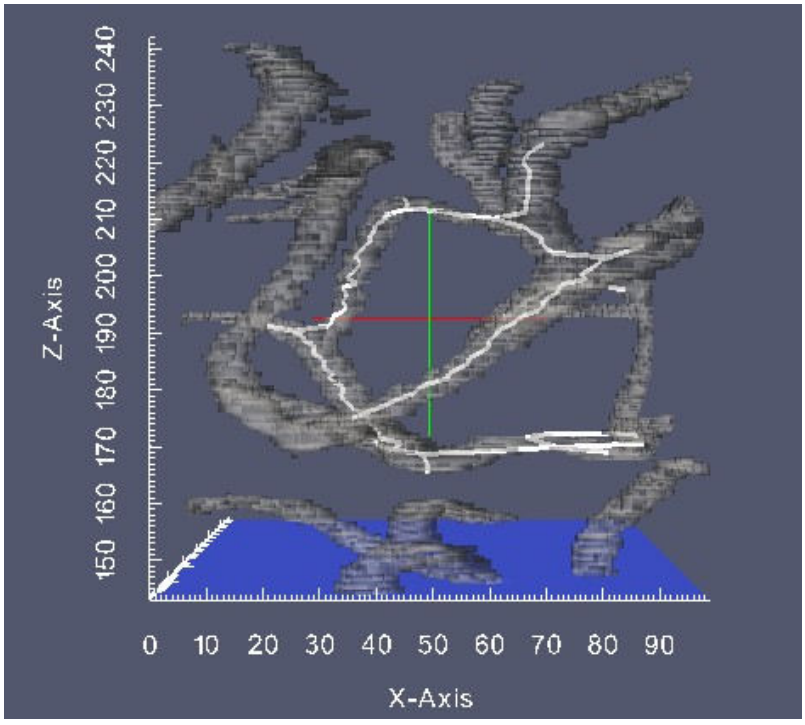

(c)

Figure 29 Continued.

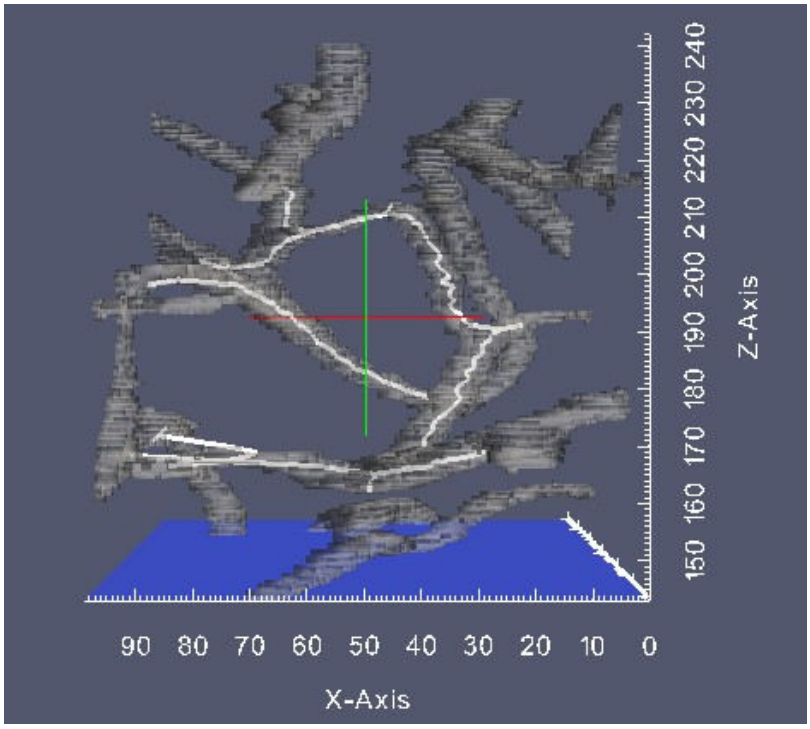

(d)

Figure 29 Continued.

4.2 Validation

In this section, I present the analysis of the accuracy of the algorithm in tracing vascular networks. In order to test the accuracy of the algorithm, I generated synthetic data and used the algorithm to reconstruct the artificial vascular network. The synthetic data was generated in Python using a series of randomised vessel segments. Only the origin point, end point, initial and final radii of the vessel segments points were fed to the program to generate the series of images. The program also added randomized jitter to each of the coordinates (x & y) as well as to the radius to simulate conditions of real-life data.

4.2.1 Synthetic Test Case 1

The seed point (10.0, 10.0) was selected from Slice No: 1 of the first synthetic data set. This synthetic vascular network has several branch points. The network was explored correctly and completely. The topology of the vascular network is illustrated in Figure 30. The 3-dimensional plot of the network is shown in Figure 31. The reconstruction report is presented in the Appendix.

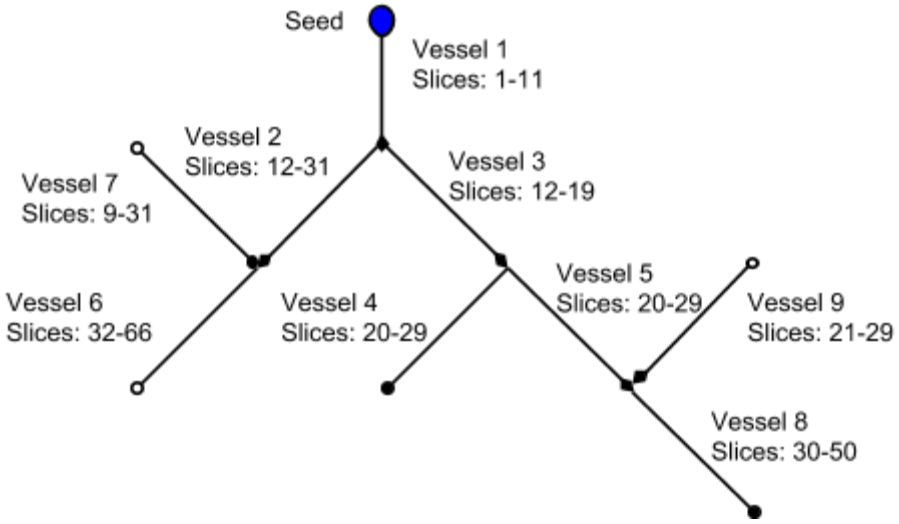

Figure 30. Topology of the vascular network for synthetic test case 1.

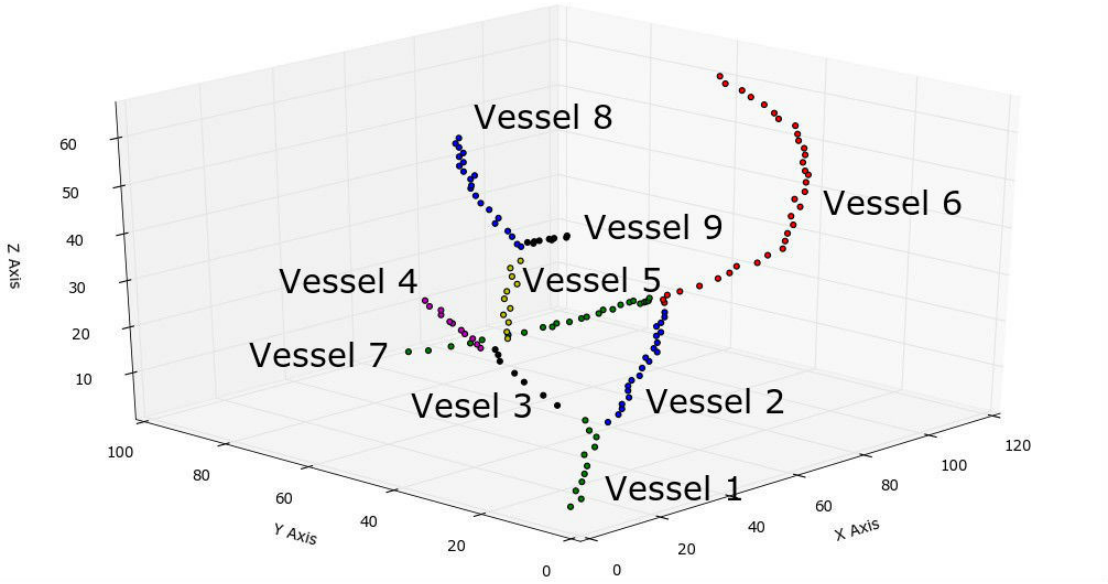

Figure 31. 3-dimensional trace of vascular network for synthetic case 1. Each segment of a vessel between distinct branching points is colored in a different color.

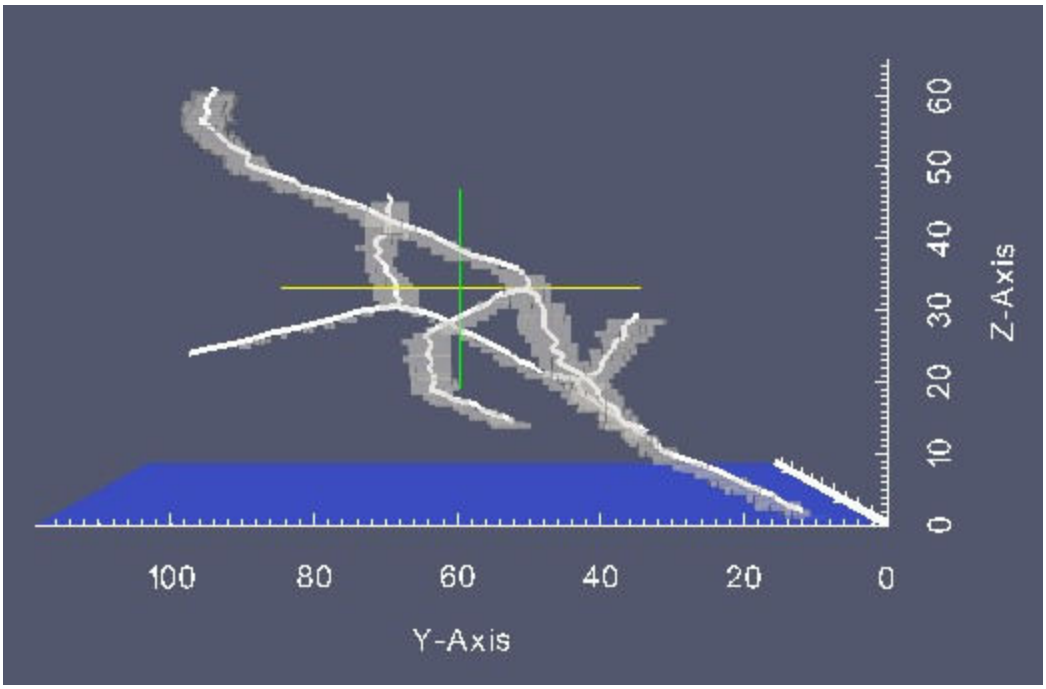

(a)

Figure 32. Image overlays for synthetic case 1. Viewed along (a) the positive X-axis, (b) the negative X-axis, (c) the positive Y-axis, (d) the negative Y-axis.

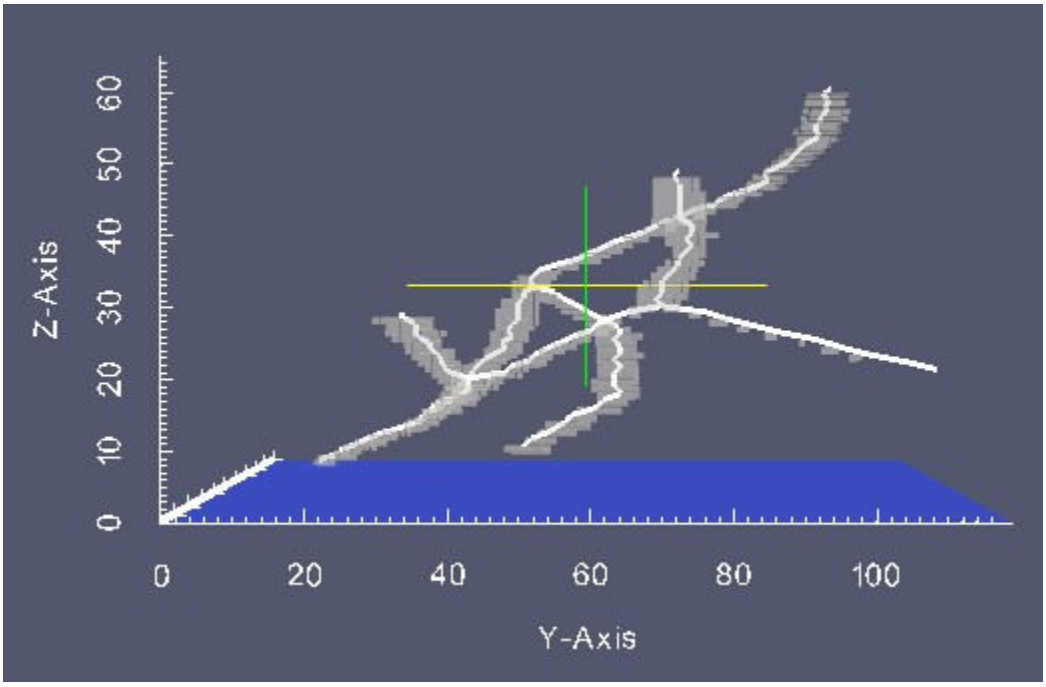

(b)

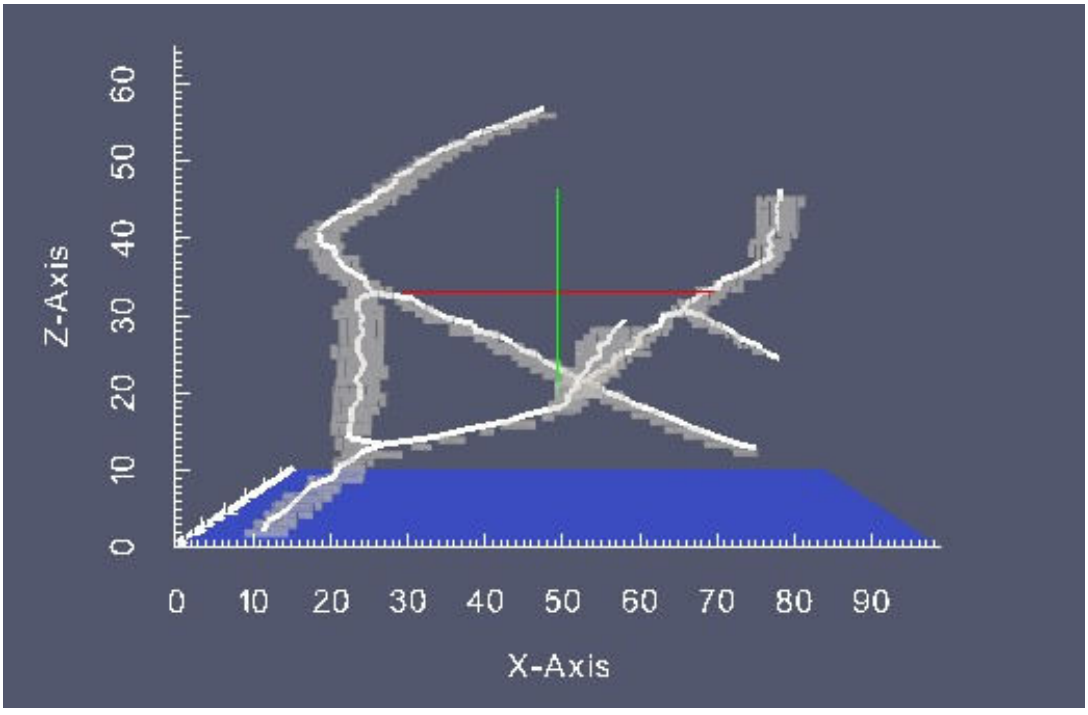

(c)

Figure 32 Continued.

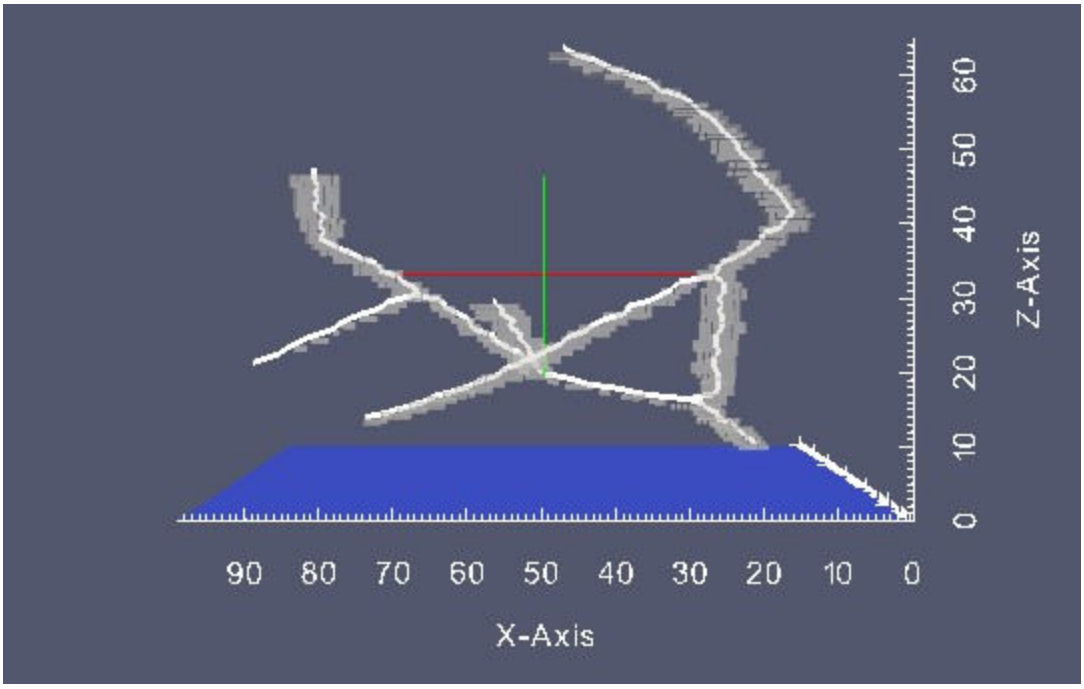

(d)

Figure 32 Continued.

The image overlay of the network generated by Paraview [18] is shown in Figure 32 above.

4.2.2 Synthetic Test Case 2

The seed point (20.0, 30.0) was selected from Slice No: 1 of the first synthetic data set. This second synthetic vascular network also has various branch points. The network was explored correctly and completely. The topology of the vascular network is illustrated in Figure 33. The 3-dimensional plot of the network is shown in Figure 34.

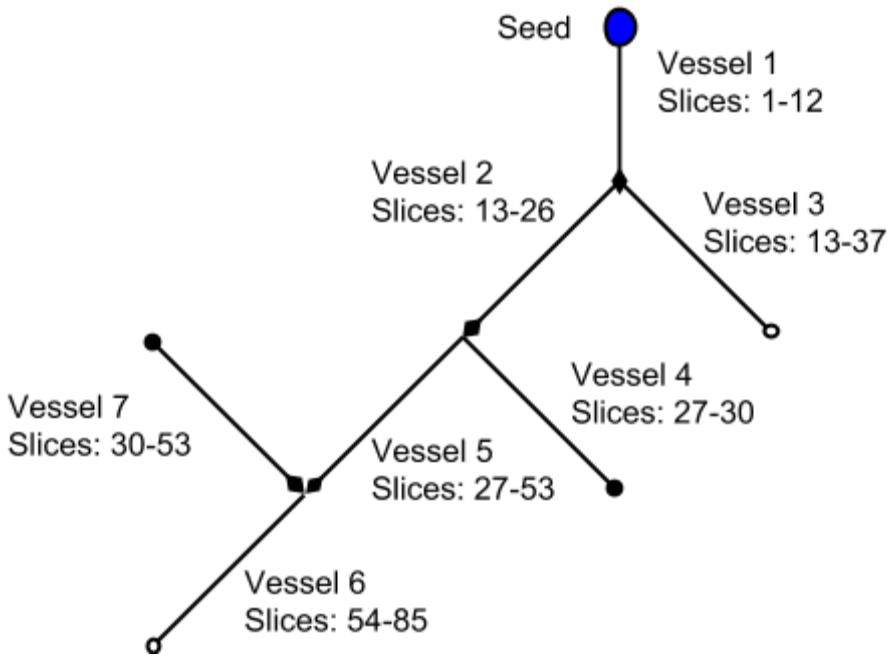

Figure 33. Topology of the vascular network for synthetic test case 2.

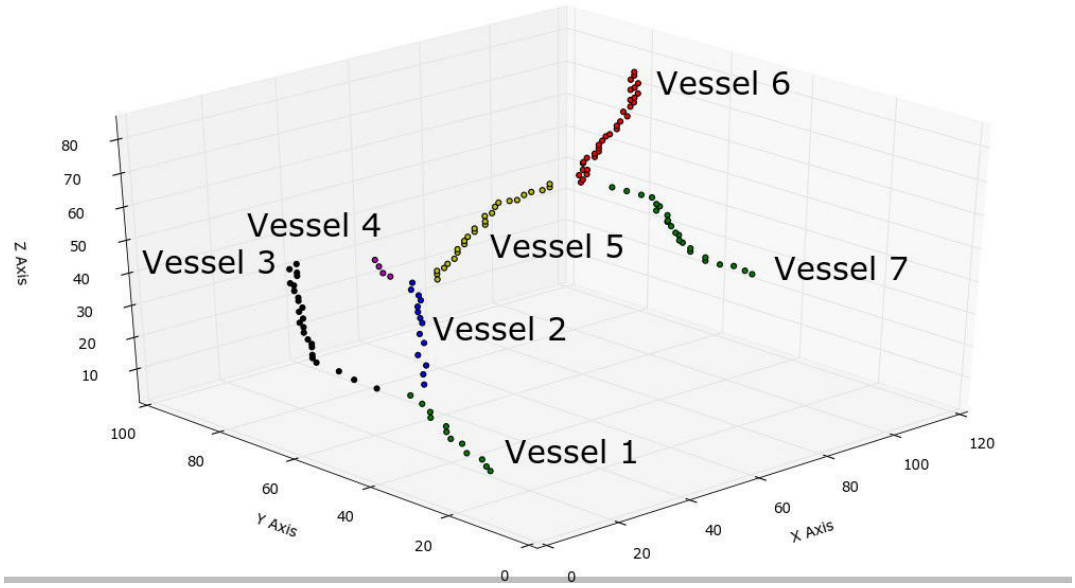

Figure 34. 3-dimensional trace of vascular network for synthetic case 2. Each segment of a vessel between distinct branching points is colored in a different color.

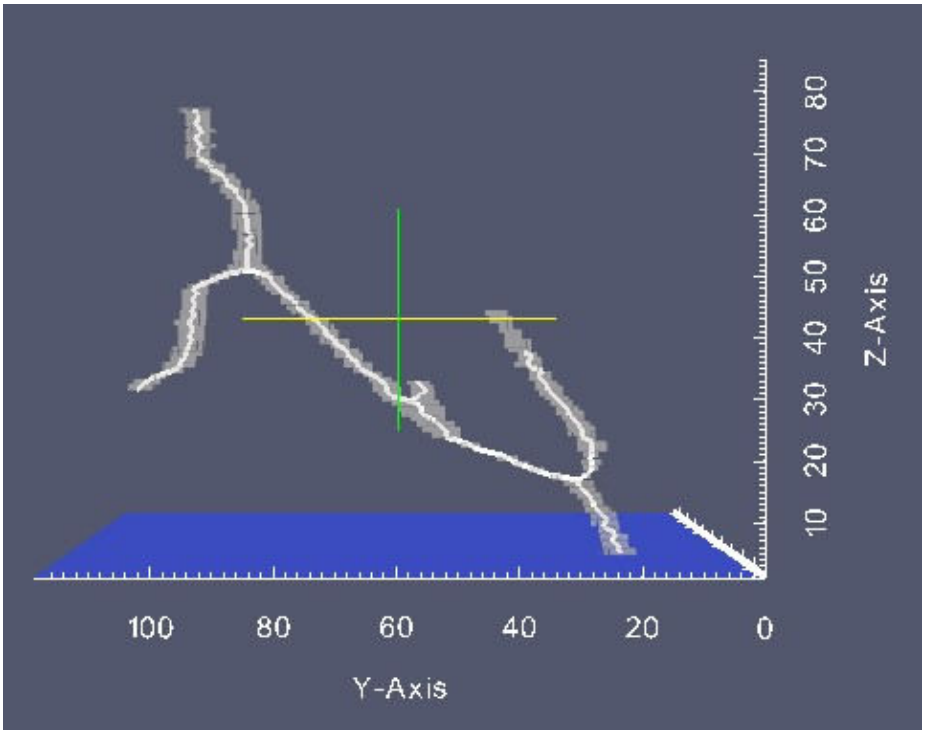

(a)

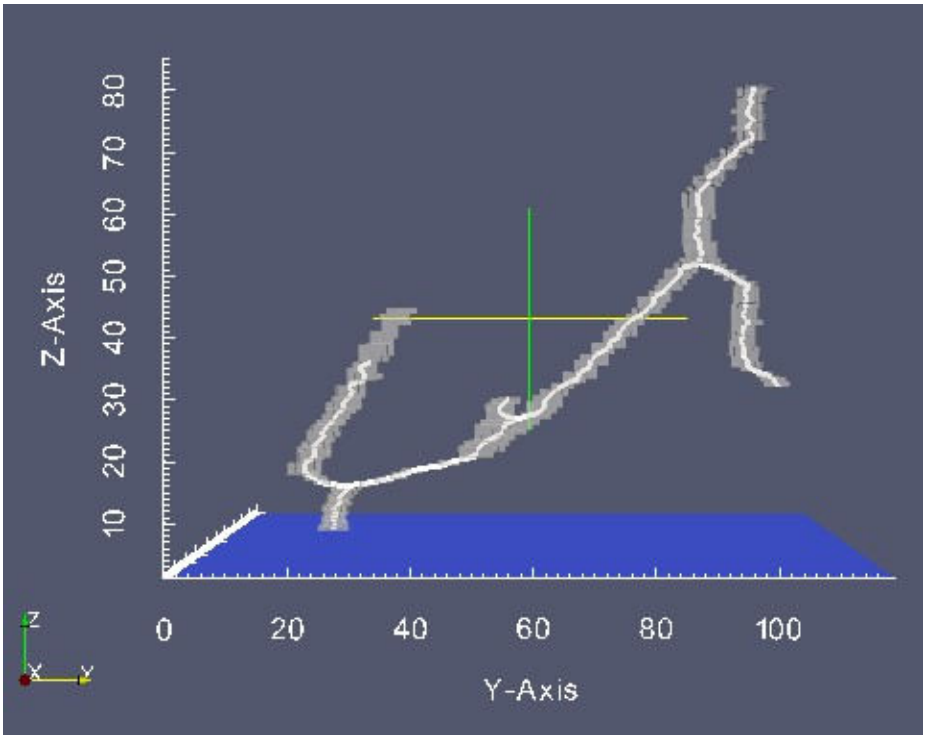

(b)

Figure 35. Image overlays for synthetic case 2. Viewed along (a) the positive X-axis, (b) the negative X-axis, (c) the positive Y-axis, (d) the negative Y-axis.

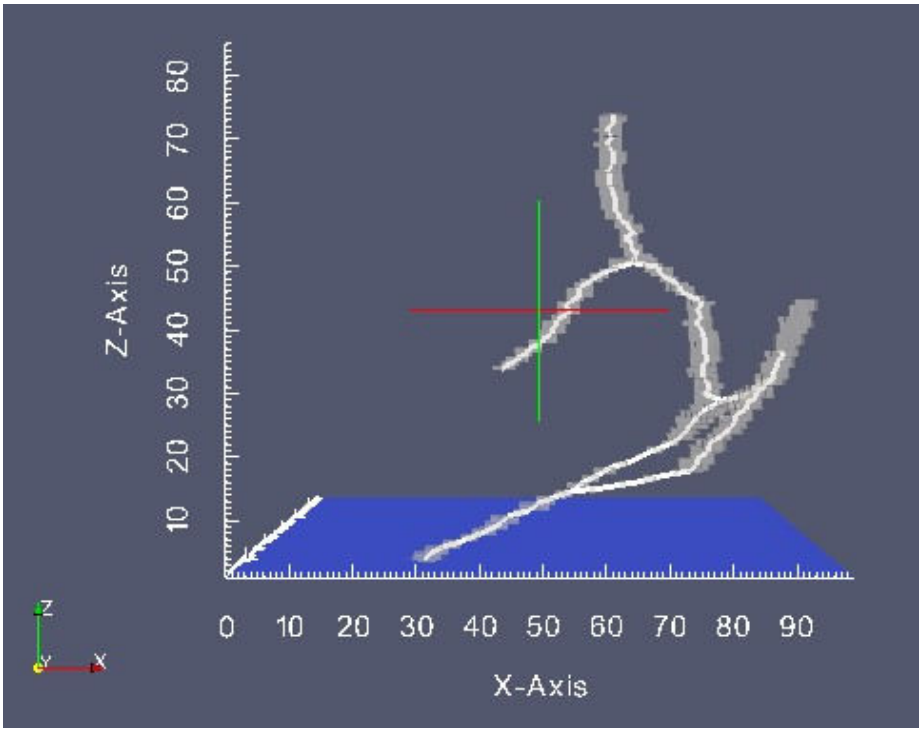

(c)

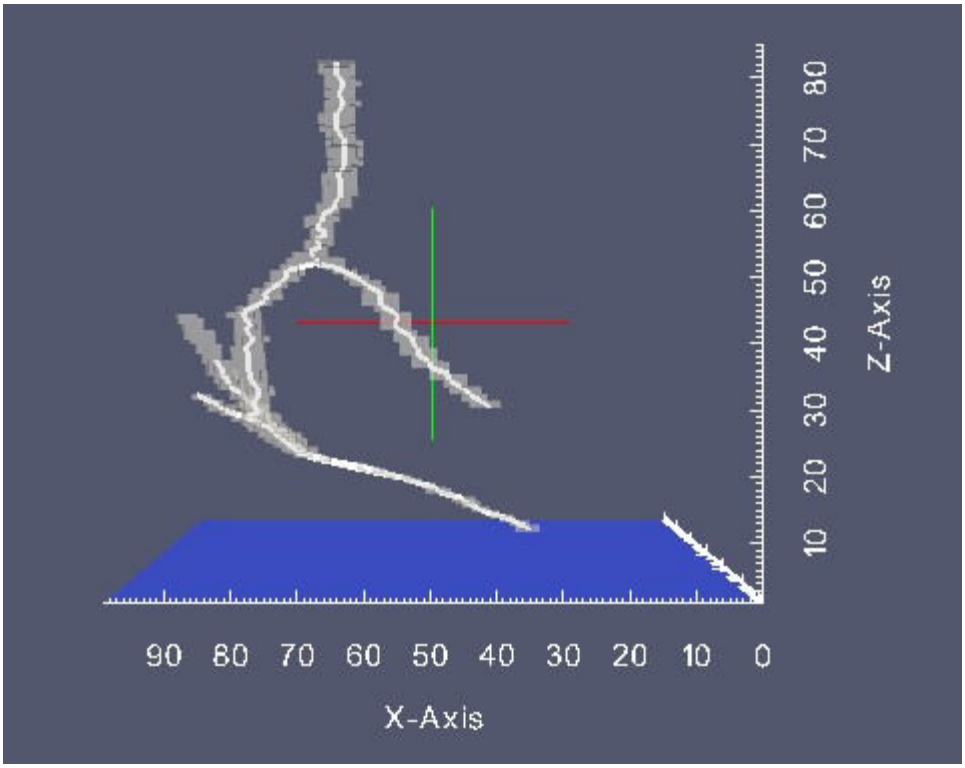

(d)

Figure 35 Continued.

The image overlay of the network generated by Paraview [18] is shown in Figure 35. The reconstruction report is presented in the Appendix.

4.2.3 Summary

In every synthetic data test case, the error measured in the pixel-wise deviation from the true centerline was 0. This was partly due to the way the synthetic data was generated and since there was no noise in the synthetic data. The error rate could increase for real life data.

CHAPTER V

DISCUSSION AND CONCLUSIONS

In this section, I discuss the contributions made by this research, open issues, future work, and conclusions.

5.1 Contributions

This thesis presents an improved methodology to reconstruct vascular networks of brain tissue from KESM image data. The algorithm and its implementation developed as part of this thesis helps the user trace the entire vascular network rooted at a particular blood vessel much faster than traditional manual methods can. The algorithm also allows for a targeted exploration of the vascular network from KESM image data: the algorithm has an interactive mode, which allows the user to direct the exploration.

5.2 Open Issues and Future Work

In this thesis, I developed a new method for performing targeted reconstruction of specific vascular networks from KESM images of sections of a whole mouse brain. However, there are certain open issues to be addressed: (1) The tool does not perform well when handling blood vessels that have segments which lie nearly perpendicular to the z-axis. (2) The methodology has not been tested on a large dataset. (3) We need to identify alternative branching events. (4) We need comprehensive exploration by expanding the image boundary and/or translating the AoI if the vessel moves out of the

image boundary. (5) Need for postprocessing of the resulting vascular network. In this section, I discuss these issues and outline future areas of work to overcome them.

5.2.1 Tracing Segments Orthogonal to the Z-axis

The software does not perform well for vessels that lie nearly perpendicular to the z-axis. This is because such vessel segments would have cross sections that lie within a limited number of slices and these cross sections would be highly elliptical or oblongated. As of now, the methodology is insensitive to the shape of the cross sections, content to reduce the cross sections to points in the image concurrent with their respective centroids. This approach is simpler and raises the efficiency of the process by handling the regions mainly through their centroids.

5.2.2 Tests on Larger KESM Data Sets.

Only a limited portion of the KESM data set was used to test this tool. The data set is made of a set of 273 images of 120x100 pixels. The tool should be tested against other portions of the data set to get a comprehensive evaluation of its efficacy. Ultimately, the tool should be able to reconstruct vascular networks rooted at any blood vessel imaged by the KESM instrument.

5.2.3 Identify Alternative Branching Events

The three branching events described in Section III were the most frequent branching events observed in the data set that was used. It is likely there could be other

variants of branching events for vessels in other data sets. Hence, a study of alternative branching events should be performed and incorporated into the tool. It would help extend the tool to handle a more diverse set of branching events in the KESM image data.

5.2.4 Comprehensive Vascular Exploration

The program in the present form focuses exploration to the 120x100 pixels of the images. In the future this could be an expandable and translatable image boundary which is adjusted to constantly track the movement of the blood vessel through the 3-dimensional volume space. It is however imperative for performance to keep the AoI as small as possible to reduce the complexity of the image processing algorithms by applying them to a limited area of the whole image. Though this is recommended for micro-vessels, when reconstructing macro-vessels it would be necessary to expand the image boundary to a much larger area.

5.2.5 Postprocessing the Vascular Network

Once the reconstruction is complete, the vascular network generated needs to be pruned for extraneous vessel segments created as part of reconstruction. For example when a vessel reverses direction along the z-axis, the trace of the vessel is interpreted by the algorithm as a merge, though technically it is not a merge. Figure 36 illustrates the creation of this extraneous vessel segment.

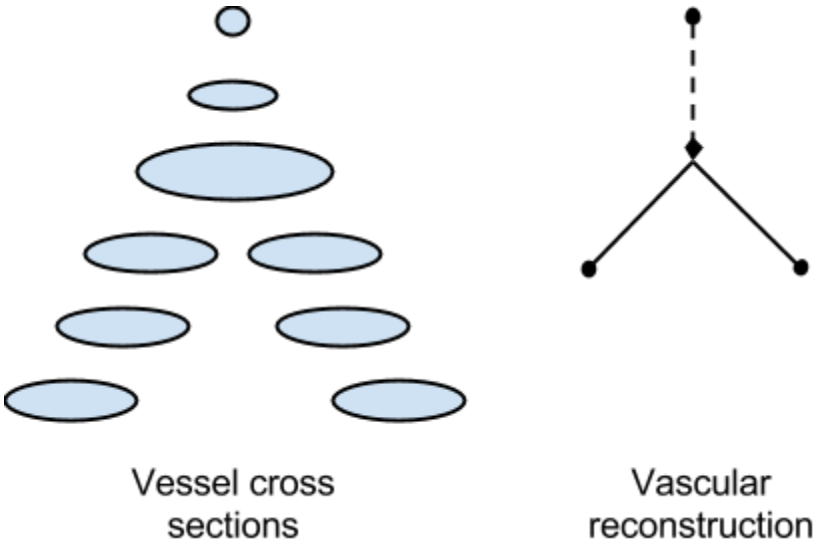

Figure 36. Extraneous vessel segment created by the algorithm. In the figure the vessel segment shown in dotted line is extraneous and typically very short. Such vessel segments can be identified and pruned.

5.3 Conclusions

The main goal of this research was to develop a novel method for targeted, interactive reconstruction of vascular networks of brain tissue from KESM image data. The algorithm outputs detailed properties for each vessel segment in the vascular network that was explored as well as a vtk file which contains the coordinates of the medial lines of the vessel segments and connections between the segments through branches. This thesis presents this new method to aid the manual reconstruction of vascular networks. This software would be more efficient than current manual methods for tracing. The accuracy of this tool was validated against synthetic vascular data. The algorithm allows for a new method to reconstruct vascular networks using targeted exploration. It can also operate in an interactive mode where the user can direct the

reconstruction. It is expected that this tool will help reconstruct larger sets of KESM images and also further discoveries in neuroscience in the process.

REFERENCES

[1] J. C. de la Torre, “Alzheimer disease as a vascular disorder: Nosological evidence”, Stroke, Volume 33, pp. 1152 - 1162, 2002.

[2] D. Mayerich, L. Abbott, and B. McCormick, “Knife-edge scanning microscopy for imaging and reconstruction of three-dimensional anatomical structures of the mouse brain”, Journal of Microscopy, Volume 231, pp. 134 - 143, 2008.

[3] D. Han, J. Keyser, and Y. Choe, “A local maximum intensity projection tracing of vasculature in knife-edge scanning microscope volume data”, IEEE International Symposium on Biomedical Imaging: From Nano to Macro (ISBI '09), pp. 1259 - 1262, 2009.

[4] J. Canny, "A computational approach to edge detection", IEEE Transactions on Pattern Analysis and Machine Intelligence, Volume PAMI-8, Issue 6, pp. 679 - 698, 1986.

[5] E. P. Meyer, A. Ulmann-Schuler, M. Staufenbiel, and Thomas Krucker, “Altered morphology and 3D architecture of brain vasculature in a mouse model for Alzheimer's disease”, Proceedings of the National Academy of Sciences, Volume 105, Issue 9, pp. 3587-3592, 2008.

[6] D. Han, “Rapid 3D tracing of the mouse brain neurovasculature with local maximum intensity projection and moving windows”, Ph.D. dissertation, Department of Computer Science and Engineering, Texas A&M University, College Station, Texas, 2009.

[7] D. Mayerich, J. Kwon, C. Sung, L. Abbott, J. Keyser, and Y. Choe, “Fast macro-scale transmission imaging of microvascular networks using KESM”, Biomedical Optics Express Volume 2, Issue 10, pp. 2888 - 2896, 2011.

[8] S. Walt, J. L. Schönberger, J. Nunez-Inglesias, F. Boulogne, J. D. Warner, N. Yager, E. Gouillart, T. Yu, and the scikit-image contributors, “scikit-image: Image processing in Python”. PeerJ 2:e453, 2014: http://dx.doi.org/10.7717/peerj.453. Scikit-image website: http://scikit-image.org, Last accessed: June 2014.

[9] W. Burger, and M. Burge, “Principles of digital image processing: Core algorithms”, Springer-Verlag, London, 2009

[10] B. Jähne, “Digital image processing”, 6th edition, Springer-Verlag, Berlin-Heidelberg, 2005.

[11] T. H. Reiss, “Recognizing planar objects using invariant image features”, Lecture notes in computer science, Volume 676. Springer, Berlin, 1993.

[12] J. R. Chung, C. Sung, D. Mayerich, J. Kwon, D. E. Miller, T. Huffman, J. Keyser, L. C. Abbot, and Y. Choe, “Multiscale exploration of mouse brain microstructures using the knife-edge scanning microscope brain atlas”, Frontiers in Neuroinformatics, Volume 5, 2011.

[13] S. Beucher, and C. Lantuejoul, “Use of watersheds in contour detection”, International Workshop on Image Processing: Real-time Edge and Motion Detection/Estimation, Rennes, 1979.

[14] Y. Choe, D. Han, P. Huang, J. Keyser, J. Kwon, D. Mayerich, and L. Abbott, “Complete submicrometer scans of mouse brain microstructure: neurons and vasculatures”, 2009 Neuroscience Meeting Planner, Society for Neuroscience, Chicago, Illinois, Program number 389.10, 2009

[15] Y. Choe, L. C. Abbott, D. Han, P. S. Huang, J. Keyser, J. Kwon, D. Mayerich, Z. Melek, and B. H. McCormick, “Knife-edge scanning microscopy: High-throughput imaging and analysis of massive volumes of biological microstructures”, In R. Rao and G. Cecchi, editors, High-throughput Image Reconstruction and Analysis: Intelligent Microscopy Applications, Series on Bioinformatics and Biomedical Imaging, Artech House Publishers, Boston, Massachusetts, 2008.

[16] S. Xue, H. Gong, T. Jiang, W. Luo, Y. Meng, Q. Liu, S. Chen, and A. Li, “Indian-ink perfusion based method for reconstructing continuous vascular networks in whole mouse brain”, PLoS ONE, Volume 9, 2014.

[17] F. Cassot, F. Lauwers, C. Fouard, S. Prohaska, and V. Lauwers-Cances, “A novel three-dimensional computer-assisted method for a quantitative study of microvascular networks of the human cerebral cortex,” Microcirculation, Volume 13, 2006.

[18] A. Henderson, “ParaView guide, a parallel visualization application”, Kitware Inc., 2007. Paraview website: http://www.paraview.org/, Last accessed: June 2014.

[19] W. S. Rasband, ImageJ, U. S. National Institutes of Health, Bethesda, Maryland. ImageJ website: http://imagej.nih.gov/ij/, Last accessed: June 2014.

[20] J. D. Hunter, “Matplotlib: A 2D graphics environment”, Computing In Science & Engineering, Volume 9, Issue 3, pp. 90-95, 2007. Matplotlib website: http://matplotlib.org/, Last accessed: June 2014.

APPENDIX

RECONSTRUCTION REPORTS

Reconstruction Experiment 1

Slice No: 1
Seed point: (22.0, 45.0)

Vessel ID: 1
Beginning explored: True
Beginning reason: out-of-scope
End explored: True
End reason: split
Length of vessel: 20 slices
Range of vessel: 1 - 20

Slice ID	Centroid	Cross section area
1	(18.86, 43.87)	164.0
2	(20.04, 44.70)	157.0
3	(19.49, 43.19)	140.0
4	(19.14, 43.72)	149.0
5	(18.84, 41.84)	154.0
6	(17.66, 42.14)	161.0
7	(17.82, 40.87)	159.0
8	(18.12, 40.81)	161.0
9	(19.55, 40.87)	166.0
10	(16.70, 40.57)	168.0
11	(18.84, 39.65)	165.0
12	(16.63, 38.74)	174.0
13	(18.42, 37.96)	175.0
14	(20.16, 38.72)	169.0
15	(19.68, 38.36)	170.0
16	(21.13, 36.03)	182.0
17	(18.93, 34.08)	223.0
18	(18.44, 32.02)	265.0
19	(18.35, 31.88)	277.0
20	(19.57, 31.70)	301.0

Next vessels:
    Vessel 3 - To be explored
    Vessel 2 - To be explored
Previous vessels:
    None

Vessel ID: 3
Beginning explored: True
Beginning reason: split
End explored: True
End reason: out-of-scope
Length of vessel: 1 slices
Range of vessel: 21 - 21

Slice ID	Centroid	Cross section area
21	(9.57, 22.77)	99.0

Next vessels:
None
Previous vessels:
Vessel 1 - Explored

Vessel ID: 2
Beginning explored: True
Beginning reason: split
End explored: True
End reason: split
Length of vessel: 24 slices
Range of vessel: 21 - 44

Slice ID	Centroid	Cross section area
21	(23.73, 34.86)	181.0
22	(24.62, 34.31)	179.0
23	(25.43, 34.61)	185.0
24	(24.19, 35.28)	194.0
25	(27.01, 34.44)	189.0
26	(27.09, 34.65)	191.0
27	(26.90, 34.84)	199.0
28	(27.25, 35.25)	192.0
29	(29.02, 35.08)	189.0
30	(28.45, 34.90)	181.0
31	(30.53, 34.70)	169.0
32	(31.56, 35.02)	172.0
33	(32.77, 34.53)	163.0
34	(33.71, 35.18)	158.0
35	(32.53, 35.24)	161.0
36	(36.42, 35.35)	155.0
37	(35.52, 35.57)	155.0
38	(36.07, 35.94)	148.0
39	(36.94, 35.86)	151.0
40	(43.65, 37.40)	154.0
41	(44.84, 31.58)	268.0
42	(45.77, 29.57)	345.0
43	(44.31, 28.32)	406.0

44	(45.86, 26.60)	442.0

Next vessels:
    Vessel 4 - To be explored
    Vessel 5 - To be explored
Previous vessels:
    Vessel 1 - Explored

Vessel ID: 4
Beginning explored: True
Beginning reason: split
End explored: True
End reason: split
Length of vessel: 25 slices
Range of vessel: 45 - 69

Slice ID	Centroid	Cross section area
45	(46.22, 34.68)	279.0
46	(48.86, 37.18)	242.0
47	(48.57, 37.49)	221.0
48	(50.42, 38.70)	179.0
49	(50.86, 39.83)	183.0
50	(53.86, 38.61)	174.0
51	(54.50, 39.50)	158.0
52	(54.84, 40.96)	155.0
53	(56.93, 41.62)	148.0
54	(56.93, 40.74)	145.0
55	(59.78, 41.31)	143.0
56	(58.99, 41.19)	153.0
57	(60.17, 43.07)	154.0
58	(61.74, 43.92)	170.0
59	(64.56, 45.11)	184.0
60	(65.03, 46.44)	177.0
61	(67.23, 47.85)	175.0
62	(71.62, 50.75)	175.0
63	(74.33, 53.08)	167.0
64	(75.90, 54.89)	167.0
65	(77.66, 57.42)	203.0
66	(78.72, 59.58)	242.0
67	(80.93, 61.98)	283.0
68	(81.64, 64.25)	310.0
69	(84.24, 65.31)	304.0

Next vessels:
    Vessel 7 - To be explored
    Vessel 6 - To be explored
Previous vessels:
    Vessel 2 - Explored

Vessel ID: 5
Beginning explored: True
Beginning reason: split
End explored: True
End reason: out-of-scope
Length of vessel: 1 slices
Range of vessel: 45 - 45

Slice ID	Centroid	Cross section area
45	(49.49, 8.86)	108.0

Next vessels:
None
Previous vessels:
Vessel 2 - Explored

Vessel ID: 7
Beginning explored: True
Beginning reason: split
End explored: True
End reason: split
Length of vessel: 9 slices
Range of vessel: 70 - 78

Slice ID	Centroid	Cross section area
70	(81.31, 52.06)	102.0
71	(81.84, 51.97)	93.0
72	(82.19, 50.98)	85.0
73	(83.33, 52.10)	92.0
74	(86.51, 49.61)	110.0
75	(88.10, 50.04)	131.0
76	(87.83, 50.83)	158.0
77	(88.37, 52.13)	170.0
78	(90.01, 51.50)	147.0

Next vessels:
Vessel 8 - To be explored
Vessel 9 - To be explored
Previous vessels:
Vessel 4 - Explored

Vessel ID: 6
Beginning explored: True
Beginning reason: split
End explored: True
End reason: out-of-scope
Length of vessel: 2 slices
Range of vessel: 70 - 71

Slice ID	Centroid	Cross section area
70	(88.15, 76.28)	172.0
71	(89.94, 82.55)	208.0

Next vessels:
None
Previous vessels:
Vessel 4 - Explored

Vessel ID: 8
Beginning explored: True
Beginning reason: split
End explored: True
End reason: out-of-scope
Length of vessel: 18 slices
Range of vessel: 79 - 96

Slice ID	Centroid	Cross section area
79	(94.89, 48.49)	81.0
80	(97.39, 47.22)	72.0
81	(98.82, 50.10)	62.0
82	(100.34, 48.84)	62.0
83	(100.19, 48.21)	58.0
84	(100.75, 47.00)	56.0
85	(103.72, 47.67)	54.0
86	(102.07, 48.57)	54.0
87	(103.19, 46.79)	53.0
88	(104.10, 45.62)	50.0
89	(106.03, 45.79)	58.0
90	(105.92, 46.11)	63.0
91	(106.67, 44.64)	58.0
92	(108.47, 44.81)	59.0
93	(109.76, 45.65)	55.0
94	(111.00, 44.50)	52.0
95	(112.42, 42.84)	55.0
96	(112.28, 42.81)	54.0

Next vessels:
None
Previous vessels:
Vessel 7 - Explored

Vessel ID: 9
Beginning explored: True
Beginning reason: split
End explored: True
End reason: out-of-scope
Length of vessel: 40 slices

Range of vessel: 79 - 118

Slice ID	Centroid	Cross section area
79	(82.67, 59.22)	27.0
80	(83.52, 59.10)	29.0
81	(84.07, 62.71)	28.0
82	(84.97, 62.39)	31.0
83	(84.23, 62.84)	31.0
84	(84.84, 62.84)	32.0
85	(87.10, 64.83)	29.0
86	(85.30, 66.06)	33.0
87	(86.00, 65.00)	31.0
88	(87.09, 65.21)	33.0
89	(88.91, 65.68)	34.0
90	(88.43, 67.54)	37.0
91	(88.94, 67.57)	35.0
92	(89.83, 68.73)	30.0
93	(90.90, 70.83)	29.0
94	(91.14, 70.83)	29.0
95	(92.00, 70.12)	32.0
96	(91.19, 71.50)	32.0
97	(90.82, 72.18)	38.0
98	(92.91, 72.53)	34.0
99	(92.87, 75.13)	30.0
100	(93.82, 75.89)	28.0
101	(93.62, 76.78)	32.0
102	(95.62, 77.76)	34.0
103	(95.50, 79.41)	34.0
104	(96.97, 78.40)	35.0
105	(97.55, 80.16)	38.0
106	(98.53, 81.42)	43.0
107	(98.02, 80.43)	47.0
108	(99.37, 81.14)	51.0
109	(100.08, 82.56)	48.0
110	(100.69, 83.33)	45.0
111	(102.67, 83.22)	40.0
112	(103.91, 84.71)	45.0
113	(104.53, 87.65)	40.0
114	(104.30, 87.50)	40.0
115	(106.24, 88.29)	42.0
116	(106.98, 87.81)	43.0
117	(109.25, 88.25)	44.0
118	(111.47, 89.00)	55.0

Next vessels:

None

Previous vessels:

Vessel 7 - Explored

Range of network: 1 - 118

Reconstruction Experiment 2 (Variant 1)

Slice No: 1
Seed point: (81.0, 25.0)

Vessel ID: 1
Beginning explored: True
Beginning reason: out-of-scope
End explored: True
End reason: split
Length of vessel: 21 slices
Range of vessel: 1 - 21

Slice ID	Centroid	Cross section area
1	(80.69, 25.03)	36.0
2	(82.32, 26.93)	41.0
3	(82.02, 26.86)	44.0
4	(82.45, 28.94)	47.0
5	(82.37, 28.57)	51.0
6	(81.98, 31.02)	59.0
7	(82.54, 32.04)	56.0
8	(83.77, 33.94)	53.0
9	(85.54, 35.41)	56.0
10	(82.96, 36.63)	49.0
11	(85.50, 37.00)	42.0
12	(83.83, 37.60)	42.0
13	(86.07, 38.31)	45.0
14	(88.15, 40.09)	46.0
15	(87.94, 41.21)	48.0
16	(89.62, 40.40)	52.0
17	(88.95, 40.45)	64.0
18	(88.75, 39.49)	101.0
19	(89.12, 40.05)	135.0
20	(91.22, 40.42)	160.0
21	(91.60, 41.01)	189.0

Next vessels:
Vessel 2 - To be explored
Vessel 3 - To be explored
Previous vessels:

None

Vessel ID: 2
Beginning explored: True
Beginning reason: split
End explored: True
End reason: out-of-scope
Length of vessel: 1 slices
Range of vessel: 22 - 22

Slice ID	Centroid	Cross section area
22	(98.50, 43.02)	124.0

Next vessels:
None
Previous vessels:
Vessel 1 - Explored

Vessel ID: 3
Beginning explored: True
Beginning reason: split
End explored: True
End reason: specialmerge
Length of vessel: 22 slices
Range of vessel: 22 - 43

Slice ID	Centroid	Cross section area
22	(83.14, 37.59)	49.0
23	(81.89, 37.79)	38.0
24	(79.42, 38.45)	31.0
25	(80.62, 37.85)	34.0
26	(79.77, 37.77)	35.0
27	(78.94, 37.91)	32.0
28	(78.65, 38.18)	34.0
29	(79.57, 37.95)	37.0
30	(78.54, 37.91)	35.0
31	(80.06, 38.09)	32.0
32	(81.00, 38.50)	34.0
33	(81.46, 38.41)	37.0
34	(81.63, 39.21)	38.0
35	(79.60, 39.48)	40.0
36	(82.67, 40.02)	42.0
37	(81.00, 40.78)	45.0
38	(81.44, 41.41)	41.0
39	(82.12, 41.84)	50.0
40	(89.84, 46.70)	44.0
41	(91.86, 47.90)	49.0
42	(93.70, 48.89)	53.0

43	(93.65, 49.90)	51.0

Next vessels:
    Vessel 4 - To be explored
Previous vessels:
    Vessel 1 - Explored

Vessel ID: 4
Beginning explored: True
Beginning reason: specialmerge
End explored: True
End reason: vanished
Length of vessel: 4 slices
Range of vessel: 44 - 47

Slice ID	Centroid	Cross section area
44	(98.80, 57.41)	152.0
45	(99.78, 55.28)	108.0
46	(101.61, 55.72)	75.0
47	(100.56, 54.10)	39.0

Next vessels:
    None
Previous vessels:
    Vessel 6 - To be explored
    Vessel 3 - Explored

Vessel ID: 6
Beginning explored: True
Beginning reason: vanished
End explored: True
End reason: specialmerge
Length of vessel: 5 slices
Range of vessel: 40 - 44

Slice ID	Centroid	Cross section area
40	(95.12, 73.53)	17.0
41	(95.57, 72.96)	94.0
42	(95.48, 72.18)	153.0
43	(93.08, 71.47)	189.0
44	(93.08, 71.47)	189.0

Next vessels:
    Vessel 5 - To be explored
    Vessel 4 - Explored
Previous vessels:
    None

Vessel ID: 5
Beginning explored: True

Beginning reason: specialmerge
End explored: True
End reason: out-of-scope
Length of vessel: 41 slices
Range of vessel: 44 - 84

Slice ID	Centroid	Cross section area
44	(83.82, 76.92)	85.0
45	(80.65, 78.40)	72.0
46	(79.95, 79.56)	64.0
47	(76.70, 78.52)	63.0
48	(74.14, 79.17)	59.0
49	(71.17, 80.36)	58.0
50	(70.21, 79.30)	63.0
51	(66.00, 79.95)	63.0
52	(62.50, 81.50)	78.0
53	(60.34, 82.52)	82.0
54	(56.56, 81.56)	81.0
55	(54.61, 81.38)	72.0
56	(49.46, 80.06)	65.0
57	(46.67, 80.02)	64.0
58	(45.10, 78.92)	61.0
59	(44.22, 78.51)	63.0
60	(40.88, 77.39)	56.0
61	(38.96, 76.30)	56.0
62	(38.09, 76.05)	55.0
63	(36.36, 74.57)	47.0
64	(34.50, 73.50)	40.0
65	(33.35, 72.28)	46.0
66	(31.22, 70.67)	49.0
67	(31.10, 69.92)	49.0
68	(29.17, 68.89)	47.0
69	(29.41, 67.23)	39.0
70	(28.39, 66.56)	41.0
71	(27.16, 66.38)	45.0
72	(25.15, 64.91)	47.0
73	(24.06, 64.82)	50.0
74	(24.61, 61.44)	54.0
75	(23.85, 60.46)	52.0
76	(22.06, 59.57)	49.0
77	(21.29, 59.62)	45.0
78	(20.37, 58.12)	49.0
79	(19.69, 57.29)	45.0
80	(19.23, 55.40)	48.0
81	(18.56, 57.27)	41.0
82	(18.12, 55.58)	50.0

83	(15.55, 53.88)	56.0
84	(13.37, 51.81)	73.0

Next vessels:
None
Previous vessels:
Vessel 6 - Explored

Range of network: 1 - 84

Reconstruction Experiment 2 (Variant 2)

Slice No: 1
Seed Point: (81.0, 25.0)

Vessel ID: 1
Beginning explored: True
Beginning reason: out-of-scope
End explored: True
End reason: split
Length of vessel: 21 slices
Range of vessel: 1 - 21

Slice ID	Centroid	Cross section area
1	(80.69, 25.03)	36.0
2	(82.32, 26.93)	41.0
3	(82.02, 26.86)	44.0
4	(82.45, 28.94)	47.0
5	(82.37, 28.57)	51.0
6	(81.98, 31.02)	59.0
7	(82.54, 32.04)	56.0
8	(83.77, 33.94)	53.0
9	(85.54, 35.41)	56.0
10	(82.96, 36.63)	49.0
11	(85.50, 37.00)	42.0
12	(83.83, 37.60)	42.0
13	(86.07, 38.31)	45.0
14	(88.15, 40.09)	46.0
15	(87.94, 41.21)	48.0
16	(89.62, 40.40)	52.0
17	(88.95, 40.45)	64.0
18	(88.75, 39.49)	101.0
19	(89.12, 40.05)	135.0
20	(91.22, 40.42)	160.0

21	(91.60, 41.01)	189.0

Next vessels:
    Vessel 3 - To be explored
    Vessel 2 - To be explored
Previous vessels:
    None

Vessel ID: 3
Beginning explored: True
Beginning reason: split
End explored: True
End reason: specialmerge
Length of vessel: 22 slices
Range of vessel: 22 - 43

Slice ID	Centroid	Cross section area
22	(83.14, 37.59)	49.0
23	(81.89, 37.79)	38.0
24	(79.42, 38.45)	31.0
25	(80.62, 37.85)	34.0
26	(79.77, 37.77)	35.0
27	(78.94, 37.91)	32.0
28	(78.65, 38.18)	34.0
29	(79.57, 37.95)	37.0
30	(78.54, 37.91)	35.0
31	(80.06, 38.09)	32.0
32	(81.00, 38.50)	34.0
33	(81.46, 38.41)	37.0
34	(81.63, 39.21)	38.0
35	(79.60, 39.48)	40.0
36	(82.67, 40.02)	42.0
37	(81.00, 40.78)	45.0
38	(81.44, 41.41)	41.0
39	(82.12, 41.84)	50.0
40	(89.84, 46.70)	44.0
41	(91.86, 47.90)	49.0
42	(93.70, 48.89)	53.0
43	(93.65, 49.90)	51.0

Next vessels:
    Vessel 4 - To be explored
Previous vessels:
    Vessel 1 - Explored

Vessel ID: 2
Beginning explored: True
Beginning reason: split

End explored: True
End reason: merge
Length of vessel: 1 slices
Range of vessel: 22 - 22

Slice ID	Centroid	Cross section area
22	(98.50, 43.02)	124.0

Next vessels:
    Vessel 7 - To be explored
Previous vessels:
    Vessel 1 - Explored

Vessel ID: 4
Beginning explored: True
Beginning reason: specialmerge
End explored: True
End reason: vanished
Length of vessel: 4 slices
Range of vessel: 44 - 47

Slice ID	Centroid	Cross section area
44	(98.80, 57.41)	152.0
45	(99.78, 55.28)	108.0
46	(101.61, 55.72)	75.0
47	(100.56, 54.10)	39.0

Next vessels:
    None
Previous vessels:
    Vessel 3 - Explored
    Vessel 6 - To be explored

Vessel ID: 7
Beginning explored: True
Beginning reason: merge
End explored: True
End reason: vanished
Length of vessel: 4 slices
Range of vessel: 23 - 26

Slice ID	Centroid	Cross section area
23	(107.62, 45.73)	234.0
24	(108.92, 46.34)	271.0
25	(110.06, 46.74)	161.0
26	(108.76, 46.67)	46.0

Next vessels:
    None
Previous vessels:
    Vessel 8 - To be explored

Vessel 2 - Explored

Vessel ID: 6
Beginning explored: True
Beginning reason: vanished
End explored: True
End reason: specialmerge
Length of vessel: 5 slices
Range of vessel: 40 - 44

Slice ID	Centroid	Cross section area
40	(95.12, 73.53)	17.0
41	(95.57, 72.96)	94.0
42	(95.48, 72.18)	153.0
43	(93.08, 71.47)	189.0
44	(93.08, 71.47)	189.0

Next vessels:
Vessel 5 - To be explored
Vessel 4 - Explored
Previous vessels:
None

Vessel ID: 8
Beginning explored: True
Beginning reason: vanished
End explored: True
End reason: merge
Length of vessel: 5 slices
Range of vessel: 18 - 22

Slice ID	Centroid	Cross section area
18	(119.00, 56.50)	4.0
19	(118.86, 54.07)	14.0
20	(118.82, 50.73)	11.0
21	(118.00, 49.39)	36.0
22	(116.98, 47.71)	59.0

Next vessels:
Vessel 7 - Explored
Previous vessels:
None

Vessel ID: 5
Beginning explored: True
Beginning reason: specialmerge
End explored: True
End reason: merge
Length of vessel: 79 slices

Range of vessel: 44 - 122

Slice ID	Centroid	Cross section area
44	(83.82, 76.92)	85.0
45	(80.65, 78.40)	72.0
46	(79.95, 79.56)	64.0
47	(76.70, 78.52)	63.0
48	(74.14, 79.17)	59.0
49	(71.17, 80.36)	58.0
50	(70.21, 79.30)	63.0
51	(66.00, 79.95)	63.0
52	(62.50, 81.50)	78.0
53	(60.34, 82.52)	82.0
54	(56.56, 81.56)	81.0
55	(54.61, 81.38)	72.0
56	(49.46, 80.06)	65.0
57	(46.67, 80.02)	64.0
58	(45.10, 78.92)	61.0
59	(44.22, 78.51)	63.0
60	(40.88, 77.39)	56.0
61	(38.96, 76.30)	56.0
62	(38.09, 76.05)	55.0
63	(36.36, 74.57)	47.0
64	(34.50, 73.50)	40.0
65	(33.35, 72.28)	46.0
66	(31.22, 70.67)	49.0
67	(31.10, 69.92)	49.0
68	(29.17, 68.89)	47.0
69	(29.41, 67.23)	39.0
70	(28.39, 66.56)	41.0
71	(27.16, 66.38)	45.0
72	(25.15, 64.91)	47.0
73	(24.06, 64.82)	50.0
74	(24.61, 61.44)	54.0
75	(23.85, 60.46)	52.0
76	(22.06, 59.57)	49.0
77	(21.29, 59.62)	45.0
78	(20.37, 58.12)	49.0
79	(19.69, 57.29)	45.0
80	(19.23, 55.40)	48.0
81	(18.56, 57.27)	41.0
82	(18.12, 55.58)	50.0
83	(15.55, 53.88)	56.0
84	(13.37, 51.81)	73.0
85	(8.79, 49.78)	151.0
86	(5.74, 50.14)	126.0

87	(4.57, 47.76)	118.0
88	(3.71, 45.75)	97.0
89	(4.10, 44.76)	99.0
90	(3.98, 43.79)	89.0
91	(6.56, 39.95)	109.0
92	(11.04, 38.44)	162.0
93	(14.81, 38.91)	172.0
94	(21.78, 40.35)	483.0
95	(21.46, 36.19)	129.0
96	(23.91, 36.81)	100.0
97	(25.06, 36.88)	85.0
98	(28.68, 36.27)	71.0
99	(29.27, 38.03)	67.0
100	(30.56, 38.46)	63.0
101	(29.93, 39.08)	59.0
102	(32.00, 39.66)	56.0
103	(30.78, 41.13)	54.0
104	(31.82, 40.09)	56.0
105	(31.65, 42.12)	49.0
106	(31.63, 43.48)	52.0
107	(30.06, 42.62)	48.0
108	(30.12, 42.98)	51.0
109	(29.48, 43.69)	48.0
110	(28.58, 43.92)	53.0
111	(29.10, 43.62)	50.0
112	(28.73, 44.23)	52.0
113	(28.46, 46.48)	54.0
114	(27.06, 45.91)	53.0
115	(27.76, 46.15)	55.0
116	(27.14, 45.50)	58.0
117	(27.06, 45.97)	64.0
118	(27.19, 46.15)	73.0
119	(26.94, 46.09)	80.0
120	(26.72, 46.98)	97.0
121	(26.58, 46.03)	116.0
122	(26.63, 45.75)	145.0

Next vessels:

Vessel 9 - To be explored

Previous vessels:

Vessel 6 - Explored

Vessel ID: 9
Beginning explored: True
Beginning reason: merge
End explored: True

End reason: split
Length of vessel: 1 slices
Range of vessel: 123 - 123

Slice ID	Centroid	Cross section area
123	(32.40, 44.59)	240.0

Next vessels:
    Vessel 11 - To be explored
    Vessel 12 - To be explored
Previous vessels:
    Vessel 10 - To be explored
    Vessel 5 - Explored

Vessel ID: 11
Beginning explored: True
Beginning reason: split
End explored: True
End reason: split
Length of vessel: 23 slices
Range of vessel: 124 - 146

Slice ID	Centroid	Cross section area
124	(41.66, 44.31)	185.0
125	(42.16, 45.53)	158.0
126	(47.44, 44.94)	62.0
127	(49.13, 39.48)	46.0
128	(48.50, 38.29)	34.0
129	(49.33, 37.50)	30.0
130	(49.68, 38.39)	31.0
131	(50.42, 39.24)	33.0
132	(51.07, 38.59)	27.0
133	(52.00, 37.50)	26.0
134	(48.92, 37.69)	26.0
135	(53.24, 38.60)	25.0
136	(52.93, 39.41)	27.0
137	(53.00, 41.37)	27.0
138	(52.31, 40.16)	32.0
139	(52.50, 41.19)	32.0
140	(53.07, 40.59)	27.0
141	(53.84, 41.08)	37.0
142	(54.92, 43.00)	59.0
143	(53.32, 46.42)	158.0
144	(53.35, 45.64)	265.0
145	(55.85, 45.45)	325.0
146	(65.99, 42.36)	211.0

Next vessels:
    Vessel 13 - To be explored

Vessel 14 - To be explored
Previous vessels:
Vessel 9 - Explored

Vessel ID: 12
Beginning explored: True
Beginning reason: split
End explored: True
End reason: merge
Length of vessel: 1 slices
Range of vessel: 124 - 124

Slice ID	Centroid	Cross section area
124	(21.85, 48.02)	99.0

Next vessels:
Vessel 15 - To be explored
Previous vessels:
Vessel 9 - Explored

Vessel ID: 10
Beginning explored: True
Beginning reason: split
End explored: True
End reason: merge
Length of vessel: 5 slices
Range of vessel: 118 - 122

Slice ID	Centroid	Cross section area
118	(55.65, 36.08)	51.0
119	(54.14, 36.67)	42.0
120	(53.06, 38.18)	34.0
121	(52.38, 37.85)	34.0
122	(50.57, 37.43)	37.0

Next vessels:
Vessel 9 - Explored
Previous vessels:
Vessel 17 - To be explored

Vessel ID: 13
Beginning explored: True
Beginning reason: split
End explored: True
End reason: merge
Length of vessel: 1 slices
Range of vessel: 147 - 147

Slice ID	Centroid	Cross section area
147	(75.99, 45.16)	133.0

Next vessels:
    Vessel 19 - To be explored
Previous vessels:
    Vessel 11 - Explored

Vessel ID: 14
Beginning explored: True
Beginning reason: split
End explored: True
End reason: vanished
Length of vessel: 10 slices
Range of vessel: 147 - 156

Slice ID	Centroid	Cross section area
147	(57.15, 32.76)	33.0
148	(54.56, 31.12)	25.0
149	(54.94, 29.55)	31.0
150	(54.57, 27.49)	37.0
151	(50.73, 24.75)	40.0
152	(52.31, 22.82)	39.0
153	(50.89, 20.49)	57.0
154	(48.25, 11.76)	124.0
155	(47.66, 10.59)	134.0
156	(45.92, 7.50)	64.0

Next vessels:
    None
Previous vessels:
    Vessel 11 - Explored

Vessel ID: 15
Beginning explored: True
Beginning reason: merge
End explored: True
End reason: vanished
Length of vessel: 21 slices
Range of vessel: 125 - 145

Slice ID	Centroid	Cross section area
125	(17.69, 52.21)	168.0
126	(18.18, 53.16)	161.0
127	(19.73, 46.95)	133.0
128	(16.79, 42.00)	107.0
129	(14.84, 40.75)	116.0
130	(13.26, 41.30)	126.0
131	(11.50, 41.45)	131.0
132	(9.90, 40.61)	111.0
133	(7.07, 36.93)	149.0

134	(3.96, 37.82)	113.0
135	(5.60, 36.55)	163.0
136	(4.58, 37.44)	131.0
137	(4.27, 38.64)	100.0
138	(3.41, 36.40)	68.0
139	(4.34, 37.07)	59.0
140	(5.43, 36.05)	60.0
141	(5.50, 35.70)	54.0
142	(6.31, 37.35)	49.0
143	(7.53, 38.07)	55.0
144	(8.52, 37.25)	60.0
145	(10.84, 37.77)	62.0

Next vessels:
    None
Previous vessels:
    Vessel 16 - To be explored
    Vessel 12 - Explored

Vessel ID: 17
Beginning explored: True
Beginning reason: vanished
End explored: True
End reason: split
Length of vessel: 3 slices
Range of vessel: 115 - 117

Slice ID	Centroid	Cross section area
115	(61.51, 30.31)	77.0
116	(60.85, 29.32)	130.0
117	(60.77, 28.75)	144.0

Next vessels:
    Vessel 10 - Explored
    Vessel 18 - To be explored
Previous vessels:
    None

Vessel ID: 19
Beginning explored: True
Beginning reason: merge
End explored: True
End reason: vanished
Length of vessel: 3 slices
Range of vessel: 148 - 150

Slice ID	Centroid	Cross section area
148	(87.44, 48.40)	182.0
149	(90.57, 48.18)	148.0

150 (91.15, 47.66) 101.0
Next vessels:
None
Previous vessels:
Vessel 13 - Explored
Vessel 20 - To be explored

Vessel ID: 16
Beginning explored: True
Beginning reason: vanished
End explored: True
End reason: merge
Length of vessel: 5 slices
Range of vessel: 120 - 124

Slice ID	Centroid	Cross section area
120	(9.68, 61.95)	57.0
121	(10.05, 59.27)	56.0
122	(10.03, 56.83)	58.0
123	(10.02, 55.69)	51.0
124	(12.48, 55.98)	54.0

Next vessels:
Vessel 15 - Explored
Previous vessels:
None

Vessel ID: 18
Beginning explored: True
Beginning reason: split
End explored: True
End reason: vanished
Length of vessel: 12 slices
Range of vessel: 118 - 129

Slice ID	Centroid	Cross section area
118	(63.40, 20.93)	55.0
119	(62.59, 18.57)	44.0
120	(61.61, 17.66)	38.0
121	(61.08, 16.00)	36.0
122	(59.53, 14.81)	36.0
123	(57.50, 14.79)	38.0
124	(57.98, 14.67)	43.0
125	(56.36, 14.51)	61.0
126	(55.26, 13.59)	70.0
127	(55.74, 6.04)	77.0
128	(54.05, 3.37)	38.0
129	(54.20, 0.40)	5.0

Next vessels:
None
Previous vessels:
Vessel 17 - Explored

Vessel ID: 20
Beginning explored: True
Beginning reason: vanished
End explored: True
End reason: merge
Length of vessel: 6 slices
Range of vessel: 142 - 147

Slice ID	Centroid	Cross section area
142	(117.06, 67.45)	31.0
143	(115.13, 66.57)	63.0
144	(111.53, 63.01)	96.0
145	(108.15, 60.42)	86.0
146	(105.35, 56.90)	62.0
147	(101.21, 54.59)	68.0

Next vessels:
Vessel 19 - Explored
Previous vessels:
None

Range of network: 1 - 156

Reconstruction Experiment 3

Slice No: 63
Seed point: (74.0, 53.0)

Vessel ID: 1
Beginning explored: True
Beginning reason: split
End explored: True
End reason: split
Length of vessel: 25 slices
Range of vessel: 45 - 69

Slice ID	Centroid	Cross section area
45	(46.22, 34.68)	279.0
46	(48.86, 37.18)	242.0

47	(48.57, 37.49)	221.0
48	(50.42, 38.70)	179.0
49	(50.86, 39.83)	183.0
50	(53.86, 38.61)	174.0
51	(54.50, 39.50)	158.0
52	(54.84, 40.96)	155.0
53	(56.93, 41.62)	148.0
54	(56.93, 40.74)	145.0
55	(59.78, 41.31)	143.0
56	(58.99, 41.19)	153.0
57	(60.17, 43.07)	154.0
58	(61.74, 43.92)	170.0
59	(64.56, 45.11)	184.0
60	(65.03, 46.44)	177.0
61	(67.23, 47.85)	175.0
62	(71.62, 50.75)	175.0
63	(74.33, 53.08)	167.0
64	(75.90, 54.89)	167.0
65	(77.66, 57.42)	203.0
66	(78.72, 59.58)	242.0
67	(80.93, 61.98)	283.0
68	(81.64, 64.25)	310.0
69	(84.24, 65.31)	304.0

Next vessels:
    Vessel 2 - To be explored
    Vessel 3 - To be explored
Previous vessels:
    Vessel 4 - To be explored

Vessel ID: 2
Beginning explored: True
Beginning reason: split
End explored: True
End reason: out-of-scope
Length of vessel: 2 slices
Range of vessel: 70 - 71

Slice ID	Centroid	Cross section area
70	(88.15, 76.28)	172.0
71	(89.94, 82.55)	208.0

Next vessels:
    None
Previous vessels:
    Vessel 1 - Explored

Vessel ID: 3

Beginning explored: True
Beginning reason: split
End explored: True
End reason: split
Length of vessel: 9 slices
Range of vessel: 70 - 78

Slice ID	Centroid	Cross section area
70	(81.31, 52.06)	102.0
71	(81.84, 51.97)	93.0
72	(82.19, 50.98)	85.0
73	(83.33, 52.10)	92.0
74	(86.51, 49.61)	110.0
75	(88.10, 50.04)	131.0
76	(87.83, 50.83)	158.0
77	(88.37, 52.13)	170.0
78	(90.01, 51.50)	147.0

Next vessels:
    Vessel 6 - To be explored
    Vessel 7 - To be explored
Previous vessels:
    Vessel 1 - Explored

Vessel ID: 4
Beginning explored: True
Beginning reason: split
End explored: True
End reason: split
Length of vessel: 24 slices
Range of vessel: 21 - 44

Slice ID	Centroid	Cross section area
21	(23.73, 34.86)	181.0
22	(24.62, 34.31)	179.0
23	(25.43, 34.61)	185.0
24	(24.19, 35.28)	194.0
25	(27.01, 34.44)	189.0
26	(27.09, 34.65)	191.0
27	(26.90, 34.84)	199.0
28	(27.25, 35.25)	192.0
29	(29.02, 35.08)	189.0
30	(28.45, 34.90)	181.0
31	(30.53, 34.70)	169.0
32	(31.56, 35.02)	172.0
33	(32.77, 34.53)	163.0
34	(33.71, 35.18)	158.0
35	(32.53, 35.24)	161.0

36	(36.42, 35.35)	155.0
37	(35.52, 35.57)	155.0
38	(36.07, 35.94)	148.0
39	(36.94, 35.86)	151.0
40	(43.65, 37.40)	154.0
41	(44.84, 31.58)	268.0
42	(45.77, 29.57)	345.0
43	(44.31, 28.32)	406.0
44	(45.86, 26.60)	442.0

Next vessels:
    Vessel 5 - To be explored
    Vessel 1 - Explored
Previous vessels:
    Vessel 8 - To be explored

Vessel ID: 6
Beginning explored: True
Beginning reason: split
End explored: True
End reason: out-of-scope
Length of vessel: 18 slices
Range of vessel: 79 - 96

Slice ID	Centroid	Cross section area
79	(94.89, 48.49)	81.0
80	(97.39, 47.22)	72.0
81	(98.82, 50.10)	62.0
82	(100.34, 48.84)	62.0
83	(100.19, 48.21)	58.0
84	(100.75, 47.00)	56.0
85	(103.72, 47.67)	54.0
86	(102.07, 48.57)	54.0
87	(103.19, 46.79)	53.0
88	(104.10, 45.62)	50.0
89	(106.03, 45.79)	58.0
90	(105.92, 46.11)	63.0
91	(106.67, 44.64)	58.0
92	(108.47, 44.81)	59.0
93	(109.76, 45.65)	55.0
94	(111.00, 44.50)	52.0
95	(112.42, 42.84)	55.0
96	(112.28, 42.81)	54.0

Next vessels:
    None
Previous vessels:
    Vessel 3 - Explored

Vessel ID: 7
Beginning explored: True
Beginning reason: split
End explored: True
End reason: out-of-scope
Length of vessel: 40 slices
Range of vessel: 79 - 118

Slice ID	Centroid	Cross section area
79	(82.67, 59.22)	27.0
80	(83.52, 59.10)	29.0
81	(84.07, 62.71)	28.0
82	(84.97, 62.39)	31.0
83	(84.23, 62.84)	31.0
84	(84.84, 62.84)	32.0
85	(87.10, 64.83)	29.0
86	(85.30, 66.06)	33.0
87	(86.00, 65.00)	31.0
88	(87.09, 65.21)	33.0
89	(88.91, 65.68)	34.0
90	(88.43, 67.54)	37.0
91	(88.94, 67.57)	35.0
92	(89.83, 68.73)	30.0
93	(90.90, 70.83)	29.0
94	(91.14, 70.83)	29.0
95	(92.00, 70.12)	32.0
96	(91.19, 71.50)	32.0
97	(90.82, 72.18)	38.0
98	(92.91, 72.53)	34.0
99	(92.87, 75.13)	30.0
100	(93.82, 75.89)	28.0
101	(93.62, 76.78)	32.0
102	(95.62, 77.76)	34.0
103	(95.50, 79.41)	34.0
104	(96.97, 78.40)	35.0
105	(97.55, 80.16)	38.0
106	(98.53, 81.42)	43.0
107	(98.02, 80.43)	47.0
108	(99.37, 81.14)	51.0
109	(100.08, 82.56)	48.0
110	(100.69, 83.33)	45.0
111	(102.67, 83.22)	40.0
112	(103.91, 84.71)	45.0
113	(104.53, 87.65)	40.0
114	(104.30, 87.50)	40.0

115	(106.24, 88.29)	42.0
116	(106.98, 87.81)	43.0
117	(109.25, 88.25)	44.0
118	(111.47, 89.00)	55.0

Next vessels:
    None
Previous vessels:
    Vessel 3 - Explored

Vessel ID: 5
Beginning explored: True
Beginning reason: split
End explored: True
End reason: out-of-scope
Length of vessel: 1 slices
Range of vessel: 45 - 45

Slice ID	Centroid	Cross section area
45	(49.49, 8.86)	108.0

Next vessels:
    None
Previous vessels:
    Vessel 4 - Explored

Vessel ID: 8
Beginning explored: True
Beginning reason: out-of-scope
End explored: True
End reason: split
Length of vessel: 20 slices
Range of vessel: 1 - 20

Slice ID	Centroid	Cross section area
1	(18.86, 43.87)	164.0
2	(20.04, 44.70)	157.0
3	(19.49, 43.19)	140.0
4	(19.14, 43.72)	149.0
5	(18.84, 41.84)	154.0
6	(17.66, 42.14)	161.0
7	(17.82, 40.87)	159.0
8	(18.12, 40.81)	161.0
9	(19.55, 40.87)	166.0
10	(16.70, 40.57)	168.0
11	(18.84, 39.65)	165.0
12	(16.63, 38.74)	174.0
13	(18.42, 37.96)	175.0
14	(20.16, 38.72)	169.0

15	(19.68, 38.36)	170.0
16	(21.13, 36.03)	182.0
17	(18.93, 34.08)	223.0
18	(18.44, 32.02)	265.0
19	(18.35, 31.88)	277.0
20	(19.57, 31.70)	301.0

Next vessels:
    Vessel 9 - To be explored
    Vessel 4 - Explored
Previous vessels:
    None

Vessel ID: 9
Beginning explored: True
Beginning reason: split
End explored: True
End reason: out-of-scope
Length of vessel: 1 slices
Range of vessel: 21 - 21

Slice ID	Centroid	Cross section area
21	(9.57, 22.77)	99.0

Next vessels:
    None
Previous vessels:
    Vessel 8 - Explored

Range of network: 1 - 118

Reconstruction Case 4

Slice No: 210
Seed point: (28.0, 68.0)

Vessel ID: 1
Beginning explored: True
Beginning reason: split
End explored: True
End reason: split
Length of vessel: 8 slices
Range of vessel: 205 - 212

Slice ID	Centroid	Cross section area
205	(25.44, 73.68)	41.0

206 (27.50, 72.29) 28.0
207 (27.57, 71.37) 35.0
208 (27.69, 71.38) 39.0
209 (28.40, 69.79) 43.0
210 (28.54, 68.16) 61.0
211 (30.37, 65.26) 106.0
212 (32.65, 62.24) 113.0
Next vessels:
Vessel 2 - To be explored
Vessel 3 - To be explored
Previous vessels:
Vessel 4 - To be explored

Vessel ID: 2
Beginning explored: True
Beginning reason: split
End explored: True
End reason: merge
Length of vessel: 2 slices
Range of vessel: 213 - 214
Slice ID Centroid Cross section area
213 (38.16, 56.61) 57.0
214 (41.15, 52.11) 47.0
Next vessels:
Vessel 6 - To be explored
Previous vessels:
Vessel 1 - Explored

Vessel ID: 3
Beginning explored: True
Beginning reason: split
End explored: True
End reason: out-of-scope
Length of vessel: 12 slices
Range of vessel: 213 - 224
Slice ID Centroid Cross section area
213 (27.91, 68.72) 43.0
214 (27.02, 68.44) 43.0
215 (26.18, 68.42) 45.0
216 (23.48, 68.48) 50.0
217 (20.90, 68.42) 48.0
218 (22.00, 68.00) 53.0
219 (19.70, 68.17) 53.0
220 (17.61, 68.16) 61.0
221 (15.38, 67.31) 58.0

222	(13.04, 67.95)	78.0
223	(10.11, 68.38)	74.0
224	(8.74, 70.47)	87.0

Next vessels:
None
Previous vessels:
Vessel 1 - Explored

Vessel ID: 4
Beginning explored: True
Beginning reason: split
End explored: True
End reason: split
Length of vessel: 14 slices
Range of vessel: 191 - 204

Slice ID	Centroid	Cross section area
191	(26.08, 64.77)	105.0
192	(27.44, 66.51)	94.0
193	(24.17, 67.76)	82.0
194	(25.85, 70.41)	71.0
195	(24.54, 71.13)	71.0
196	(24.29, 71.54)	72.0
197	(23.69, 73.59)	68.0
198	(23.75, 74.47)	77.0
199	(21.89, 74.68)	105.0
200	(22.48, 79.09)	139.0
201	(21.71, 78.70)	168.0
202	(19.77, 80.25)	187.0
203	(20.61, 81.49)	202.0
204	(19.38, 83.30)	212.0

Next vessels:
Vessel 5 - To be explored
Vessel 1 - Explored
Previous vessels:
Vessel 8 - To be explored

Vessel ID: 6
Beginning explored: True
Beginning reason: merge
End explored: True
End reason: vanished
Length of vessel: 3 slices
Range of vessel: 215 - 217

Slice ID	Centroid	Cross section area
215	(47.82, 45.58)	98.0

216	(46.99, 45.10)	89.0
217	(46.43, 44.43)	42.0

Next vessels:

None

Previous vessels:

Vessel 2 - Explored

Vessel 7 - To be explored

Vessel ID: 5
Beginning explored: True
Beginning reason: split
End explored: True
End reason: out-of-scope
Length of vessel: 2 slices
Range of vessel: 205 - 206

Slice ID	Centroid	Cross section area
205	(15.08, 86.92)	136.0
206	(15.13, 89.33)	135.0

Next vessels:

None

Previous vessels:

Vessel 4 - Explored

Vessel ID: 8
Beginning explored: True
Beginning reason: out-of-scope
End explored: True
End reason: split
Length of vessel: 17 slices
Range of vessel: 174 - 190

Slice ID	Centroid	Cross section area
174	(19.16, 35.61)	168.0
175	(24.01, 38.10)	98.0
176	(26.12, 41.29)	56.0
177	(27.17, 43.97)	63.0
178	(28.00, 46.92)	63.0
179	(28.82, 47.72)	60.0
180	(28.85, 49.42)	53.0
181	(29.07, 53.32)	44.0
182	(29.50, 53.76)	34.0
183	(29.24, 55.21)	42.0
184	(28.78, 57.65)	37.0
185	(28.92, 57.79)	39.0
186	(28.59, 59.84)	44.0
187	(32.06, 61.96)	81.0

188	(32.32, 61.75)	146.0
189	(36.64, 62.57)	244.0
190	(38.37, 63.29)	302.0

Next vessels:

Vessel 9 - To be explored

Vessel 4 - Explored

Previous vessels:

None

Vessel ID: 7
Beginning explored: True
Beginning reason: split
End explored: True
End reason: merge
Length of vessel: 24 slices
Range of vessel: 191 - 214

Slice ID	Centroid	Cross section area
191	(55.64, 28.50)	22.0
192	(57.88, 29.53)	17.0
193	(55.80, 29.87)	15.0
194	(57.93, 31.86)	14.0
195	(57.00, 32.00)	15.0
196	(56.69, 31.81)	16.0
197	(56.60, 32.93)	15.0
198	(57.50, 32.50)	20.0
199	(56.93, 31.14)	14.0
200	(58.00, 34.00)	15.0
201	(58.33, 32.50)	18.0
202	(57.40, 33.07)	15.0
203	(58.50, 34.00)	16.0
204	(58.22, 35.22)	18.0
205	(57.12, 34.18)	17.0
206	(58.42, 34.58)	19.0
207	(58.00, 35.44)	18.0
208	(58.06, 36.65)	17.0
209	(57.39, 37.11)	18.0
210	(56.50, 37.79)	24.0
211	(55.04, 38.75)	24.0
212	(55.33, 38.42)	24.0
213	(54.75, 40.04)	24.0
214	(53.85, 40.19)	27.0

Next vessels:

Vessel 6 - Explored

Previous vessels:

Vessel 10 - To be explored

Vessel ID: 9
Beginning explored: True
Beginning reason: split
End explored: True
End reason: merge
Length of vessel: 9 slices
Range of vessel: 191 - 199

Slice ID	Centroid	Cross section area
191	(51.84, 64.09)	134.0
192	(58.85, 65.34)	116.0
193	(60.91, 65.94)	94.0
194	(66.13, 68.06)	78.0
195	(67.10, 68.67)	79.0
196	(69.75, 70.27)	83.0
197	(71.90, 72.81)	73.0
198	(74.32, 74.88)	78.0
199	(75.16, 75.52)	82.0

Next vessels:
    Vessel 12 - To be explored
Previous vessels:
    Vessel 8 - Explored

Vessel ID: 10
Beginning explored: True
Beginning reason: split
End explored: True
End reason: split
Length of vessel: 27 slices
Range of vessel: 164 - 190

Slice ID	Centroid	Cross section area
164	(77.43, 42.60)	60.0
165	(78.00, 43.50)	46.0
166	(76.83, 39.65)	40.0
167	(74.10, 38.73)	41.0
168	(74.33, 38.02)	45.0
169	(73.27, 37.40)	45.0
170	(72.83, 36.87)	46.0
171	(71.02, 36.42)	45.0
172	(69.76, 35.17)	41.0
173	(67.02, 33.89)	45.0
174	(66.70, 32.50)	40.0
175	(67.28, 31.62)	40.0
176	(65.07, 30.84)	43.0
177	(63.85, 31.22)	46.0

178	(63.27, 31.17)	41.0
179	(62.56, 29.46)	39.0
180	(61.36, 28.11)	45.0
181	(60.46, 29.10)	41.0
182	(60.51, 27.60)	43.0
183	(59.60, 27.36)	42.0
184	(58.94, 27.70)	47.0
185	(58.14, 25.50)	42.0
186	(57.02, 25.18)	45.0
187	(58.82, 25.12)	51.0
188	(56.02, 23.23)	65.0
189	(55.49, 23.24)	79.0
190	(54.60, 21.87)	94.0

Next vessels:
    Vessel 7 - Explored
    Vessel 11 - To be explored
Previous vessels:
    Vessel 14 - To be explored

Vessel ID: 12
Beginning explored: True
Beginning reason: merge
End explored: True
End reason: out-of-scope
Length of vessel: 1 slices
Range of vessel: 200 - 200

Slice ID	Centroid	Cross section area
200	(79.28, 87.10)	152.0

Next vessels:
    None
Previous vessels:
    Vessel 9 - Explored
    Vessel 13 - To be explored

Vessel ID: 11
Beginning explored: True
Beginning reason: split
End explored: True
End reason: out-of-scope
Length of vessel: 1 slices
Range of vessel: 191 - 191

Slice ID	Centroid	Cross section area
191	(51.87, 16.96)	76.0

Next vessels:
    None

Previous vessels:
    Vessel 10 - Explored

Vessel ID: 14
Beginning explored: True
Beginning reason: split
End explored: True
End reason: split
Length of vessel: 1 slices
Range of vessel: 163 - 163

Slice ID	Centroid	Cross section area
163	(84.23, 41.09)	193.0

Next vessels:
    Vessel 10 - Explored
    Vessel 15 - To be explored
Previous vessels:
    Vessel 16 - To be explored

Vessel ID: 13
Beginning explored: True
Beginning reason: out-of-scope
End explored: True
End reason: merge
Length of vessel: 1 slices
Range of vessel: 199 - 199

Slice ID	Centroid	Cross section area
199	(79.18, 93.46)	65.0

Next vessels:
    Vessel 12 - Explored
Previous vessels:
    None

Vessel ID: 15
Beginning explored: True
Beginning reason: split
End explored: True
End reason: out-of-scope
Length of vessel: 4 slices
Range of vessel: 164 - 167

Slice ID	Centroid	Cross section area
164	(89.85, 37.73)	136.0
165	(92.87, 37.18)	142.0
166	(93.94, 31.27)	165.0
167	(93.08, 27.95)	185.0

Next vessels:

None
Previous vessels:
Vessel 14 - Explored

Vessel ID: 16
Beginning explored: True
Beginning reason: vanished
End explored: True
End reason: split
Length of vessel: 5 slices
Range of vessel: 158 - 162

Slice ID	Centroid	Cross section area
158	(81.43, 49.29)	7.0
159	(80.44, 49.46)	100.0
160	(82.51, 49.07)	167.0
161	(82.08, 48.54)	224.0
162	(84.48, 48.48)	293.0

Next vessels:
Vessel 17 - To be explored
Vessel 14 - Explored
Previous vessels:
None

Vessel ID: 17
Beginning explored: True
Beginning reason: split
End explored: True
End reason: merge
Length of vessel: 1 slices
Range of vessel: 163 - 163

Slice ID	Centroid	Cross section area
163	(78.56, 59.99)	108.0

Next vessels:
Vessel 18 - To be explored
Previous vessels:
Vessel 16 - Explored

Vessel ID: 18
Beginning explored: True
Beginning reason: merge
End explored: True
End reason: split
Length of vessel: 1 slices
Range of vessel: 164 - 164

Slice ID	Centroid	Cross section area

164 (78.89, 78.09) 331.0
Next vessels:
Vessel 20 - To be explored
Vessel 21 - To be explored
Previous vessels:
Vessel 17 - Explored
Vessel 19 - To be explored

Vessel ID: 20
Beginning explored: True
Beginning reason: split
End explored: True
End reason: merge
Length of vessel: 3 slices
Range of vessel: 165 - 167
Slice ID Centroid Cross section area
165 (81.83, 74.48) 221.0
166 (81.69, 71.90) 157.0
167 (79.26, 77.37) 19.0
Next vessels:
Vessel 22 - To be explored
Previous vessels:
Vessel 18 - Explored

Vessel ID: 21
Beginning explored: True
Beginning reason: split
End explored: True
End reason: out-of-scope
Length of vessel: 1 slices
Range of vessel: 165 - 165
Slice ID Centroid Cross section area
165 (76.15, 97.90) 41.0
Next vessels:
None
Previous vessels:
Vessel 18 - Explored

Vessel ID: 19
Beginning explored: True
Beginning reason: out-of-scope
End explored: True
End reason: merge
Length of vessel: 1 slices
Range of vessel: 163 - 163

Slice ID	Centroid	Cross section area
163	(77.80, 89.26)	166.0

Next vessels:
    Vessel 18 - Explored
Previous vessels:
    None

Vessel ID: 22
Beginning explored: True
Beginning reason: merge
End explored: True
End reason: out-of-scope
Length of vessel: 2 slices
Range of vessel: 168 - 169

Slice ID	Centroid	Cross section area
168	(62.48, 93.31)	118.0
169	(57.02, 92.67)	120.0

Next vessels:
    None
Previous vessels:
    Vessel 20 - Explored
    Vessel 23 - To be explored

Vessel ID: 23
Beginning explored: True
Beginning reason: out-of-scope
End explored: True
End reason: merge
Length of vessel: 1 slices
Range of vessel: 167 - 167

Slice ID	Centroid	Cross section area
167	(64.75, 94.78)	110.0

Next vessels:
    Vessel 22 - Explored
Previous vessels:
    None

Range of network: 158 - 224